
Reviews
of Physiology,
Biochemistry and
Pharmacology
162
Springer

Reviews of Physiology, Biochemistry and Pharmacology

For further volumes:
http://www.springer.com/series/112

Bernd Nilius · Susan G. Amara ·
Thomas Gudermann · Reinhard Jahn ·
Roland Lill · Stefan Offermanns ·
Ole H. Petersen
Editors

Reviews of Physiology, Biochemistry and Pharmacology
162

Springer

Editors
Bernd Nilius
Full Professor of Physiology
KU Leuven, Department Cell Mol Medicine
Laboratory Ion Channel Research
Campus Gasthuisberg
Herestraat 49 bus 802
B-3000 Leuven
Belgium

Susan G. Amara
University of Pittsburgh
Pittsburgh, PA
USA

Thomas Gudermann
Walther-Straub-Institut für Pharmakologie
und, Toxikologie
München
Germany

Reinhard Jahn
Max-Planck-Institute for Biophysical
Chemistry
Göttingen
Germany

Roland Lill
University of Marburg
Medical Biotechnology Center
Marburg
Germany

Stefan Offermanns
Max-Planck-Institut für Herz- und
Lungenforschung
Bad Nauheim
Germany

Ole H. Petersen
School of Biosciences
Cardiff University
Museum Avenue
Cardiff, UK

ISSN 0303-4240 ISSN 1617-5786 (electronic)
ISBN 978-3-642-29255-2 ISBN 978-3-642-29256-9 (eBook)
DOI 10.1007/978-3-642-29256-9
Springer Heidelberg New York Dordrecht London

Contents

Cardiac Ion Channels and Mechanisms for Protection Against Atrial Fibrillation

Morten Grunnet, Bo Hjorth Bentzen, Ulrik Svane Sørensen, and Jonas Goldin Diness

Abstract Atrial fibrillation (AF) is recognised as the most common sustained cardiac arrhythmia in clinical practice. Ongoing drug development is aiming at obtaining atrial specific effects in order to prevent pro-arrhythmic, devastating ventricular effects. In principle, this is possible due to a different ion channel composition in the atria and ventricles. The present text will review the aetiology of arrhythmias with focus on AF and include a description of cardiac ion channels. Channels that constitute potentially atria-selective targets will be described in details. Specific focus is addressed to the recent discovery that Ca^{2+}-activated small conductance K^+ channels (SK channels) are important for the repolarisation of atrial action potentials. Finally, an overview of current pharmacological treatment of AF is included.

Abbreviations

aERP	Atrial effective refractory period
AF	Atrial fibrillation
APD	Action potential duration
AV	Atrioventricular
AV-ERP	AV-nodal effective refractory period
BCL	Basic cycle length
BPM	Beats per minute
CV	Conduction velocity
DAD	Delayed afterdepolarisations
EAD	Early afterdepolarisations

M. Grunnet (✉)
NeuroSearch A/S, Pederstrupvej 93, 2750, Ballerup, Denmark
e-mail: mgr@neurosearch.com

Rev Physiol Biochem Pharmacol, doi: 10.1007/112_2011_3,

SA	Sinoatrial
SK channel	Small conductance Ca^{2+} activated K^+ channel
TdP	Torsades de pointes
vERP	Ventricular effective refractory period
VF	Ventricular fibrillation
WL	Wavelength

Introduction

The mammalian heart is a mechanical pump with the function of assuring pulmonary and systemic blood circulation. This secures the crucial transport of nutrients, removal of waste products, circulation of hormones and antibodies and exchange of gases. Under normal non-diseased conditions, the heart will exert its mechanical pumping in a continuous fashion with a stable rhythm while changing rate according to systemic needs. This implies that the human heart is capable of performing approximately 3.000.000.000 beats in an average life span. It also implies that, in principle, a single inappropriate electrical signal can disturb the delicate balance between excitation and contraction. In the worst case such an event can ultimately result in sudden cardiac arrest. Appropriate contraction and thus pumping of the heart is initiated and controlled by cardiac impulses or electrical signals that on a cellular level are recognised as cardiac action potentials.

The contrast to the highly stable rhythm of a normal functional heart is categorised as arrhythmias (from Greek a + rhythmos = loss of rhythm). In its broadest meaning, arrhythmias can be anything from single events with diminutive palpitations to fibrillations in the ventricles that can lead to sudden cardiac death. With the multifaceted and complicated nature of the cardiac excitation-contraction coupling in mind, it is fascinating that arrhythmias nevertheless are an unusual incident in young and middle age people.

Excitability of cardiac myocytes is obtained by transient changes in ion permeability across the cell surface membrane. The generation of the cardiac action potentials therefore relies on the delicate orchestration of openings and closures of many different ion channels that can allow the selective passage of ions across the lipophilic plasma membrane. Compared to neuronal action potentials, cardiac action potentials are unique in appearance as a consequence of a prolonged plateau phase that can last for several hundred milliseconds. The exact shape and duration of cardiac action potential is different in different areas of the heart as a consequence of the subtle composition and interplay between different ion channels in different parts of the heart. Generally, action potentials recorded from the atria will appear more triangulated in shape compared to ventricular action potentials which have a more stable plateau phase and thereby a dome-like shape. Both types of action potentials are different from the electrical activity that can be recorded from the sinoatrial (SA) and atrioventricular (AV) nodes, where a sliding baseline in the

membrane potential gives rise to spontaneous electrical activity. In addition, the width and shape of the dome-like structure of a ventricular action potential differ between different regions of the heart. A thorough understanding of the ion channels underlying these differences is valuable in the search for drugs that can selectively target a specified part of the heart as for example the atria. Representative examples of action potentials recorded from different cardiac regions are depicted in Fig. 1.

The profound regulation of ion channels and some redundancy in the excitation-contraction system are probably important for the stability of the system. Good examples of partial redundancy is the participation of a number of different K^+ channels responsible for repolarising the action potential in both atria and ventricles. In the ventricles at least three different potassium currents named I_{Kr}, I_{Ks} and I_{K1} participate in repolarisation. This phenomenon has been characterised as the "repolarisation reserve" (Roden 1998) to underline the overlapping function and, in this manner, the redundancy in the system. In the atria, a number of different K^+ channels also participate in terminating or repolarising the action potential. Importantly, from a functional perspective some of these channels are almost exclusively active in the atria, thereby giving the opportunity to specifically target these ion channels with a reduced risk of ventricular side effects. Examples of K^+ channels that are selectively expressed in the atria are $K_v1.5$ as responsible for I_{Kur},

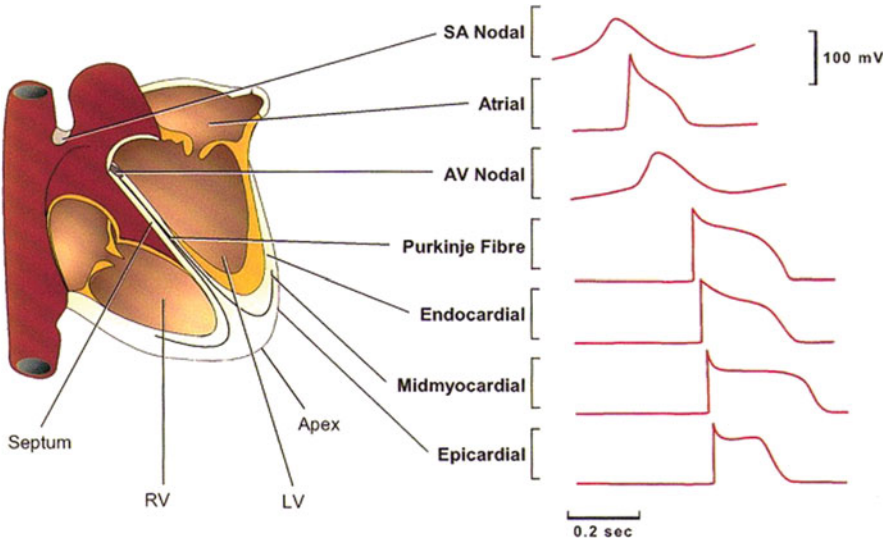

Fig. 1 Differences in action potential morphology in various regions of the heart. Notice how differences exist both transmurale in ventricles (epicardial to endocardial) and between chambers. Furthermore, the action potential morphology is unique in nodes with a sliding diastolic baseline and more depolarised resting membrane potentials (membrane potential not indicated). From (Nerbonne 2000)

$K_{ir}3.1/K_{ir}3.4$ as accountable for I_{KACh} and, more recently, small conductance Ca^{2+}-activated K^+ channels responsible for I_{KCa} (Boyle and Nerbonne 1992; Ravens and Dobrev 2003; Xu et al. 2003).

The term "arrhythmia" includes a number of diverse diseases. In the attempt to understand and treat arrhythmic conditions, it is a requirement to understand the regulation and function of cardiac ion channels. Furthermore, it is important to acknowledge the diverse compositions and distributions of ion channels in the heart to be able to selectively treat specific diseases such as AF. In the following, we will give a general description of the prerequisites for obtaining an arrhythmia as well as an introduction to cardiac ion channels. Special emphasis will be on the recent discovery that Ca^{2+}-activated small conductance K^+ channels (SK channels) are important for the repolarisation of atrial action potentials. Finally, an overview of mode of action of different anti-AF drugs targeting ion channels will be given.

Mechanisms and Aetiology of Arrhythmias

In a wide sense, any kind of abnormal heart rhythm can be regarded as an arrhythmia. Events can vary from a gentle transient palpitations to much more severe conditions that can ultimately lead to cardiac arrest and thereby sudden death. Simple arrhythmias can be a too slow heart beat frequency which is termed bradycardia (in humans less than 60 beats per minute), or an abnormally fast heart beat frequence known as tachycardia (in humans more than 100 beats per minute at rest). Tachycardia will be monomorphic or polymorphic in origin and can progress into fibrillation that describes a completely uncoordinated electrical activity of the heart. A common denominator for complex arrhythmias is the initiation by a trigger and the sustainability that depends on the presence of a substrate. In the following we will give a description of the mechanisms behind both triggers and substrates and also introduce re-entry based arrhythmias based upon the leading circle and spiral wave theories.

Triggers of Arrhythmias

Arrhythmias are always initiated by a trigger. Abnormal focal automaticity is a typical trigger of AF. "Automaticity" is the basis of cardiac pacemaking function. Several areas of the heart show automaticity, but normally the SA node is the fastest pacemaker and therefore the one that controls the heart rate. If an area outside the SA or the AV nodes starts an impulse it is considered as abnormal automaticity, and such an area is called an ectopic focus. Acute myocardial ischaemia, increased sympathetic drive or remodeling of ion channel expression as a consequence of AF can enhance the risk for unwanted atypical automaticity (Boyle and Nerbonne 1992; Ravens and Dobrev 2003).

Abnormal focal activity can also arise from so-called afterdepolarisations (Fig. 2a). During the plateau of the action potential (phase 2), the free intracellular concentration of Ca^{2+} increases sharply. This free intracellular Ca^{2+} is returned to baseline level by

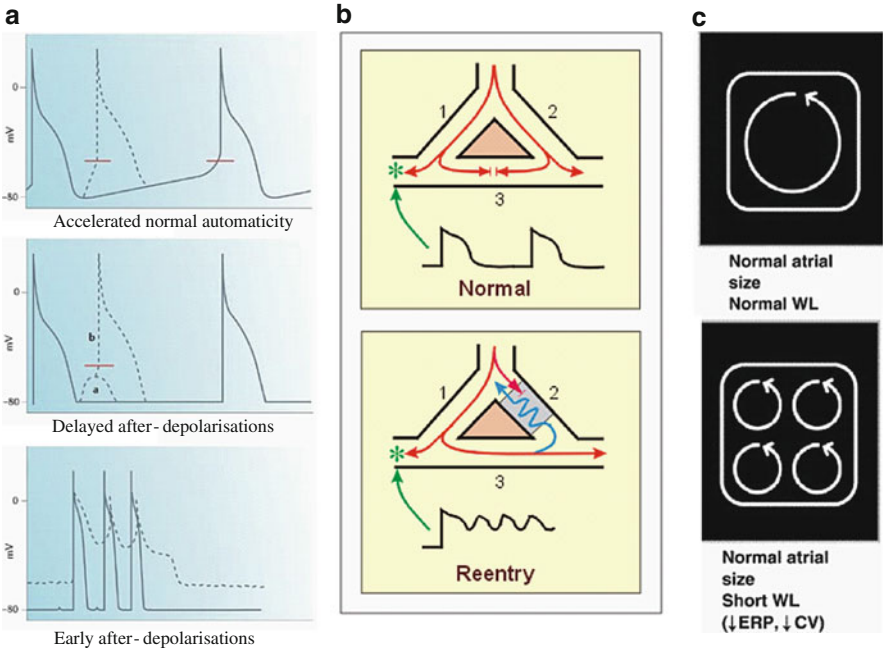

Fig. 2 Triggers and substrates for arrhythmias. Arrhythmias are initiated by a triggering event. Three examples are demonstrated in **a**. The *upper panel* depicts how accelerated normal automaticity will increase the heart rate. Delayed afterdepolarisations (DADs) taking place in the diastolic interval are shown in the middle panel in **a**. An extra beat will occur if the depolarisation is adequate for Na^{+} channel activation. The lower panel in **a** demonstrates an early afterdepolarisations (EADs). EADs are unintended re-activations of voltage gated Ca^{2+} channels that disturb the normally repolarising. DADs and EADs can both trigger arrhythmias. Normal and re-entry propagation of electrical signals are demonstrated in **b**. In a non-disturbed situation the electrical signal extends around a non-conducting are a with equal velocity (1 and 2). The two signals will propagate in the *left* and *right direction* with equal velocity. When colliding in point 3 they will therefore encounter refractory tissue and die out. In contrast the presence of a unidirectional block, represented by the *grey area*, can act as the substrate for a re-entry based arrhythmia. The signal can only pass in one direction represented by branch 1. If the conducting signal re-encounters point 1 at a time where the tissue is no longer refractory re-excitation can happen and result in self sustained wave propagation. The green star represents a recording electrode recording arrhythmogenic or normal action potentials. The principle of decreased wavelengths according to the leading circle re-entry is illustrated in **c**. Wavelengths will normally be sufficiently long to encompass only few re-entry waves. Since the wavelength is defined as the product of conduction velocity (CV) times effective refractory period (ERP) it is evident that decreased CV, decreased ERP or a combination of both will shorten wavelengths. The more wavelengths that can be encompassed in a given area of tissue the greater is the likelihood for a re-entry based arrhythmias. **a** is from (Nattel and Carlsson 2006) and **c** is from (Nattel et al. 2005)

uptake into the sarcoplasmatic reticulum or by transmembrane extrusion via the Na^+/Ca^{2+} exchanger. The latter process exchanges three Na^+ ions for one Ca^{2+} ion. In effect, one positive charge is moved into the cell for each Ca^{2+} ion leaving via this mechanism, thereby producing a net inward current. This can give rise to a delayed afterdepolarisation (DAD) in the diastolic interval (phase 4 of the action potential) (Zygmunt et al. 1998; Nagy et al. 2004; Homma et al. 2006; Venetucci et al. 2007).

Another kind of afterdepolarisation is the early afterdepolarisation (EAD) which takes place during the repolarizing phase of the action potential (phase 3). Mechanistically, EADs are associated with inappropriate reactivation of L-type Ca^{2+} channels. The initial depolarisation in the cardiac action potential (phase 0) will activate the voltage gated Ca^{2+} channels in a process that is followed by both voltage and Ca^{2+} dependent inactivation. Consequently, inactivation can be released by a reduction in the membrane potential and in intracellular Ca^{2+} concentrations. If this release of inactivation happens at a membrane potential that is still sufficiently depolarised to allow activation of L-type Ca^{2+} channels, an inappropriate reopening of these channels will instigate an EAD (Shorofsky and January 1992; Yamawake et al. 1992; Zeng and Rudy 1995). The time interval where reactivation of the L-type Ca^{2+} channels is possible during the repolarisation phase of the action potential, is defined as a "vulnerable window". This will typically be between 30% to 90% repolarisation of the action potential (APD_{30}–APD_{90}). Even though EADs typically originate in tissue areas with long action potentials, such as the Purkinje system, this trigger has been associated with AF (Yamashita et al. 1997; Satoh and Zipes 1998; Burashnikov and Antzelevitch 2003). It should also be mentioned that it is not only the action potential duration *per se* that determines whether an EAD might originate. The exact morphology of the reactivation phase is also very central (Hondeghem et al. 2001). In situations with increased triangulation of action potentials, which can be observed in atria from patients with AF, the vulnerable window will typically increase and thereby enhance the probability for EADs. Prolongation of the action potentials without increasing triangulation can actually be antiarrhythmic (Hondeghem et al. 2001).

Substrates of Arrhythmias

In order for sustained AF to occur, the trigger must initiate a self-sustained event of action potential propagation and a prerequisite for such an accidental continued circulation of action potentials is a so-called substrate (Fig. 2b). This can be an anatomical obstacle or be based upon inappropriate electrophysiological heterogeneity. The common denominator is that the substrate will permit sustained excitation and propagation of the electrical signals. This can happen if the electrical propagation is sufficiently slow, or if the travelled path is sufficiently long for the tissue to regain its excitability once the action potentials reach their original starting point. Such self-sustained continuous propagation of electrical signals is therefore referred to as re-entry arrhythmias.

The hypothesis that AF is a result of multiple re-entrant wavelets was put forward by Moe et al. more than 60 years ago and has been the dominant theory for many years (Moe et al. 1964; Nattel 2002). The theory was substantiated by the work of Allessie et al. who proposed the "leading circle" mechanism of re-entry and showed that re-entry can occur in tissue even when no obvious anatomical obstacle is present (Allessie et al. 1973, 1975, 1976, 1977). According to Allessie et al. ". . . the smallest possible pathway in which the impulse can continue to circulate is the circuit in which the stimulating efficacy of the circulating wavefront is just enough to excite the tissue ahead which is still in its relative refractory phase. In other words, in this smallest circuit possible, which we designated as the "leading circle," the head of the circulating wavefront is continuously biting in its own tail of refractoriness. Because of this tight fit, the length of the circular pathway equals the "wavelength" of the circulating impulse"(Allessie et al. 1977). In brief, the wave length (WL) depends on the product of the effective refractory period (ERP) and the conduction velocity (CV) as WL = ERP x CV. The shorter the WL the more current circuits can be encompassed in a given tissue area and consequently a decreased WL is considered to be pro-arrhythmic. From this perspective it is also worth mentioning that remodelling conditions leading to atrial dilatation or enlargement will also be pro-arrhythmic since more tissue area is available to encompass circulatory current propagation. Atrial enlargement is seen as a consequence of both congestive heart failure and atrial tachycardia and is believed to be an important predictor for clinical maintenance of atrial fibrillation (Henry et al. 1976; Shi et al. 2001). It follows accordingly, that anti-arrhythmic effects can be obtained by an increased WL. This will typically be achieved by an increased ERP obtained by a prolongation of the action potential duration or less commonly by an increased CV (Fig. 2c) (Nattel et al. 2005). It should be emphasized that this approach calls for an atria-selective effect since it has clearly been demonstrated that especially heterogenic prolongation of ventricular action potentials is potentially devastating due to increased risk for ventricular fibrillation (Pratt et al. 1998; Conrath and Opthof 2006; Antzelevitch et al. 2007).

The leading circle theory does not, however, explain why blockers of I_{Na} are effective in terminating arrhythmias. On the contrary, according to this theory, I_{Na} blockers should promote AF by decreasing the conduction velocity and consequently decreasing the wavelength. It is however apparent that inhibition of cardiac Na^+ channels can be a useful anti-arrhythmic principle in many cases as demonstrated by class Ia-c compounds that by different modes of action all reduce functional Na^+ current (Okishige et al. 2000). This perceptible contradiction can be addressed using a more novel and complex model of cardiac re-entry; the so-called "spiral wave" model of re-entry (Davidenko et al. 1992; Pertsov et al. 1993; Skanes et al. 1998; Wijffels et al. 2000; Kneller et al. 2005). According to this model, a spiral wave continuously and rapidly rotates around a central core. Re-entry of a curved spiral wave necessitates a highly excitable substrate with short refractoriness that supports the angle of spiral curvature. In contrast to the leading circle model, where the central cores of the re-entry circuits are constantly

refractory because of continual excitation, the core of the spiral wave is non-activated and excitable. When I_{Na} is decreased the source current is decreased. According to the spiral wave model, this reduction of diffusive current leads to an increased meandering of the core as well as increased core size and decreased curvature, all of which can be antiarrhythmic. An excellent overview of the biophysical differences between the leading circle and spiral wave theories has been given by Comtois et al. (Comtois et al. 2005).

During the last 60 years most attention has been given to the principle of multiple circuit re-entries such as illustrated for the leading circle and spiral wave theories. More recent results, however, indicate that ectopic foci and single re-entry circles especially around the pulmonary veins or mitral valve act as the foundation for AF. Depending on the conditions, ectopic foci, single re-entry circles and multiple re-entry circles can probably all be involved in AF (Nattel et al. 2005).

Atrial Fibrillation

Atrial fibrillation (AF) was first described in 1906, and is characterized by a rapid and uncoordinated electrical activation of the atria (Fye 2006).

Several classification systems and various labels have been used to describe the pattern of AF, including acute, chronic, paroxysmal, intermittent, constant, persistent, and permanent fibrillation. The current international guidelines recommend distinguishing the first-detected episode of AF whether symptomatic and/or self-limited or not (Fig. 3). When a patient has had two or more episodes, AF is considered recurrent. If the recurrent AF terminates spontaneously within a week it is designated as *paroxysmal* and if the fibrillation is sustained for more than 7 days it is designated as *persistent*. The term *permanent* AF is a clinical designation given to ongoing long-term episodes where cardioversion has either failed or not been attempted.

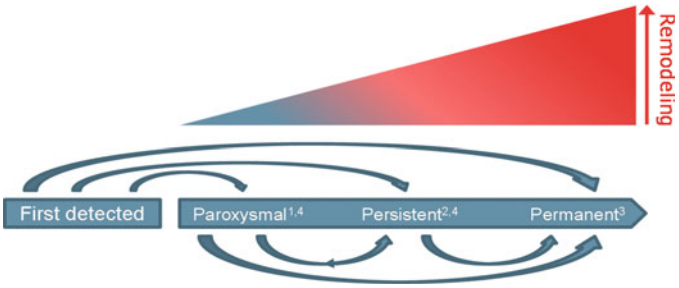

Fig. 3 Patterns of atrial fibrillation. (1) Episodes that generally last 7 days or less. (2) Episodes that usually last longer than 7 days. (3) Cardioversion failed or not attempted. (4) Both paroxysmal and persistent AF may be recurrent. The progression from paroxysmal to permanent AF is associated with increased degree of atrial remodeling

As a result of the lack of coordinated atrial contraction the ventricular filling is reduced and blood stasis occurs in the atria, which predispose to heart failure and thromboembolic stroke, respectively (Wolf et al. 1991; Wang et al. 2003). AF increases the risk for stroke nearly fivefold and it is estimated that 15% of all strokes are attributable to AF – a proportion which increases markedly with age (Wolf et al. 1991). Even though AF is not *per se* a fatal arrhythmia, there is a significantly increased risk of death after the onset of AF, primarily due to the increased risk of stroke (Kannel et al. 1983).

Among cardiac arrhythmias, AF is the most common, accounting for approximately one third of hospitalizations for heart rhythm disturbances (Fuster et al. 2011). The lifetime risk for developing AF is approximately 25% in the general population (Lloyd-Jones et al. 2004).

Ion Channel Composition in Atria and Ventricles

Although the mammalian heart is from an overall morphological perspective more or less identical in different species, there is nevertheless a large degree of variation in ion channel compositions. This is reflected both as variation in the actual shape and duration of action potentials and in the actual heart rates in different species. An illustrative example is the tenfold difference between the resting heart rates of man and mouse being approximately 60 and 600 beats per minute. To add further to the variation in shape and duration of action potentials, ion channel distribution will also vary within the same species according to their intra-cardiac location. As illustrated in Fig. 1, variations can be observed between atria, ventricles, the conduction system and the nodes. Also, more local differences are evident for example between different transmural ventricular layers. The action potential in both atria and ventricles is divided into five distinct phases (phase 0–4, Fig. 4). The following section will give an account on ion channels occupied in shaping the human cardiac action potential. For ion channels involved in both atrial and ventricular electrical activity, a brief description will be included while more emphasis will be given to atria-selective channels. Finally, it should be emphasised that atrial fibrillation *per se* can lead to a change in the overall presence of cardiac ion channels in a qualitative and quantitative fashion in a process recognised as remodeling. The following description will focus on action potentials in sinus rhythm and subsequently give an account of important changes in ion channel distribution as a consequence of remodeling of cardiac tissue.

Phase 0

This initial phase of the action potential represents the transition from the diastolic to systolic interval. Activation of voltage gated cardiac Na^+ channels drives the corresponding depolarising of the membrane potential. The predominant cardiac

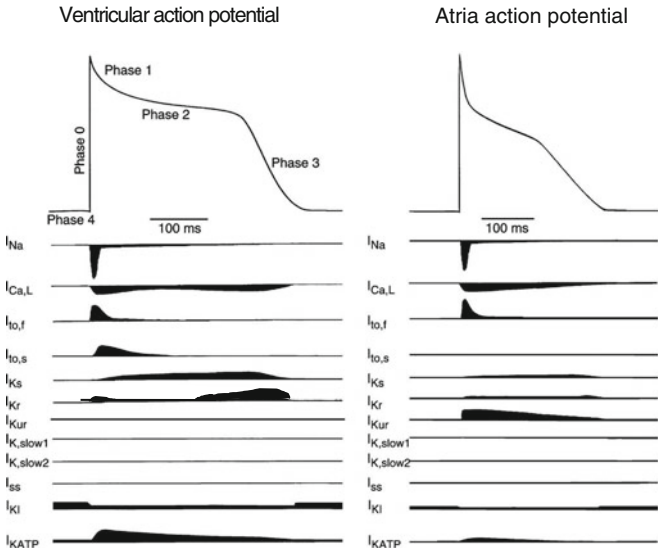

Fig. 4 Ionic currents in atrial and ventricular action potentials. Phase 0 is defined by activation of voltage-dependent Na^+ channels giving rise to inward movement of Na^+. Phase 1 is the combined inactivation of Na^+ channels, activation of Ca_V channels and transient K^+ channels. Phase 2 results from Ca^{2+} influx via sustained activation of voltage gated Ca^{2+} channels. Phase 3 repolarisation is accomplished by Ca_V channel inactivation and increased conduction through different K^+ channels and phase 4 is the resting phase, controlled mainly by K^+ channels. The relative contribution from the different ion currents, in time and amplitude, to the different phases of the action potential is illustrated by the black shading. The figure is modified from (Nerbonne and Kass 2005)

Na^+ current is conducted by $Na_v1.5$ and encoded by the gene *SCN5A*. Cardiac $Na_v1.5$ channels are characterised by the very low sensitivity to the neurotoxin tetrodotoxin (TTX) (Fozzard and Hanck 1996; Yu and Catterall 2003). Few reports have identified other Na^+ channels in the cardiac myocardium than $Na_v1.5$. At least mRNA has been identified for $Na_v1.1$, $Na_v1.3$ and $Na_v1.4$ (encoded by the genes *SCN1A, SCN3A and SCN4A,* respectively) (Rogart et al. 1989; Sills et al. 1989; Dhar Malhotra et al. 2001; Zimmer et al. 2002). It should however be emphasised that only very few studies have succeeded in identifying TTX sensitive voltage gated Na^+ current in cardiac myocytes (Rogart et al. 1989; Sills et al. 1989; Dhar Malhotra et al. 2001; Zimmer et al. 2002). The notion that cardiac Na^+ current is predominantly conducted by $Na_v1.5$ channels therefore seems justified. $Na_v1.5$ channels are responsible for the initial depolarisation in atria, ventricles and the Purkinje system while depolarisation in the nodes relies on voltage gated Ca^{2+} channels (Nerbonne and Kass 2005).

Activation of $Na_v1.5$ channels is fast and is characterised by a steep voltage dependency starting from potentials around −55 mV (Fozzard and Hanck 1996). In addition to the fast peak current, which drives the initial depolarisation, $Na_v1.5$

channels also conduct a more persistent current. The biophysical explanation for this persistent current is the partial voltage overlap between activation and inactivation. This generates a co-called "window" or persistent Na^+ current (Attwell et al. 1979). The persistent Na^+ current is absolutely minor compared to the initial peak current constituting 1‰ to 1% of the total current (Wang et al. 1996). The persistent Na^+ current can anyhow have a substantial impact on the action potential morphology and thereby also for the probability for developing arrhythmias (Weidmann 1951; Bennett et al. 1995).

Finally, it should be emphasised that even though $Na_v1.5$ channels are encoded from the same gene and are expressed in both atria and ventricles, a functional difference exists between the two types of chambers. The half inactivation voltage ($V_{0.5}$) for $Na_v1.5$ channels is more negative, or left-ward shifted, in atria compared to ventricles in both canine and guinea pig (Li et al. 2002; Burashnikov et al. 2007).

Phase 1

The initial depolarisation in phase 0 is followed by a transient repolarisation termed phase 1. This phase is evident in both atria and ventricles but is most prominent in atria. In ventricles the regional differences in the amplitude is seen with a more pronounced repolarisation in epicardium compared to endocardium. The transient repolarisation is ascribed to voltage dependent inactivation of $Na_v1.5$ channels in combination with activation of transient voltage gated K^+ channels giving rise to an outward current. This current is named I_{to} that is further divided into $I_{to,\ fast}$ or $I_{to,f}$ and $I_{to,\ slow}$ or $I_{to,\ s}$ (Xu et al. 1999). Both are activated at potentials above −30 mV and are characterised by a fast inactivation (Nerbonne and Kass 2005). The pore forming subunit of $I_{to,f}$ is $K_v4.2$ and $K_v4.3$ channels. These proteins are encoded by the genes *KCND2* and *KCND3,* respectively. $K_v4.2$ and $K_v4.3$ channels are expressed in both Purkinje fibers, in atria and in ventricles in many different species excluding guinea pig and rabbit (Fermini et al. 1992; Inoue and Imanaga 1993; Nerbonne and Kass 2005). The K^+ channel underlying $I_{to,s}$ is $K_v1.4$ (*KCNA4)* (Guo et al. 1999). In smaller mammals, heteromeric $K_v4.2/4.3$ subunits will constitute $I_{to,f}$ while in larger species such as canine and human $I_{to,f}$ largely consists of $K_v4.3$ (Kong et al. 1998; Guo et al. 2002). In addition, the accessory subunits KChIP2 and DPP6 are necessary to recapitulate native $I_{to,f}$ (Guo et al. 2002; Radicke et al. 2005). In large mammals the transmural gradient of KChIP2 is likely responsible for the more prominent $I_{to,f}$ in epicardium as compared to the endocardium (Rosati et al. 2001; Soltysinska et al. 2009).

An important electrophysiological difference between atria and ventricles is the presence of the atria-selective ultra-rapid delayed rectifier current, $I_{Kur,}$. I_{Kur} is conducted by $K_v1.5$ channels encoded by the gene *KCNA5*. This potassium current will further add to the transient repolarisation in phase 1 and is one of the reasons why atrial action potentials appear more triangulated in shape relative to ventricular action potentials. Because of its slow and partial inactivation, I_{Kur} plays a role during both phase 1, 2, and 3, and will be described further in section "Phase 3".

Phase 2

The primary difference between cardiac action potentials and their neuronal counterparts is the long lasting phase 2 or plateau phase of the cardiac action potential. The extended phase 2 is primarily a consequence of activation of voltage gated Ca^{2+} channels (Bers 2002). This activation is necessary and sufficient to initiate excitation-contraction coupling in the myocardium. Influx of Ca^{2+} through the voltage gated Ca^{2+} channels in the plasma membrane (or sarcolemma) activates ryanodine receptors located intracellular in the sacroplasmic reticulum. This results in a Ca^{2+} dependent Ca^{2+} release from intracellular stores that serves as a trigger for muscle contraction (Bers 2002). Voltage gated Ca^{2+} channels of two different types are present in mammalian myocardium. The most commonly accepted nomenclature for these channels are T-type and L-type Ca_v channels (Nilius et al 1985; Bean 1985). It has been argued that humans express only L-type channels (Perez-Reyes 2003). This notion is however challenged by the fact that mibefradil is effective against stable angina pectoris. This compound is selective for T-type channels pointing to the fact that functional T-type channels exist in humans at least in vessel related cardiac tissue (Lee et al. 2002). The nomenclature L- and T-types are based upon biophysical properties and names were given before the molecular compositions of these channels were known. The T-type name refers to the fact that channels have a transient current and a tiny single channel conductance (Nilius et al. 1985). In contrast L-types have long lasting currents and large single channel conductance (Nilius et al. 1985). When cloning became obtainable, it was demonstrated that most cardiac L-type channels are encoded by the gene *CACNA1C* that translates into the protein $Ca_V1.2$ or α_{1C} (Soldatov 1994). L-type channels are expressed ubiquitously in the heart including both the SA and AV nodes (Munk et al. 1996; Boyett et al. 2000). It has been suggested that T-type channels could be functionally more important than L-type channels in the nodes (Zhang et al. 2002). Another feature of the T-type channels is their activation at only slightly depolarised potentials (more positive than −50 mV) (Bean 1985; Perez-Reyes 2003). In contrast, activation of L-type channels requires more depolarised membrane potentials (more positive than −30 to −20 mV) (Bean 1985). Activation and inactivation are both fast processes (Carbone and Lux 1987). Inactivation is a slow process lasting up to hundreds of milliseconds, which secure sufficient Ca^{2+} inflow in the systolic interval for proper contraction and encompasses a voltage dependent and a Ca^{2+}/calmodulin dependent component (Marban and O'Rourke 1995; Bers and Perez-Reyes 1999; DeMaria et al. 2001). Termination of phase 2 of the action potential is due to the combined effect of L-type channel inactivation and the simultaneous activation of K^+ channels.

A final electrogenic component worth mentioning in phase 2 is the Na^+/Ca^{2+} exchanger encoded by the *SLC8A1* gene. This co-transporter can in the initial part of the phase 2 contribute to inward Ca^{2+} flux. The stoichiometry of the protein is 3 Na^+ for 1 Ca^{2+}, resulting in a net movement of a positive charge. Under normal circumstances this will result in a reversal potential around −30 mV. As a

consequence the initial phase 0 depolarisation reaching slightly positive membrane potentials will drive the Na^+/Ca^{2+} exchanger in reverse mode resulting in an influx of Ca^{2+}. This Ca^{2+} influx is however a very transient phenomenon giving rise to only a minor part of Ca^{2+} influx during phase 2 in normal hearts (Bers 2002; Armoundas et al. 2003).

Phase 3

Phase 3 of the action potential represents the transition from plateau phase to reestablishment of the diastolic resting membrane potential. As mentioned previously, the phase 3 repolarisation is as a consequence of two concurrent events; the Ca^{2+} and voltage dependent inactivation of voltage gated Ca^{2+} channels and an increased activity of K^+ channels. In humans and other large mammals three different potassium currents are mainly responsible for the repolarisation. These are named I_{Kr}, I_{Ks} and I_{K1} and have diverse but partly overlapping functions. To emphasize this redundancy in the repolarisation process a common denominator for these three currents has therefore been the "repolarisation reserve" (Roden 1998).

The molecular components for the three currents are as follows;

I_{Kr} is conducted via the protein $K_v11.1$ also known as ERG1 or just hERG. This channel is encoded by the gene *KCNH2*. $K_v11.1$ exists in two different variants called $K_v11.1a$ (ERG1a) and $K_v11.1b$ (ERG1b). In general, literature describing $K_v11.1$ channels only refers to the Kv11.1a variant. However, functional I_{Kr} is likely to consist of a mixture of both $K_v11.1a$ and $K_v11.1b$ (London et al. 1997; Larsen et al. 2008). Additionally, it has been argued that the presence of β-subunits might be necessary to recapitulate native I_{Kr}. Two different β-subunits, namely KCNE1 and KCNE2 have been described to interact with $K_v11.1$ (McDonald et al. 1997; Abbott et al. 1999). The proposed $K_v11.1$/KCNE1 interaction has not been confirmed. For the $K_v11.1$/KCNE2 combinations some evidence has emerged even though the interaction is still controversial (Weerapura et al. 2002).

I_{Ks} is conducted via the pore forming α-subunit $K_v7.1$ *(KCNQ1)* in obligate conjunction with the β-subunit KCNE1 (or minK) (Barhanin et al. 1996; Sanguinetti et al. 1996). $K_v7.1$ channels seem to be rather promiscuous in their interaction with β-subunits in the KCNE family that consist of five members (KCNE1-5) (McCrossan and Abbott 2004). All five subunits are found in the heart and have been demonstrated to have a functional interaction with $K_v7.1$. The relative expression of *KCNE* genes in human hearts is *KCNE4*≥*KCNE1*>*KCNE3*>*KCNE2*>*KCNE5* (Bendahhou et al. 2005). It is however likely that the only functional important interaction is the $K_v7.1$/KCNE1, since both KCNE4 and KCNE5 dramatically right-shift the activation curve for the channel complex making them non-functional at physiologically relevant membrane potentials and interaction between $K_v7.1$ and KCNE2 and KCNE3 seem to be most important in non-cardiac tissue

(Angelo et al. 2002; Grunnet et al. 2002, 2005; Bendahhou et al. 2005; Jespersen et al. 2005).

I_{K1} is conducted via $K_{ir}2.X$ proteins. Four members named $K_{ir}2.1$ (IRK1/*KCNJ2*), $K_{ir}2.2$ (IRK2/*KCNJ12*), $K_{ir}2.3$ (IRK3/*KCNJ4*) and $K_{ir}2.4$ (IRK4/*KCNJ14*) have been identified (Kubo et al. 1993; Bond et al. 1994; Takahashi et al. 1994; Bredt et al. 1995; Topert et al. 1998).

The contribution to phase 3 repolarisation and the partly overlapping function of the three repolarisation reserve currents can be elegantly explained by their biophysical properties. I_{Kr} and I_{Ks} are voltage gated currents even though with different capabilities. I_{Kr} is characterised by a fast activation and even faster inactivation approximately 10 times faster than the activation process (Piper et al. 2005). Since an inactivated channel is functionally equivalent to a closed condition, I_{Kr} will contribute only very little to phase 0–2 of the action potential. The opposite is valid in phase 3. The initiation of the repolarising process will release I_{Kr} from inactivation and bring the underlying channel into an open state. The subsequent deactivation of the channel, or transition to the closed state, is a relatively slow process. Consequently, I_{Kr} will be in a conducting state during phase 3 and part of the diastolic phase 4 of the action potential. I_{Ks} is also voltage gated but the biophysical properties is very different from I_{Kr}. Due to the presence of the KCNE1 β-subunit the activation curve for the I_{Ks} is right-shifted to a degree that requires membrane potentials more positive than −20 mV before activation is initiated. Activation is also characterised by very large τ-values being equivalent to slow activation (Jespersen et al. 2005). Finally, inactivation of I_{Ks} is almost absent (Splawski et al. 1997). To recapitulate, these properties sums up to a current that will slowly build in amplitude during phase 2 and finally become an important potassium conductance in phase 3. I_{K1} is fundamentally different from voltage gated I_{Kr} and I_{Ks} since $K_{ir}2.X$ channels only consist of 2 transmembrane regions and thereby is without the normal voltage sensing part of voltage gated ion channels (Heginbotham et al. 1994). $K_{ir}2.X$ channels are however recognised as inward rectifiers. Even though this name implies some kind of voltage dependency this is apparently not the case but rely on the fact that K_{ir} channels are inhibited by intracellular Mg^{2+} and polyamines such as spermine (Vandenberg 1987; Fakler et al. 1995; Guo and Lu 2000; Lopatin and Nichols 2001). A consequence of this is that K^+ flux through $K_{ir}2.X$ channels will be larger in amplitude in the inward direction compared to the outward direction. From a biophysical perspective this is equivalent to a strong rectification (McAllister and Noble 1966). From a physiological perspective only outward current flow is possible through these potassium channels. A consequence of the strong rectification of K_{ir} channels is therefore that conduction will be absent at positive potentials meaning that these channels will not participate in phase 0–2 of the action potential. When phase 3 repolarisation has reached a value of approximately −40 mV the $K_{ir}2.X$ channels will be released from intracellular inhibition and I_{K1} will therefore especially contribute to repolarisation in the late part of phase 3 (Lopatin and Nichols 2001). This also implies that I_{K1}will be important for controlling diastolic or resting membrane potential. This is emphasised by the fact that ventricles with high I_{K1} expression

have a resting membrane potential around −80 mV while the resting membrane potential in nodes lacking I_{K1} is approximately −50 mV (Schram et al. 2002). The relative conductance of the three repolarising reserve currents I_{Kr}, I_{Ks} and I_{K1} during the action potential and their partly overlapping functions are illustrated in Fig. 5.

In addition to the repolarisation reserve currents I_{Kr}, I_{Ks} and I_{K1} other potassium currents can have a significant impact on repolarisation of cardiac action potentials. Some examples that are especially important for the atria are:

The $K_v1.5$ potassium channels encoded by the gene *KCNA5* that underlies the cardiac current I_{Kur} as mentioned under phase 1, (Boyle and Nerbonne 1992).

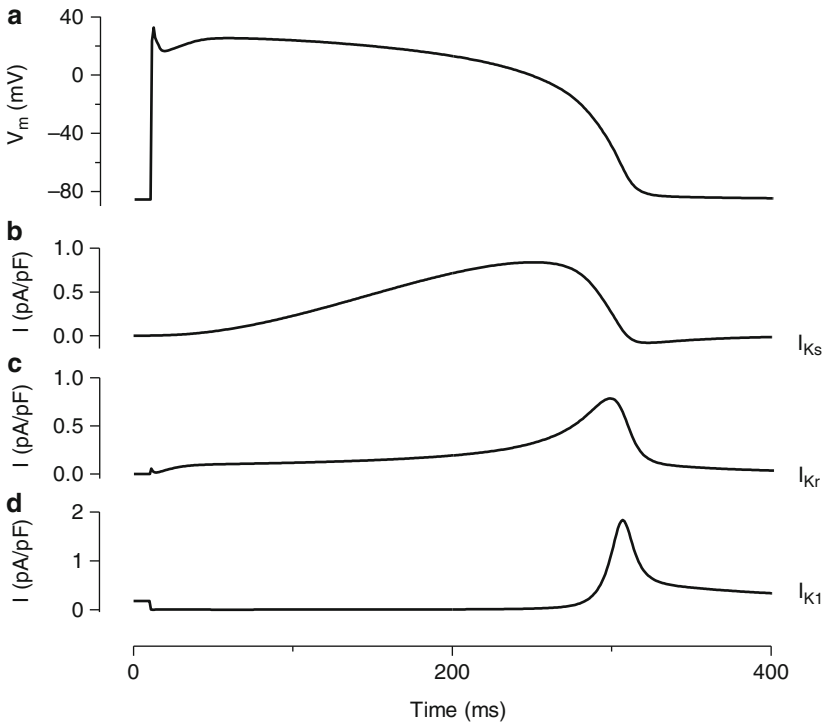

Fig. 5 The repolarisation reserve constituted by combined biophysical properties of I_{Kr}, I_{Ks} and I_{K1}. A typical ventricular action potential is illustrated in **a**. Repolarisation is in a different species, including humans, due to the highly coordinated function of the three currents I_{Kr}, I_{Ks} and I_{K1}. The current development for these currents during the action potential are shown in **b**, **c** and **d**. Due to slow activation of I_{Ks} this current will increase progressively through the plateau phase to a level where it can impact repolarisation. Repolarisation will release I_{Kr} from inactivation and consequently this current will give a profound impact to the continued repolarisation due to slow deactivation kinetics. Finally, when reaching sufficiently repolarised potentials, I_{K1} will come into play and participate in the last part of repolarisation. The cooperation between these channels therefore elegantly demonstrates how distinct biophysical properties can be very well matched to perform a given physiological function. The partly overlapping physiological role of these currents has lead to the "repolarisation reserve" name. The figure is a courtesy from Anders-Peter Larsen

I_{Kur} has a fast activation and only partly inactivates during the entire phase 2 and 3 of the action potential. This channel will therefore participate in repolarisation in both phase 1, 2 and 3. In mice, functional I_{Kur} has been demonstrated in both atria and ventricles. In contrast, in larger mammals, including humans, I_{Kur} is believed to be atria-specific (Nerbonne and Kass 2005). I_{KAch} is another potassium current also generally believed to be atria-specific. The two genes *KCNJ3* and *KCNJ5* encoding $K_{ir}3.1/K_{ir}3.4$ (or GIRK1/GIRK4) proteins is the molecular entity of I_{KAch}. Within the potassium channel family I_{KAch} is unusual as it is directly activated by interaction with the βγ part of G_i-proteins connected to muscarinic 7TM receptors. In contrast to most other G_i proteins these muscarinic acetylcholine receptors have the dual property of both inhibiting adenylyl cyclase and moreover activating ion channels (Brown and Birnbaumer 1990; Hille 1992). $K_{ir}3.1/K_{ir}3.4$ thereby become cornerstones in controlling heart rate. As a consequence of vagal stimulation cardiac muscarinic receptors will be activated. The dissociation of the βγ part of the G-protein will subsequently increase the activity of I_{KAch}. $K_{ir}3.1/K_{ir}3.4$ channels are important in both the SA node and in the atria. In the SA node the increased K^+ conductance will give rise to a slower depolarisation of the pacemaker potential and therefore result in a slowing of the heart rate (Medina et al. 2000; Ravens and Dobrev 2003). $K_{ir}3.1/K_{ir}3.4$ channels are also important for atrial repolarisation and activating these channels will therefore increase the repolarisation capacity and shorten the atrial action potential.

Ca^{2+}-activated K^+ channels have not received much attention in cardiac tissue. The last couple of years have however provided evidence for important cardiac functions for this channel family. There is in addition an emerging support for this channel family being an interesting target for development of new drugs against AF. A separate overview of cardiac Ca^{2+}-activated K^+ channels is given in section "Cardiac Calcium Activated K^+ Channels".

I_{KATP} is another non-voltage gated potassium channel in cardiac tissue. This current is conducted by the pore-forming α-subunit $K_{ir}6.2$ *(KCNJ11)* that is associated with the β-subunit SUR2A *(ABCC9)* (Burke et al. 2008; Flagg et al. 2008). This channel is actually one of the more abundant ones in the heart but will during normal physiological conditions remain quiescent or non-conducting. This is due to the fact that the normal intracellular ATP level is sufficiently high to inhibit the channels. In situations such as hypoxia and ischemia the intracellular ATP level will be diminished and consequently result in an activation of $K_{ir}6.2$ channels (Isomoto and Kurachi 1997; Findlay 2004). $K_{ir}6.2$ channels have an overall membrane topology similar to $K_{ir}2.X$ channels conducting $I_{K1.}$ They do however possess a smaller degree of rectification relative to $K_{ir}2.x$ channels and will therefore, when activated, conduct current during the entire phase 0–3. As a result a marked triangulation of the action potential can be observed.

Finally, it should be mentioned that various 2-pore K^+ channels have been identified in cardiac tissue. These also belong to non-voltage gated channels and are thought to comprise a leak or background current (Backx and Marban 1993; Zhang et al. 2008; Gurney and Manoury 2009).

Phase 4

Phase 4 describes the interval between two successive action potentials and thereby represents the resting membrane potential. In broad terms, this will be equivalent to the diastolic interval. Phase 4 is characterized by very limited net charged movement. This does not imply that all ion channels will be closed. The resting membrane potential is generally in closest proximity to the equilibrium potential for potassium. Though small in amplitude, relatively more K^+ conductance will prevail compared to Na^+ and Ca^{2+} conductance during phase 4. Due to their biophysical properties, 2-pore and K_{ir} potassium channels are active in phase 4. Additional channels with slow deactivation kinetics, that being $K_v11.1$ and $K_v7.1$, can also remain active at least in the initial part of phase 4. This overall persistent K^+ current will counteract possible depolarizing events from DAD's. The impact from this K^+ conductance is however seldom enough to withstand massive depolarising impacts such as a new wave of action potentials. The most efficient way to prolong the effective refractory period is therefore still to prolong the action potential.

Finally, it should be mentioned that the duration and the degree of hyperpolarisation in phase 4 will impact the morphology of the subsequent action potential. This arises from the fact that both Ca^{2+} and Na^+ channels undergo voltage and time dependent release from inactivation. The number of Na^+ and Ca^{2+} channels that can be engaged in a subsequent action potential will therefore increase if more time at more hyperpolarised potentials is spent in phase 4.

Remodeling

Atrial fibrillation is a disease that tends to progress over time. When AF is present, a remodeling of the atria, both structurally and electrically, takes place. Electrical remodeling involves changes in the overall presence of cardiac ion channels in a qualitative and quantitative fashion and structural remodeling can involve changes such as increased amounts of unconductive fibrotic tissue, atrial dilatation, and hypertrophy. Many patients with few episodes of paroxysmal AF eventually progress to persistent atrial fibrillation (Fig. 3). The phenomenon that AF is self-perpetuating, has given rise to the expression "AF begets AF." As a consequence of atrial remodeling the propensity for subsequent incidences of AF will increase as atrial tissue will become more vulnerable to premature beats that can serve as triggers for AF and, once initiated, AF sustainability will be increased (Wijffels et al. 1995; Allessie et al. 2002; Nattel 2002; Dobrev and Ravens 2003). In addition to being a direct consequence of AF, remodelled atria can also be a secondary effect of cardiac diseases not directly related to arrhythmia. Examples of this are acute myocardial infarction and congestive heart failure (Nattel et al. 2007). The following description of remodeling will focus on atrial effects. It should be underlined

that effects on specific proteins can be completely opposite in ventricles but extending this paragraph to also encompass these effects is beyond the scope of the present review.

From an acute perspective the immediate remodeling response to increased atrial contractility is beneficial but the long term perspectives are unfortunately potentially devastating. A very consistent observation after tachypacing or AF is a reduction in L-type Ca^{2+} channels and thereby an acute reduction in the Ca^{2+} influx to the myocytes. This is a logical response to prevent Ca^{2+} overload that can potentially be lethal. This phenomenon has been confirmed in many different species (Yue et al. 1997; Bosch et al. 1999, 2003; Workman et al. 2001; Yagi et al. 2002; Christ et al. 2004). The reduction in inward Ca^{2+} seems to be obtained without involving a remodeling of T-type Ca^{2+} channels (Yue et al. 1997). The apparent benefit of reducing Ca^{2+} overload by a reduction in L-type Ca^{2+} channels is in longer perspective jeopardized by the fact that decreased Ca^{2+} current will reduce action potential duration and reduce the plateau phase, or phase 2, thereby creating a shorter and more triangulated action potential. This has pro-arrhythmic consequences due to a concomitant increased risk of triggers and especially a reduction in atrial ERPs. The propensity for EADs is dually affected by the remodeling. Triangulation will increase the vulnerable window for reactivation of L-type Ca^{2+} channels while the concomitant reduction in the expression of these channels will counteract this tendency. The exact outcome is therefore complex but it should be mentioned that atrial EAD related arrhythmias have indeed been reported (Satoh and Zipes 1998; Burashnikov and Antzelevitch 2003).

Another important contributor to the action potential shortening is the up-regulation of K^+ channels. As described in detail previously, $K_{ir}2.1$ channels are the main component of I_{K1} current and both mRNA and protein levels are increased for this channel as a consequence of AF (Hara et al. 1999; Gaborit et al. 2005; Pandit et al. 2005; Zhang et al. 2005). Such an increase in one of the K^+ channel components of the repolarization reserve will naturally add to the shortening of the action potential duration and a hyperpolarization of the resting membrane potential. The upregulation of I_{K1} seems to be exclusively related to tachypacing or AF since remodeling models based upon congestive heart failure and myocardial infarction both results in a reduced I_{K1} level or no change in the atrial content of I_{K1} (Pinto and Boyden 1998; Li et al. 2000).

A consistent finding in remodelled atria seems to be a down-regulation of I_{to} (Van Wagoner et al. 1997; Workman et al. 2001; Bosch et al. 2003). The functional consequence of this is distorted by the fact that reduced I_{to} has a relatively small but complex impact on action potential duration in the atria. An implication of reduced I_{to} might be indirect increase in peak Na^+ current as a result of less K^+ conductance to balance the upstroke of the action potential (Nattel et al. 2008).

Few and conflicting results are reported for remodeling of $Na_v1.5$ and thereby the cardiac I_{Na}. A reduction has been observed in dogs after sustained tachypacing (Gaspo et al. 1997). Peak I_{Na} density was also found to be significantly reduced by 16% in atrial (right appendage) cardiomyocytes from patients in AF as compared to

sinus rhythm (Sossalla et al. 2010). However, other studies on human atrial tissue did not observe similar effects of AF (Bosch et al. 1999; Gaborit et al. 2005).

Finally, it is worth mentioning that connexins and thereby gap junctions can be affected by atrial remodeling. Effects on the overall expression level demonstrates some inconsistency among different studies with reports of both reduced, enhanced or unchanged connexion levels (Nattel et al. 2007). More important for the propensity to promote AF might actually be the subcellular distribution rather than the total amount of connexin 40 and 43. A result of AF remodeling is a translocation of connexin from intercalated disks to lateral membranes (Polontchouk et al. 2001; Kostin et al. 2002), and such distributional change will increase the heterogeneity of impulse propagation and likely increase the propensity for AF.

Lastly, some remodeling consequences not directly related to ion channels and tachypacing should be briefly mentioned. Conditions such as atrial dilation, inflammation and acute ischemia can also contribute to increased substrate necessary for maintenance of AF (Nattel et al. 2008). Atrial dilation and thereby enlargement of the tissue area will give a situation that can encompass more re-entry circuits and therefore be pro-arrhythmic. This condition can be obtained both by tachypacing and as a consequence of heart failure (Shi et al. 2001). Another important contributor to substrates is the increased amount of fibrotic atrial tissue primarily seen in conjunction with AF associated to heart failure (Li et al. 1999; Shinagawa et al. 2002). For a brief overview of decrease in conduction velocity and shortening and triangulation of atrial action potentials see Fig. 6.

Remodeling of Atria-Selective Currents

Remodeling is also evident for the three potassium currents that have demonstrated some degree of atrial selectivity, namely I_{KACh}, I_{Kur} and I_{KCa}. In AF based remodeling, the effect of I_{KACh} is actually that a reduction is seen in the agonist dependent component of this channel. However, the constitutive, or agonist independent, component of the channel conductance is increased thereby increasing the pro-arrhythmic consequences of I_{KACh} remodeling (Dobrev et al. 2005; Voigt et al. 2008). It should additionally be mentioned that increased parasympathetic tone, or vagal activation, promotes AF also in clinical settings (Yeh et al. 2007). This phenomenon is from a mechanistic perspective explained by the activation of I_{KACh} and consequently shortened atrial effective refractory period that is likely to stabilize atrial re-entrant rotors (Kneller et al. 2002).

Remodeling in AF of I_{Kur} (conducted by $K_v1.5$ channels) is more equivocal. Results are pointing in the direction of no changes or reduction in current density (Van Wagoner et al. 1997; Bosch et al. 1999; Brandt et al. 2000; Workman et al. 2001). Finally, it is worth mentioning that in rare cases of lone AF, where a heritable component has been identified, a few reports have associated loss of function mutations in *KCNA5*, and thereby I_{Kur}, to an increased risk for AF (Olson et al. 2006;

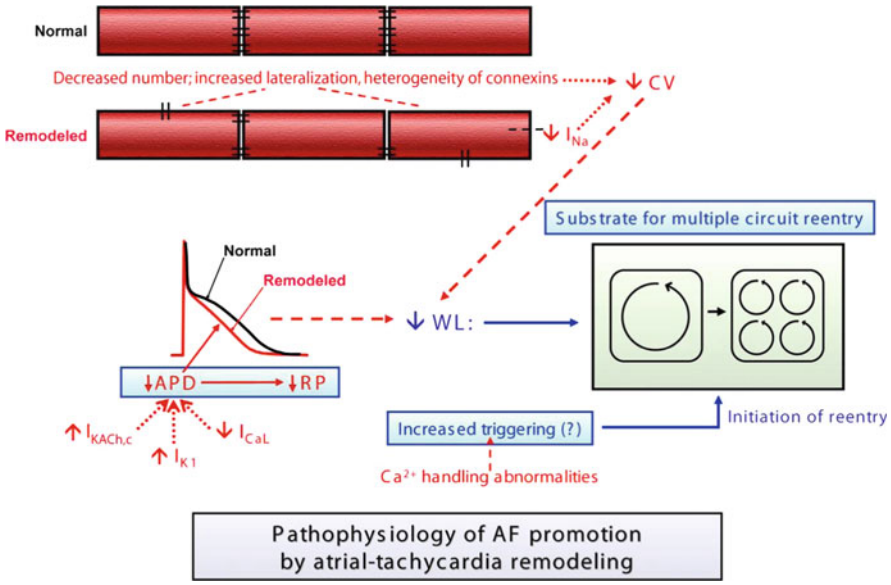

Fig. 6 Remodeling as a consequence of atrial tachycardia. The wavelength is decrease as a consequence of decreased conduction velocity (CV), decreased effective refractory period (ERP) or a combination of both. CV can be reduced as a consequence of diminished gap junction or subcellular re-location of gap junctions resulting in increased lateralisation that will disturb and reduce normal conduction. Action potential shortening and increased triangulation is the consequence in the expression pattern of a number of ion channels as mentioned in the text. From (Nattel et al. 2007)

Yang et al. 2009). An overview of consequences of atrial remodeling is given in Figs. 6 and 7.

Not much is known about remodeling as a consequence of AF of the small conductance Ca^{2+} activated K^+ (SK) channels conducting the I_{KCa}. Increased membrane trafficking of SK2 and progressive shortening of pulmonary vein action potentials due to increased I_{KCa} has been observed as a result of intermittent burst pacing of pulmonary vein cardiomyocyte sleeves (Ozgen et al. 2007). Furthermore, very recently an article published in Chinese reported an upregulation of apamin-sensitive current in cardiomyocytes from patients with persistent AF (Li et al. 2011).

Cardiac Calcium Activated K^+ Channels

Recently, small-conductance Ca^{2+}-activated potassium (SK) channels have emerged as a seemingly atria-selective target (Nattel 2009). Overall, the Ca^{2+}-activated K^+ channel family consist of three subfamilies of channel subunits,

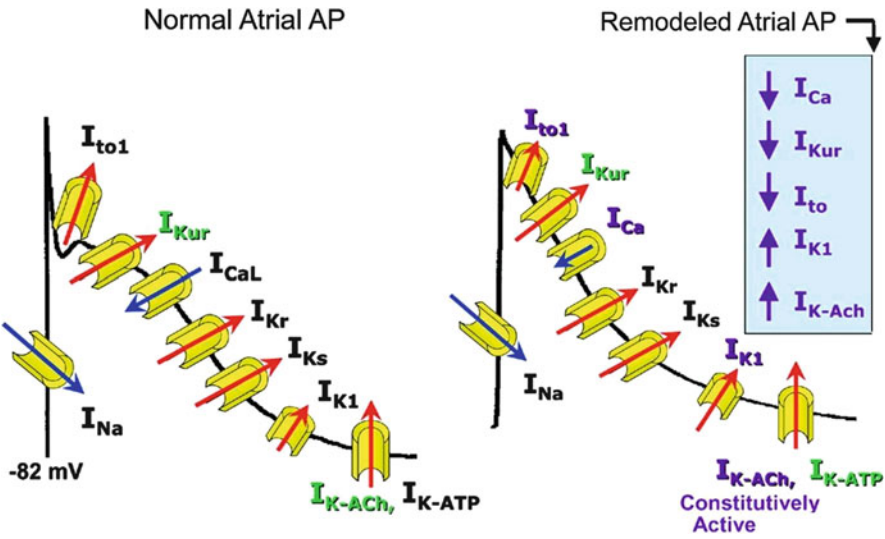

Fig. 7 Important ion channel changes as a consequence of atrial remodeling. Significant changes for the remodelled atria are a down regulation of I_{Ca}, I_{Kur}, and I_{to}. Equally central is upregulation of I_{K1} and constitutively active part of $I_{K\text{-}ACh}$. A consequence of these changes is abbreviation of action potential duration and increased triangulation. From (Antzelevitch and Burashnikov 2009)

traditionally named after their single channel conductance; big (BK/K_{Ca}1.1/*KCNMA1*), intermediate (IK/K_{Ca}3.1/*KCNN4*), and small (SK1, SK2, SK3/K_{Ca}2.1, K_{Ca}2.2, K_{Ca}2.3/*KCNN1, KCNN2, KCNN3*) conductance potassium channels (Grunnet et al. 2009; Berkefeld et al. 2010; Weatherall et al. 2010). Of these, only SK channels have been demonstrated to be functional in surface membranes of cardiomyocytes. These channels have been described in the hearts of mice, rats, guinea pigs, rabbits, dogs and humans (Xu et al. 2003; Tuteja et al. 2005; Ozgen et al. 2007; Li et al. 2009; Nagy et al. 2009; Diness et al. 2010, 2011). An SK channel consists of four α-subunits, each possessing six-transmembrane domains with intracellular N- and C-termini, that associate to form a tetramer (Vergara et al. 1998). Cardiac SK channels have been shown to form both homo- and heteromultimers (Tuteja et al. 2010).

SK channels represent a unique family of K^+ channels because they are gated solely by intracellular Ca^{2+} in a time- and voltage-independent manner and they thereby integrate changes in intracellular Ca^{2+} with changes in K^+ conductance (Weatherall et al. 2010). The Ca^{2+}-sensitivity of SK channels is conferred by the calcium-binding protein calmodulin, which binds constitutively to the calmodulin-binding domain at the C-terminus of the α-subunit. The activation of SK channels is steeply Ca^{2+} dependent with a Hill coefficient of approximately 4–5 and a half-maximal activation at ~300 nM (Xia et al. 1998).

A functional coupling between voltage gated L-type Ca^{2+} channels and SK channels has been described in cardiac tissue via the cytoskeletal linker protein α-actinin2 (Lu et al. 2007).

Historically, a defining feature of native SK channels has been considered to be the block by apamin, even though it has long been known that not all SK channels are apamin-sensitive (Romey et al. 1984; Vergara et al. 1998). Apamin is a highly potent and specific peptide isolated from bee venom and inhibits all three subtypes of SK channels at nM concentrations whereas it is inactive on BK and IK channels as well as Na^+, Ca^{2+}, and Cl^- channels. By many, apamin has been considered a state-of-the-art blocker of SK, and it has been used extensively as a tool to elucidate a number of physiological roles of SK channels in neurons, skeletal muscle, hepatocytes, and T lymphocytes (Bond et al. 1999; Pribnow et al. 1999; Jager et al. 2000; Barfod et al. 2001).

Several toxins isolated from scorpion venom, e.g. scyllatoxin and tamapin, also block the pore of SK channels (Stocker 2004; Wulff et al. 2007). Small molecule compounds such as tubocurarine and UCL1684 (Rosa et al. 1998) mimic the structural elements of the binding residues on these selective SK neurotoxins whereas another class of small molecules, represented by *N*-(pyridin-2-yl)-4-(pyridin-2-yl)thiazol-2-amine, has been suggested to act by blocking the channels through its chelation to a cation (Gentles et al. 2008). All the above compounds displace [^{125}I]-apamin binding and are considered as pore blockers acting at the apamin binding site (for reviews see (Liegeois et al. 2003; Wulff et al. 2007)).

Another class of selective SK channel inhibitors, exemplified by the compound NS8593, that do not block the channel pore, has recently been described (Strobaek et al. 2006; Sorensen et al. 2008). [^{125}I]-Apamin is not displaced by these compounds in binding studies, and they still inhibit SK channels in which point mutations of essential amino acids have disrupted the apamin binding site (Sorensen et al. 2008). NS8593 indiscriminately modulates all SK1-3 subtypes negatively by decreasing the sensitivity towards Ca^{2+} (Strobaek et al. 2006). Although it could therefore be speculated that they interact with the C-terminal region near the calcium-binding protein calmodulin, it has recently been elucidated, by a chimeric approach and subsequent point mutations, that this class of SK channel modulators interact with gating structures deep within the channel pore (Jenkins et al. 2011).

Literature on SK Channels in the Atria

Interestingly, shortly after the separation of bee venom into its chemical components, a technical report from Edgewood Arsenal, Maryland, reported on the effects of apamin in isolated, perfused hearts from mongrel dogs and rhesus monkeys as well as in intact animals (Vick et al. 1972). This was before the pharmacological actions of apamin on any ion channel were known, but nevertheless apamin was found to be clearly antiarrhythmic, increasing the heart rate and the force of contraction with no effects on blood pressure or electrocardiogram (ECG). However, the apamin used in this study was not entirely pure and the findings did

apparently not lead to follow-up studies of this interesting effect of apamin (Gauldie et al. 1976).

The hypothesis that Ca^{2+}-activated K^+ channels are present in the heart is not new. Several reports of supposed I_{KCa} currents in the heart were made in the 1970s (Eisner and Vaughan-Jones 1983). The presence of Ca^{2+}-activated K^+ channels relating intracellular free Ca^{2+} with the opening of K^+ channels would in principle make a lot of sense and explain many of the effects that free cytosolic Ca^{2+} has on transmembrane currents. However, not until 1999, when Wang et al. reported of $K_{Ca}2.3$/SK3 subunits and I_{KCa} currents in myocytes from a cell-line derived from rat ventricles, were there any convincing evidence of the presence of cardiac Ca^{2+} activated K^+ channels (Wang et al. 1999). In 2003, Xu et al. provided evidence for substantial apamin-sensitive current in human and mouse atrial myocytes with a surprisingly low concentration of only 50 pM apamin. In mouse, the amount of apamin-sensitive current was found to be significantly larger in atrial myocytes than in ventricular myocytes which was in line with the finding that the SK2 channel has an atria-selective distribution in human and mouse hearts (Xu et al. 2003). In 2005, Tuteja et al. detected all three SK channel subtypes in mouse hearts, with $K_{Ca}2.1$/SK1 and $K_{Ca}2.2$/SK2 showing an atria-selective distribution (Tuteja et al. 2005).

In 2007, Özgen et al. provided the first – however only circumstantial – evidence for a potential role of I_{KCa} in AF (Ozgen et al. 2007). They observed increased membrane trafficking of $K_{Ca}2.2$/SK2 and progressive shortening of pulmonary vein action potentials due to increased I_{KCa} as a result of intermittent burst pacing of pulmonary vein cardiomyocyte sleeves.

More direct evidence for a role of I_{KCa} in AF was given by Li et al. in early 2009 (Li et al. 2009) where they showed that atrial myocytes isolated from mice lacking $K_{Ca}2.2$/SK2 upon genetic knockout had prolonged atrial APD's, and had inducible EADs under certain conditions. Furthermore, in vivo experiments showed that the $K_{Ca}2.2$/SK2-deficient mice could have AF induced by premature extrastimulation protocols. These findings are counterintuitive, as prolongation of the atrial effective refractory period (aERP) would be expected to be antiarrhythmic. Also, the premature extrastimulation protocol is much more effective in causing re-entry than the EAD arrhythmias postulated by Li, but re-entry should in principle be less likely due to the APD prolongation (Nattel 2009).

Later in 2009, a study was published by Nagy et al. reporting no functional role for SK channels in rat, dog and human ventricular cells under normal physiological conditions (Nagy et al. 2009). The Nagy study did not observe any effects of 100 nM apamin on atrial nor ventricular APDs from rat and dog (and a single human) multicellular preparations as well as from single cardiomyocytes, even though care was taken to allow any SK channels to be activated by high intracellular Ca^{2+} concentrations before applying apamin, thus seriously contradicting the findings by Xu et al. in 2003 (Xu et al. 2003).

The first direct link between clinical AF and SK channels was provided in 2010 when a meta-analysis of genome-wide association studies in 1,335 individuals with lone AF and 12,844 individuals with no AF, conducted by Ellinor et al., concluded

that common variants in the gene encoding $K_{Ca}2.3$/SK3, *KCNN3*, are associated with lone AF (Ellinor et al. 2010).

Shortly after the publication by Ellinor et al., it was demonstrated that I_{KCa} inhibition is antiarrhythmic in models of AF in isolated perfused heart preparations from rat, guinea pig, and rabbit as well as in an in vivo model of AF in rat (Fig. 8) (Diness et al. 2010). These findings were further substantiated in 2011 with two publications documenting that inhibition of SK channels can prolong aERP in vivo in rat, and that this prolongation of aERP correlates to antiarrhythmic activity (Diness et al. 2011; Skibsbye et al. 2011). Furthermore, the effects of I_{KCa} inhibition were examined in aging, spontaneously hypertensive rats, which have earlier been shown to exhibit atrial remodeling and increased susceptibility to atrial tachyarrhythmias (Choisy et al. 2007). SK channel inhibition was as effectively antiarrhythmic in this setting of hypertension-induced atrial remodeling as in younger, normotensive rats (Diness et al. 2011).

In the beginning of 2011, two articles (written in Chinese) regarding atrial SK channels were published (Li et al. 2011; Yu et al. 2011). According to both abstracts, apamin-sensitive current is present in cardiomyocytes from AF patients in sinus rhythm, and one of the abstract reports of an upregulation of apamin-sensitive current in cardiomyocytes from patients with persistent AF (Li et al. 2011).

Discussion of Data on the Effects of Apamin in Atrial SK Channels

The peptide apamin is considered the state-of-the art blocker of SK channels, but nevertheless the evidence for the effects of apamin in cardiac preparations appear to be conflicting. The significant prolongation of APD by 50 pM apamin in murine and human atrial myocytes reported by Xu et al. (Xu et al. 2003) could not be reproduced by Nagy et al. (Nagy et al. 2009) in single- and multicellular preparations from rat and dog cardiomyocytes with a concentration apamin 2,000 times higher than that used by Xu et al. According to two Chinese publications, apamin sensitive current is present, and 100 nM apamin is able to increase APD significantly in human atrial myocytes (Li et al. 2011; Yu et al. 2011). When tested in cardiac myocytes from guinea pig, apamin has been reported to slightly increase APD at 2 Hz pacing rate and to show no significant effect at 1 Hz (Diness et al. 2010).

In models of AF, apamin has also shown non-uniform results (Diness et al. 2010; Skibsbye et al. 2011). When tested in an in vivo rat model of AF, apamin (0.1 mg/kg) did not affect aERP significantly even though a trend towards an increase was seen, and some protection against AF was also demonstrated, although not as pronounced as the effects seen with small-molecule SK channel inhibitors. In two experiments in a model of AF in guinea pig Langendorff hearts, concentrations of apamin as high as 1 μM did not revert sustained AF. Although apamin has some effects in models of AF, these effects seem to be much less pronounced

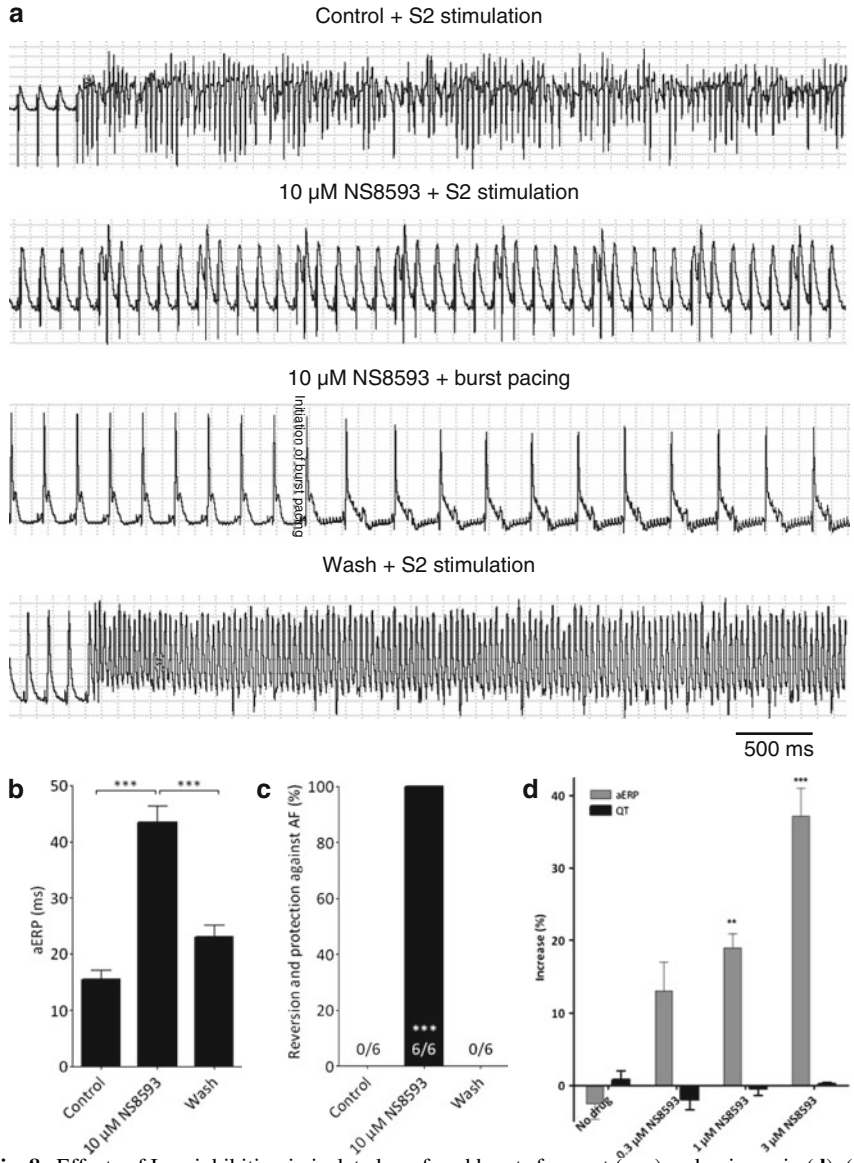

Fig. 8 Effects of I_{KCa} inhibition in isolated, perfused hearts from rat (**a**–**c**) and guinea pig (**d**). (**a**) Representative recordings from isolated, perfused rat heart of ECG and MAPs from left ventricle and left atrium in the presence of no drug, 10 μM NS8593 (representing a negative modulator of SK channels), and after washing combined with S2 stimulation and with 10 μM NS8593 also combined with burst pacing. S2 stimulation elicits sustained AF in the presence of no compound. Perfusion with 10 μM NS8593 terminates AF and protects against the re-induction of AF by S2 stimulation and by burst pacing. After washing, AF can be re-induced by S2 stimulation. (**b**) Application of 10 μM NS8593 prolongs the atrial effective refractory period (aERP) in the rat hearts from 15.5 ± 3.8 ms in the control situation to 43.5 ± 7.0 ms ($p < 0.001$, $n = 6$). After wash-out aERP is shortened to 23.0 ± 5.2 ms, which is not significantly different from the control

than the effects seen with a range of small-molecule inhibitor of SK channels. This apparent lack of effect of apamin could have a number of explanations. At supramaximal concentrations (1 μmol/L), apamin has been found to leave almost half of the SK currents unblocked in Chinese hamster ovary cells stably expressing K_{Ca}2.1–3/SK1–3 (Dale et al. 2002). Several possible explanations to this could in principle be postulated. One hypothesis could be the existence of auxiliary subunits able to prevent apamin binding. SK channels have been reported to heteromeric channel complexes, and it could be speculated that some of these have decreased sensitivity towards apamin (Tuteja et al. 2010). Other possibilities could be that apamin block is modulated by phosphorylation or that apamin might have separate mechanisms for binding and blocking that allow the channel to be in a conducting state even when apamin is bound – as opposed to other blockers of SK channels (Dale et al. 2002; Weatherall et al. 2010). Thus, apamin may constitute its own third class of SK channel inhibitors different from both the negative modulators and the small-molecule pore blockers such as dequalinium or UCL1684. Also, the existence of an apamin- and scyllatoxin-insensitive isoform of the human K_{Ca}2.3/SK3 channel has been reported (Wittekindt et al. 2004). In conclusion, it appears possible that SK channels in the heart have properties that decrease the blocking effects of apamin and, whether or not that is the case, the ambiguous results obtained so far with apamin in cardiac preparations could indicate that apamin is unsuited for addressing SK currents in the heart.

Management of AF

The two principal strategies in the management of AF are rhythm- and rate control. Rate control aims to reduce the ventricular rate while the atria are still fibrillating, whereas the goal of rhythm control is to restore and maintain sinus rhythm. Rate control is accomplished by prolonging the AV nodal refractoriness and slowing the conduction through the AV node using beta blockers, calcium channel blockers, digoxin or amiodarone.

Several large clinical studies have compared the effects of rhythm control to those of rate control and found that rhythm control was not superior to rate control in reducing the occurrence of major endpoints such as stroke or death (AFFIRM, RACE, PIAF, STAF, and HOT CAFÉ trials) (Hohnloser et al. 2000; Van Gelder et al. 2002; Wyse et al. 2002; Carlsson et al. 2003; Opolski et al. 2004). The non-superiority of rhythm control in these studies is counter-intuitive, since rhythm control would be expected to have advantages over rate control by reducing the risk

Fig. 8 (continued) situation. (**c**) S2 stimulation elicits sustained AF in the presence of no compound in all hearts. Perfusion with 10 μM NS8593 terminates AF and protects against the re-induction of AF by S2 stimulation and by burst pacing in all hearts. After washing, AF can be re-induced by S2 stimulation in all hearts. (**d**) NS8593 concentration-dependently increases aERP with no effect on QT interval in concentrations from 0.3 to 3 μmol/L

of stroke, increasing the hemodynamic parameters and alleviating the symptoms of atrial fibrillation.

As a consequence of these studies one could speculate, that this would spell an end to the era of rhythm control in the treatment of atrial fibrillation. However, this has not been the case.

For one thing, the RACE and AFFIRM trials did not address atrial fibrillation in younger, symptomatic patients with little underlying heart disease, and the international guidelines still consider restoration of sinus rhythm by cardioversion with antiarrhythmic drugs or nonpharmacological interventions a useful therapeutic approach in these patients (Fuster et al. 2011).

Secondly, in a later on-treatment analysis of the AFFIRM trial it was determined that the presence of sinus rhythm was an independent predictor of a reduction of the risk of death, consistent with the findings in the DIAMOND study (Pedersen et al. 2001; Corley et al. 2004). However, in the same on-treatment analysis, the use of rhythm control drugs was associated with a significantly increased mortality (hazard ratio = 1.49). One explanation to these seemingly conflicting data could be that the currently available drugs for rhythm control are not very effective in actually obtaining sinus rhythm and that they have poor safety profiles including long term extracardiac toxicity and potentially fatal proarrhythmic effects in the ventricles. E.g. proarrhythmic effects of encainide, flecainide, and moricizine were shown in the Cardiac Arrhythmia Suppression Trial (CAST) (Echt et al. 1991; Epstein et al. 1991). Also, in the SWORD Trial, *d*-sotalol increased mortality when given prophylactically after myocardial infarction (Waldo et al. 1996).

The AFFIRM on-treatment analysis treated the presence of sinus rhythm and treatment with an antiarrhythmic drug as separate variables, and found that the antiarrhythmic drugs only had deleterious effects after adjustment for the presence of sinus rhythm. When the models were not adjusted for sinus rhythm, the antiarrhythmic drugs were no longer associated with adverse outcomes (Corley et al. 2004).

The results of the AFFIRM on-treatment analysis suggest that if an effective method for restoring and maintaining sinus rhythm with fewer adverse effects were available, it might improve survival. Consequently, ongoing drug development has focused on increasing safety by developing atrial-specific agents.

The two main determinants of AF initiation and maintenance are ectopic activity and re-entry formation (Nattel et al. 2008). The aim of rhythm control therapy is therefore to remove the ectopic trigger and to disrupt the re-entry circuits. Currently this can be achieved by non-pharmacological procedures such as ablation therapy and electrical cardioversion, or by pharmacological conversion and maintenance of sinus rhythm. Depending on patient category, the guidelines for management of AF recommend the use of amiodarone, dofetelide, flecainide ibutilide and propafenone for pharmacological conversion of AF. In addition to these drugs, sotalol, beta blockers disopyramide and dronedarone have also been proven effective in maintaining sinus rhythm (Fuster et al. 2011; Wann et al. 2011). The anti-arrhythmic drugs work by suppressing the excitability of the atrial tissue and by prolonging the refractory period.

Reduction of excitability can be achieved by Na^+ channel block, which is the hallmark of Vaughan- Williams class I anti-arrhythmic agents. Flecanide and propafenone are members of this class, but they also inhibit a number of K^+ channels (for review see (Tamargo et al. 2004)). Both drugs have proven effective in converting AF and maintaining sinus rhythm, but they also increase adverse events (Lafuente-Lafuente et al. 2006).

The second strategy for terminating AF is to prolong the refractoriness of the atria. This can be accomplished by potassium channel blockers. With respect to the traditional anti-arrhythmic drugs it is achieved by blocking the repolarising K^+ currents, which results in a prolongation of the cardiac action potential and refractory period. This will increase the wavelength of the re-entrant wave that sustains the AF and thereby cause the wave front to reach refractory atrial tissue, resulting in collapse of the wavelets and ultimately in termination of AF (Comtois et al. 2005). Dofetilide and ibutilide are archetypical class III drugs. The former is a specific I_{Kr} blocker, while the latter also inhibits the late Na^+ current (Carmeliet 1992; Lee 1992). Drugs belonging to class III, including sotalol prolong the action potential duration and ERP of both the atria and ventricles. The ventricular effects are not surprising considering that these drugs were originally developed for treating ventricular arrhythmia. Excessive prolongation of the ventricular APD might produce ventricular EADs which can trigger polymorphic ventricular tachycardia, also known as torsades de pointes (TdP) that can potentially degenerate into ventricular fibrillation (Sanguinetti and Tristani-Firouzi 2006). This was also demonstrated in the "Survival With Oral d-Sotalol" SWORD clinical trial, which was terminated due to increased mortality (Waldo et al. 1996). One problem shared by sotalol and other traditional class III anti-arrhythmic drugs is that their ERP prolonging effect declines when the heart rate increases. This reverse use-dependence is unfavourable as these drugs show least efficacy during tachycardia, and induce maximal ADP prolonging effects during bradycardia or during the consecutive beat following an extrasystole. However, prolongation of the QT-interval is *per se* not pro-arrhythmic. An example of this is the currently most effective drug for sinus rhythm maintenance, amiodarone, which when chronically administered prolongs the QT-interval while displaying no reverse use-dependence and is associated with little probability of inducing TdP (Hondeghem and Snyders 1990; Kaufman et al. 2004).

For now, the multi ion channel blocker amiodarone is the most effective compound for maintenance of sinus rhythm in AF patients. However, its chronic use is associated with non-cardiac toxicity. In comparison, the follow-up and recently approved drug dronedarone, a structurally close analogue of amiodarone, has a better safety profile but is less effective in terminating AF (Piccini et al. 2009).

Ideally, novel drugs for the treatment of AF should be devoid of unwanted ventricular effects and extra cardiac toxicity and display improved efficacy. This might be achieved by targeting ion channels that are predominantly expressed in the atria, or by taking advantage of chamber specific electrophysiological differences. The former is achieved for the $K_V1.5$, $K_{ir}3.1/K_{ir}3.4$ and SK channels, whereas the latter holds for certain drugs targeting the sodium channel and a potential benefit

of atrio-ventricular differences in resting membrane potential, differences in action potential morphology and in the inactivation kinetics between atria and ventricles. The pathological state of AF might also contribute to atrial selectivity. In this way, rapid activation rate during AF, or electrical remodeling, might confer atrial selectivity.

With time, many of the drugs that have been introduced and claimed to be specific modulators of a single ion channel group have in fact turned out to affect a broader range of cardiac ion channels. Despite this, often a single ion channel can be identified which is primarily responsible for the anti-AF effects. In the following we will look into more detail on compounds developed to selectively target the apparently atrial specific currents I_{KACh}, and I_{Kur}.

I_{KACh} Blockers

The acetylcholine activated K^+ channels $K_{ir}3.1/K_{ir}3.4$ are predominantly found in the atria, where they are important for repolarising the atrial cardiac action potential (Ravens and Dobrev 2003). Therefore, $K_{ir}3.1/K_{ir}3.4$ could constitute an important drug target for the treatment of AF as inhibition of the channel would be expected to leave the ventricles unaffected and so holds minimal risk for ventricular proarrhythmia. Furthermore, studies have found that the I_{KACh} density is increased in atrial cells from electrically remodelled canine hearts and that these cells display I_{KACh} activity in the absence of muscarinic stimulation (Cha et al. 2006). Importantly, the fraction of such constitutively active $K_{ir}3.1/K_{ir}3.4$ channels has also been found to be increased in atrial cells isolated from patients with chronic AF (Dobrev et al. 2005). Further evidence for $K_{ir}3.1/K_{ir}3.4$ channel involvement in AF has been obtained from $K_{ir}3.4$ knock-out mice. Under normal condition parasympathetic activation, and thereby $K_{ir}3.1/K_{ir}3.4$ channel activation, will increase the propensity for AF. This was not observed in $K_{ir}3.4$ knock-out mice (Kovoor et al. 2001). Therefore, I_{KACh} is not only a "selective" atrial target, but might also be a pathophysiological target. It should be mentioned that a recent study identified a loss-of-function mutation in *KCNJ5* in a large Chinese family with congenital long QT syndrome, suggesting a role of I_{KACh} in the ventricles (Yang et al. 2010).

Many compounds that display multi channel blocking effects have also been found to inhibit I_{KACh}. These include amiodarone, dronedarone, AVE0118, E-4031, vernakalant, sotalol and flecanid (Mori et al. 1995; Watanabe et al. 1996; Guillemare et al. 2000; Gogelein et al. 2004; Fedida 2007).

NTC-801

Until recently, no compounds had been reported to selectively target the $K_{ir}3.1/K_{ir}3.4$ channel. However, Machida et al. recently demonstrated that the compound NTC-801 selectively inhibits I_{KACh} with a margin of >1,000-fold over other

cardiac ion channels (Machida et al. 2011). Furthermore, this compound shows subtype selectivity having a 34-fold higher potency on heteromeric channels composed of $K_{ir}3.1$ and $K_{ir}3.4$ (IC_{50} of 0.7 nM) compared to $K_{ir}3.1/K_{ir}3.2$. This selectivity is of interest as $K_{ir}3.1/K_{ir}3.2$ channels are primarily found in the CNS. Inhibition of I_{KACh} by NCT-801 reversed the action potential shortening induced by carbachol or adenosine in isolated atrial guinea pig cardiomyocytes. The anti-AF potential of NTC-801 was investigated in three in vivo dog models and found to dose-dependently convert AF induced by either ectopic automaticity (by aconitine) or by vagal nerve stimulation.

Rapid pacing of the canine atrium generates electrical remodeling and has been found to generate constitutively active K_{ACh} channels. In this model NTC-801 was found to reduce the inducibility of AF and to prolong the atrial ERP regardless of pacing frequency. ERP measurements on the ventricles and atria were conducted in the vagal nerve stimulated dogs and here NTC-801 produced a dose dependent prolongation of the atrial ERP but had no effects on the ventricular ERP (Machida et al. 2011). The atria-selective effect together with the findings of no QT prolongation in conscious dogs indicates that NTC-801 is unlikely to induce adverse ventricular effects.

NTC-801 is developed by Nissan Chemical Industries, and in Japan it is currently under Phase II clinical trial with Teijin Pharma Limited. A licensing agreement was announced in 2009 with Bristol-Myers Squibb Company (BMS) for development and marketing outside Japan.

NIP-151 and NIP-142

Another selective I_{KACh} inhibitor, NIP-151, has also been reported by Nissan Chemical Industries. It potently inhibits I_{KACh} with an in vitro IC_{50} of 1.6 nM in HEK293 cells expressing the $K_{ir}3.1/K_{ir}3.4$ channel, and showed dose-dependent effect in terminating AF induced in beagle dogs by either vagal nerve stimulation or by aconitine stimulation (Hashimoto et al. 2008). As expected the compound prolongs the aERP without significant effect on ventricular ERP. NIP-142 is an in vitro less potent inhibitor of human $K_{ir}3.1/K_{ir}3.4$ (IC_{50} 0.64 μM in HEK-293 cells) which in isolated guinea-pig atrial tissue reversed the shortening of the APD action potential duration induced by either carbachol or adenosine. NIP-142 also inhibits other potassium, calcium and sodium channels but the atria-selective antiarrhythmic effects are assigned to a predominant block of I_{Kur} and I_{KACh} currents (Tanaka and Hashimoto 2007). Further data on the in vitro profile of NIP-142 are the recent reports of inhibition of the KCNQ1/KCNE1 channel current (I_{Ks}), with and IC_{50} of 13.2 μM (Namekata et al. 2011) as well as a blockade in Xenopus laevis oocytes of mouse $K_v1.5$, $K_v4.2$ and $K_v4.3$ channel current, with the most prominent effect on $K_v1.5$ (Tanaka et al. 2010). These effects may contribute to the anti-arrythmic effect of NIP-142 and this latter study also reported a prolongation of APD, aERP and contractility in isolated mouse atrial myocardium.

I_{Kur} Blockers

$K_v1.5$ is expressed predominantly in atria (Nerbonne and Kass 2005) and consequently I_{Kur} is almost absent from ventricles (Amos et al. 1996). Blocking I_{Kur} could therefore produce atria-selective effects by prolonging the atrial ERP without affecting QT, and this has resulted in substantial interest in developing selective I_{Kur} blockers for the treatment of AF (Ford and Milnes 2008). However, this concept has also been challenged in a study where the compound 4-aminopyridine showed a prolongation of canine ventricular action potentials in I_{Kur} sensitive (micromolar) concentrations (Sridhar et al. 2007).

Block of I_{Kur} with low concentrations of 4-aminopyridine in atrial trabeculae from patients in sinus rhythm elevates the AP plateau to more positive potentials and shortens the APD (Wettwer et al. 2004). How a block of a repolarising current (I_{Kur}) results in shortened action potential duration is explained by the changes in action potential morphology after inhibition of I_{Kur}. The elevation of the plateau phase allows for more I_{Kr} activation, which accelerates repolarisation. This possible explanation was found using computer simulation and verified by electrophysiological recordings (Wettwer et al. 2004). In AF the action potential triangulates as a result of electrical remodeling. Inhibition of I_{Kur} in cardiomyocytes from chronic AF results in only a slight elevation of the plateau potential, and in contrast to measurement on atrial tissue from patients in sinus rhythm; it causes a prolongation of the action potential duration. The reduced elevation in plateau potential and the increase in I_{K1} in AF will shorten the period where I_{Kr} is activated. This might explain the prolongation in APD observed after I_{Kur} block in tissue from AF patient (Wettwer et al. 2004).

The question however still remains whether a pure I_{Kur} blocker is sufficient for AF suppression. It is noteworthy that chronic AF in humans has been reported to result in reduced $K_v1.5$ expression and I_{Kur} density (Van Wagoner et al. 1997; Christ et al. 2008), and that I_{Kur} density is reduced at high stimulation frequencies, as occur in AF (Feng et al. 1998). Furthermore, a safety concern has appeared as it has been found that loss of function mutation in *KCNA5* (I_{Kur}) is associated with familial AF (Olson et al. 2006; Yang et al. 2009). Several drugs targeting $K_v1.5$ have been discovered.

AVE0118

AVE0118 is a blocker of I_{Kur} (IC_{50} 1.1 μM), but it also inhibits I_{to} and I_{KACh} in similar concentration ranges, and $K_v11.1$ with an IC_{50} of 10 μM. (Gogelein et al. 2004).

In conscious goats and anaesthetised pigs, AVE0118 prolongs the atrial ERP, without affecting the QT-interval. It furthermore reduces the inducibility of AF and converts AF to sinus rhythm (Wirth et al. 2003; Blaauw et al. 2004; de Haan et al. 2006).

Studies on isolated human cardiomyocytes have found that AVE0118 prolongs the APD_{90} and ERP of atrial cardiomyocytes from chronic AF patients. Notably, atrial cardiomycocytes from chronic AF patients demonstrated a large fraction of AVE0118 insensitive I_{Kur} (Christ et al. 2008).

Thromboembolism is one of the major complications of AF. Studies have found that thrombus formation not only occurs during AF but also after conversion to sinus rhythm (Black et al. 1994; Fatkin et al. 1994). To circumvent the mechanical stunning of atria after cardioversion and consequently reduce the risk of thrombus formation, positive inotropic agents have been tested; however they show limited safety and efficacy (DeCara et al. 2000; Date et al. 2002; Sanders et al. 2003). AVE0118 was found to enhance the contractility of atrial muscle strips obtained from patients in both sinus rhythm and AF. The positive inotropic effect was likely due to changes in the shape of the action potential, elevated and prolonged plateau potential, which enhances Ca^{2+} entry primarily via reverse mode Na^{+}/Ca^{2+} exchange (Schotten et al. 2007). In comparison the I_{Kr} blocker dofetilide prolonged the action potential but only produced small effects on the plateau potential. Because the amount of calcium that enters the cells during the late repolarisation is small, dofetilide was found not to have any significant effects on contractility (Schotten et al. 2007). The combination of anti-AF and positive inotropy is an interesting new therapeutic principle for AF management.

AVE0118 has been abandoned for further clinical development.

An analogue of AVE0118, AVE12231, for oral administration has also demonstrated anti-AF properties (Wirth et al. 2007).

DPO-1

DPO-1 is an open channel blocker of I_{Kur} but also affects I_{K1} and I_{Ks}. Expectedly, the potency of the I_{Kur} block increases with pacing frequency. This use-dependency would be beneficial in the setting of AF, where rapid activation rates are encountered (Lagrutta et al. 2006). It furthermore prolongs atrial APD and elevates the atrial action potential plateau level, without affecting ventricular APD measured from isolated human cardiomyocytes. In accordance, a study on African green monkey found that 10 mg/kg DPO-1 elicited significant increases in atrial refractoriness (approximately 15% increase), with no change in ventricular refractory period (Regan et al. 2006).

S9947

S9947 was found to be primarily an open state blocker of both heterologously expressed $K_v1.5$ and native (I_{Kur}) cardiac potassium currents (Bachmann et al. 2001; Strutz-Seebohm et al. 2007). In anaesthetised pig studies, S9947 was found to be atria-selective and it prolonged the atrial ERP with no apparent effect on ventricular repolarisation (Knobloch et al. 2002). The effects of S9947 on

atrial ERP were larger on the left atrium than on the right atrium, and it reduced the vulnerability to arrhythmia induced by premature (S2) stimulation (Knobloch et al. 2002).

KVI-020/WYE-160020

KVI-020 is reported as a selective $K_V1.5$ blocker, with IC_{50} values many fold higher then for other cardiac currents, including $K_v11.1$. It prolonged the atrial ERP, whereas ventricular ERP remained unchanged in beagle dogs. These studies also demonstrated no significant effects on cardiac function after treatment with KVI-020 as compared to vehicle treatment. In a atrial/ventricular tachypacing canine cardiac model, oral administration of KVI-020 was found to decrease the success rate of inducing AF by burst pacing, and it also decreased the total time in AF (AF burden) by 52% (Blass et al. 2009).

XEN-D0101 and XEN-D0103

XEN-D0101 is a compound currently under development (Phase 1) by Xention for the treatment of AF. XEN-D0101 inhibits $K_V1.5$ and human atrial I_{Kur} with an IC_{50} of 241 and 154 nM, respectively (Ford and Milnes 2008). XEN-D0103 is, according to Xention, a more potent and more selective Kv1.5 inhibitor with high selectivity over non-atrial ion channels such as $K_v11.1$, $Na_V1.5$ and the L-type cardiac calcium channel. XEN-D0103 is claimed to cause a significant prolongation of the APD in human atrial tissue with no effect on the APD in ventricular tissue. XEN-D0103 is a follow-up to XEN-D0101 and has recently completed pre-clinical development.

Atria-Selective Sodium Channel Block

Inhibition of atrial sodium channels is able to terminate AF, but sodium channel block in the ventricles can be proarrhythmic, particularly in patients with myocardial infarction (Echt et al. 1991; Fuster et al. 2011). To avoid potential ventricular proarrhythmic effects, atria-selective sodium channel blockers are warranted.

The more depolarised resting membrane potential in atrial as compared to ventricular cardiomyocytes prevents a larger proportion of sodium channels to recover from inactivation during diastole. At least in guinea pig and dog, the potential for half maximum inactivation is more negative in atria versus ventricles (Li et al. 2002; Burashnikov et al. 2007). This means that more negative voltages are required to obtain full availability of sodium channels in the atria compared to ventricles. Taken together, this increases the fraction of inactivated sodium channels and reduces the number of channels in the resting state in the atria as

compared to the ventricles (Comtois et al. 2008; Antzelevitch and Burashnikov 2009). Because recovery from sodium channel block, for most sodium channel blockers, occurs in the resting state of the Na^+ channel, there will be a predominant accumulation of sodium channel block in the atria.

Due to the slower phase III repolarisation in the atrial action potential as compared to the ventricular action potential, rapid activation rates diminish the diastolic interval in the atria but not in the ventricles. Therefore, in the atria, less time will be spent in the resting state of the sodium channel where the drug can dissociate from the channel, and more time is spent in the open/inactivated state where drug binding occurs. Consequently, during AF an atrial specific use-dependent sodium channels block develops (Antzelevitch and Burashnikov 2009).

Not all sodium channel blockers display atrial selectivity. It requires that the dissociation of the drug from the ventricular sodium channel is fast enough to allow complete unbinding of the compound during diastole at the ventricular resting membrane potential and at physiological ventricular rates. Ranolazine is an example of a compound with a relatively fast dissociation constant and it indeed displays atrial selectivity. In contrast, propafenone has slow dissociation kinetics and show limited atrial selectivity (Antzelevitch and Burashnikov 2009). Despite this, lidocaine, which holds rapid dissociation constants, did not show any significant AF suppressing effects in a clinical trial (Marrouche et al. 2000). This argues for that a pure sodium channel block in the absence of concomitant APD prolonging by K^+ channel inhibition might not be sufficient for conversion of AF (Antzelevitch and Burashnikov 2009). However, agents that combine a sodium channel block with inhibition of I_{Kr} have been found to be anti-arrhythmic, including ranolazine, vernakalant, amiodarone, dronedarone, AZD1305 and AZD7009. These agents will be described in separate sections. Whether it is the inhibition of K^+ channels or the block of I_{Na} that is predominantly responsible for the atria-selective prolongation of ERP and anti-AF properties is not clear.

It is important to mention that electrical remodeling of the atria as a consequence of AF or other pathological condition can change the pharmacological response of Na^+ channel blockers. Changes in peak Na^+ current density and $Na_V1.5$ channel expression caused by AF has been studied in both humans and dogs. Peak I_{Na} density was found to be significantly reduced by 16% in atrial (right appendage) cardiomyocytes from patients in AF as compared to sinus rhythm (Sossalla et al. 2010). Another study, using similar cell preparations, found that peak I_{Na} was not significantly reduced (Bosch et al. 1999), but that the voltage-dependent inactivation of I_{Na} was shifted to more positive potentials in cells isolated from AF patients. This would result in fewer channels in the inactivated state and less sodium channel block accumulation. Peak I_{Na} was also found to be decreased in atrially tachypaced dogs (Gaspo et al. 1997; Yagi et al. 2002).

In addition to atria-specific effects of blocking peak sodium currents, inhibition of the late sodium current, $I_{Na,\ late}$, has also attracted attention. Sossalla et al. found that $I_{Na,\ late}$ current density was significantly increased in atrial cardiomyocytes isolated from patients in permanent AF as compared to $I_{Na,\ late}$ measured in cells from patients in sinus rhythm (Sossalla et al. 2010). It was hypothesised that the

increased $I_{Na,\ late}$ causes accumulation of intracellular Na^+ and consequently cytosolic Ca^{2+} overload due to reverse mode Na^+/Ca^{2+} exchanger activity. This causes spontaneous release of calcium from the sarcoplasmic reticulum, which may result in triggered activity and initiation of atrial arrhythmia. Inhibition of the $I_{Na,\ late}$, using ranolozine, demonstrated anti-arrhythmic effects in isolated human atrial trabeculae (Sossalla et al. 2010). However, selective inhibition of $I_{Na,\ late}$, would be expected to further shorten the APD in AF patients and promote re-entry arrhythmia. Application of ranolazine does however not shorten the atrial APD, likely due to its additional class III effects (Antzelevitch et al. 2004).

Ranolazine

Ranolazine is approved for use in chronic angina pectoris. The MERLIN-TIMI 36 trial also demonstrated that ranolazine significantly reduced the occurrence of supraventricular tachycardia (Scirica et al. 2007). This finding has been followed up by several smaller clinical studies where ranoalzine has proven efficacious in terminating newly onset or paroxysmal AF (Kumar et al. 2009; Murdock et al. 2009). However, larger controlled prospective trials are needed to investigate the efficacy and safety of ranolazine in AF. Ranolazine has demonstrated beneficial effects in several experimental models of AF. In isolated perfused dog atria, ranolazine suppresses both vagally and adrenergic induced AF (Burashnikov et al. 2007). In the same preparation, ranolazine demonstrated atrial predominant use-dependent reduction of V_{max} of the action potential upstroke and atrial conduction velocity and an increase in diastolic threshold of excitation. There was also a marked rate dependent prolongation of atrial ERP, which was not observed in the ventricles. This resulted in atrial refractoriness that exceeded the APD (post repolarisation refractoriness) (Burashnikov et al. 2007). Studies using the same experimental setup have found that in concentrations where ranolazine only produces modest effects on sodium channel parameters, ERP and AF suppression, co-administration of amiodarone or dronedarone results in synergistic effects (Burashnikov et al. 2010b; Sicouri et al. 2010). This synergism was suggested to stem from the fact that amiodarone and dronedarone are primarily inactivated-state sodium channel blocker whereas ranolazine is an open-state sodium channel blocker. The combination would therefore inhibit the sodium channel by two independent mechanisms (Burashnikov et al. 2010b; Sicouri et al. 2010). In anaesthetised pigs, it was found that ranolazine prolonged atrial ERP two times more than ventricular ERP. It also increased conduction time and lowered AF inducibility (Kumar et al. 2009). Intrapericardial infusion of ranolazine in anaesthetised pigs also demonstrated atrial predominant effects on ERP and increased fibrillation inducability (Carvas et al. 2010).

Ranolazine is a multi ion channel blocker, and blocks I_{Kr}, I_{Ks}, $I_{Ca,l}$, $I_{Na,\ late}$, $I_{Na,\ peak}$ (Antzelevitch et al. 2004). The atrial predominant reduction in V_{max} and conduction velocity as well as the increased ERP and diastolic threshold for excitation are all due to atrial specific block of peak I_{Na}. This can be explained by atrio-ventricular

differences in factors such as the biophysical properties of the sodium channel, resting membrane potential, morphology of the action potential and faster activation rates in the atria during AF (Li et al. 2002; Burashnikov et al. 2007). The inhibition of peak I_{Na} is both voltage and rate dependent and it is believed to be the primary mechanism behind the antifibrillatory effects of ranolazine (Antzelevitch et al. 2011). In addition, the inhibition of I_{Kr} also plays a role by eliminating the diastolic interval in the atria during AF, which aids in sodium channel block accumulation. The I_{Kr} block could potentially result in ventricular arrhythmia, but this is counteracted by the inhibition of the persistent $I_{Na,\ late}$ (Burashnikov and Antzelevitch 2010).

Whether ranolazine will be capable of terminating and preventing AF in more advanced AF where both electrical and structural remodeling is present needs further experimental and clinical investigation.

Multichannel Blockers

In addition to the atria-selective ion channel blockers, a range of multichannel blocking drugs with class III properties are under development for the treatment of AF, some of which (amiodarone) have been on the market for years whereas others only recently have been approved (dronedarone). In addition to their anti-AF effects these drugs also demonstrate ventricular effects.

Amiodarone

Amiodorane was originally used for treatment of angina pectoris, but today it stands as the most effective anti-arrhythmic drug for AF treatment. However, amiodarone is associated with extracardiac toxic effects such as thyroid dysfunction, hepatic toxicity, pulmonary fibrosis, photosensitivity and neurological disorders, which makes it a second in line drug in many cases. However, in patients with left ventricular hypertrophy, heart failure and ischemic heart disease, amiodarone is associated with low proarrhythmic potential and can be used to prevent AF recurrence (Fuster et al. 2011). Amiodarone both displays acute and chronic effects and has properties of class I, II, III and IV. It inhibits both inward Ca^{2+} and Na^{+} currents and outward K^{+} currents. The sodium channel block is stronger at less negative diastolic potentials and at higher frequencies, which might account for the atrial selectivity of the I_{Na} block. Many of the cardiac potassium currents are inhibited by amiodarone, including I_{Kr}, I_{Ks}, I_{Kach}, I_{to}, I_{Kur} and I_{K1}. In addition, amiodarone has adrenoceptor blocking effects, which is beneficial in obtaining ventricular rate control. Chronic treatment with amiodarone causes electrical remodeling of the heart, and changes in the repolarising potassium current gene expression has been found, likely mediated by triiodothyronine antagonism. This effect on the repolarising current probably explains the APD prolongation observed after chronic treatment (for review see (Kodama et al. 1997)). Despite the observed QT

prolongation, amiodarone treatment is associated with little probability of inducing TdP (Kaufman et al. 2004). This safer profile has been suggested to be a result of the block of $I_{Na,\ late}$ which helps to keep the I_{Kr} inhibition in check and counteracts the proarrhythmic effects of I_{Kr} inhibition (Burashnikov and Antzelevitch 2010). The anti-arrhythmic properties of amiodarone are likely a consequence of reduced excitability and prolonged refractoriness.

K201 (JVT-519)

K201 (JTV-519) was originally discovered as an effective suppressant of sudden cardiac cell death due to Ca^{2+} overload. It has been tested and found to produce beneficial effects in models of heart failure, ischemic heart disease, AF and VF. It is a multichannel blocker and inhibits I_{Na}, I_{Ca}, I_{Kr}, I_{KAch}, I_{K1} (for review see (Kaneko et al. 2009)), consequently it also affects the ventricles causing a prolongation of the QTc-interval. However, it was reported not to induce TdP in the methoxamine sensitised rabbit model of TdP (Hasumi et al. 2007). It also suppresses spontaneous Ca^{2+} release (sparks) from the sarcoplasmic reticulum by inhibiting the sarcoplasmatic reticulum Ca^{2+}-ATPase *(SERCA2a/ATP2A2)* and the ryanodine receptor *(RyR2)* (Loughrey et al. 2007). The reduction of sarcoplasmatic reticulum Ca^{2+} overload could provide anti-arrhythmic effects through reduction of DADs. Most recently, the effect of K201 was assessed in isolated working rabbit heart where it significantly improved mechanical function of the heart during pharmacologically-induced Ca^{2+} overload (Kelly et al. 2011). Sequel Pharmaceuticals is currently developing K201 for the treatment of AF.

Tedisamil

Tedisamil is a multichannel blocker which has been found to block I_{Kur}, I_{to}, I_{KATP}, I_{Kr}, and I_{Ks}. It has demonstrated anti-VF abilities in ischemic animal models and anti-AF properties in canines, with the underlying antifibrillatory mechanism being a prolongation of the action potential. In both animals and humans QT prolongations were observed (for review see (Freestone and Lip 2004)), and in healthy volunteers tedisamil caused a reverse use-dependent QT-interval prolongation (Demolis et al. 1997). A clinical trial performed in patients with symptomatic AF or atrial flutter of 3 to 48 h duration; found that tedisamil was superior to placebo in converting AF or atrial flutter. Significant prolongations of QTc-intervals were observed and in the highest dosing group one episode of TdP and one of a self-terminating monomorphic ventricular tachycardia were observed (Hohnloser et al. 2004).

AZD1305

AstraZeneca, the company behind AZD1305, another multi/combined ion channel blocker, in 2010 decided to discontinue the development of this compound due to an

unfavarouble risk-benefit profile. Intravenous infusion of AZD1305 was found to effectively convert AF to sinus rhythm, but produced a dose-dependent increase in QTc and was associated with induction of TdP in two patients (Ronaszeki et al. 2011). The pharmacological profile of AZD1305 has been investigated, and it blocks $I_{Kr} > I_{Ca,l} > I_{Na}$ and delays repolarisation and increases the refractoriness of both atria and ventricles (Carlsson et al. 2009). This profile is associated with prolongation of the QT-interval but, in contrast to the clinical trials in human, the QT prolongation observed in animals was found to have low pro-arrhythmic potential. The delayed repolarisation was not associated with any changes in pro-arrhythmic markers such as beat to beat variability of repolarisation, instability and it did not induce TdP. In comparison, "pure" I_{Kr} blockers (dofetilide and E4031) were found to induce instability, which resulted in TdP (Carlsson et al. 2009; Andersson et al. 2010). It was suggested that the mechanism behind the lack of increase in pro-arrhythmic signs, despite a delayed repolarisation, was the inhibition of $I_{Na,\ late}$ and I_{Ca}, which antagonizes the effect of AZD1305 on the outward I_{Kr} (Carlsson et al. 2009; Andersson et al. 2010). In dogs, AZD1305 was found to have atrial predominant depressive effects on sodium channel dependent parameters such as diastolic threshold of excitation, V_{max}, and conduction time. AZD1305 also preferentially prolonged the atrial APD. It was found that AZD1305 produced much greater effects on the atrial I_{Na} as compared to ventricular I_{Na} (Burashnikov et al. 2010c). In the atria, during rapid pacing, the APD prolonging effect of AZD1305 diminished the diastolic interval (Burashnikov et al. 2010c). This is a stage where Na^+ channels would normally be released from inactivation, and AZD105 should dissociate from the sodium channel. This, together with the finding of a tonic block, contributed to the inhibition of the sodium channel preferentially in the atria at high heart rates, and allowed for accumulation of the use-dependent sodium channel block (Burashnikov et al. 2010c). AZD1305 was found to prolong post repolarisation refractoriness and to prevent and suppress the induction of AF in an acetylcholine induced canine AF model (Burashnikov et al. 2010c). In the canine pulmonary sleeve preparations AZD1305 was found to suppress DAD triggered activity in (Sicouri et al. 2010). As it was found in animal models, invasive electrophysiological investigations in patients with atrial flutter found that AZD1305 prolonged the ERP of both the atria and right ventricle (Toivonen et al. 2010). Another compound from AstraZeneca (AZD7009), with similar ion channel blocking properties, also demonstrated anti-AF effects in humans, but was discontinued due to induction of flu like symptoms in elderly on repeated oral administration (comment in (Toivonen et al. 2010)).

Derivatives of Existing Drugs

An alternative strategy used in the development of new anti-AF drugs is to take advantage of drugs that have already demonstrated effects in the clinic and modify these to improve efficacy, safety and pharmacokinetic properties.

Dronedarone

Dronedarone (SR33589) is a non-iodinated analogue of amiodarone developed by Sanofi-Aventis. The iodine groups are considered to be responsible for the toxicity of amiodarone (Mason 1987), and so the lack of the iodine group is expected to result in better drug tolerance while maintaining the anti-arrhythmic potential (Sun et al. 1999). Like amiodarone, dronedarone is a multi ion channel blocker and a β1 adrenoceptor antagonist (for review see (Patel et al. 2009)). It blocks the repolarising potassium currents (I_{Kr}, I_{Ks}, I_{K1}, I_{to}) and the depolarising I_{Na}, $I_{Ca,l}$ with higher potency compared to amiodarone. Dronedarone also shows a 100-fold higher potency for blockage of I_{KACh} as compared to amiodarone (Guillemare et al. 2000). There are only a few experimental studies published addressing the atrial effects of dronedarone, and divergent data are found (Manning et al. 1995; Sun et al. 2002; Burashnikov et al. 2010a). Acute superfusion of isolated rabbit atrial tissue with dronedarone abbreviates APD and atrial ERP to a similar extend as for amiodarone. In comparison, four weeks treatment with dronedarone or amiodarone resulted in an increased APD and aERP. However, both durations of treatment slowed the action potential upstroke velocity (Sun et al. 2002). The APD shortening in the acute setting is likely a consequence of the I_{Na} and I_{Ca} block whereas the chronic effects could represent sustained block of the repolarising potassium currents (Sun et al. 2002). In contrast, when comparing the acute effects of amiodarone and dronedarone on coronary-perfused canine atrial preparations, both compounds prolonged the atrial refractoriness, but amiodarone was found to produce significantly greater prolongation of APD_{90} and atrial ERP (Burashnikov et al. 2010a). The acute atrial ERP prolonging effects of dronedarone was also observed in anaesthetised dog experiments (Manning et al. 1995). Results from the isolated perfused canine atrial preparation also demonstrated that the action potential upstroke velocity, diastolic threshold of excitation and conduction velocity were decreased significantly more for amiodarone as compared to dronedarone. When the atrial tissue was exposed to acetylcholine, AF could easily be induced and amiodarone was superior in terminating AF compared to dronedarone. Likewise, pretreatment with amiodarone prevented the induction of AF to a greater extent than dronedarone (Burashnikov et al. 2010a). These differences are explained by a much greater development of post repolarisation refractoriness in the amiodarone treated hearts. The experimental difference in anti-AF efficacy found in this study has also been found in clinical trials comparing the efficacy of the two drugs (Le Heuzey et al. 2010).

A number of clinical studies on the effects of dronedarone have been conducted. In the DAFNE trial, dronedarone reduced ventricular rate and prevented AF relapse after cardioversion in patients with persistent AF, but only in the lowest dose tested (Touboul et al. 2003). Dronedarone treatment resulted in a dose-dependent prolongation of QTc-interval and one case of TdP was reported (Hohnloser et al. 2009). However, dronedarone was not associated with any thyroid, ocular, or pulmonary toxicity. The rhythm control effect was also demonstrated in the

ADONIS and EURIDIS studies where dronedarone postponed the time to first AF recurrence in paroxysmal AF patients (Singh et al. 2007). Furthermore, the ventricular rate was also found to be lowered in these twin trials. This rate control effect was further substantiated in the ERATO study which demonstrated a reduction in sinus rate of ~12 BPM (Davy et al. 2008) in patients with paroxysmal AF. In the ANDROMEDA trial, the effect of dronedarone on mortality was compared to placebo in patients with systolic left ventricular dysfunction. The study was prematurely discontinued due to increased mortality. In the ATHENA study, patients with paroxysmal AF or persistent AF that received dronedarone experienced a significant reduction in mortality and cardiovascular admissions as compared to the placebo group (Hohnloser et al. 2009). A comparative study of amiodarone and dronedarone (DIONYSOS) in patients with persistent AF found that dronedarone was better tolerated but less efficient in decreasing AF recurrence (Le Heuzey et al. 2010). Very recently the FDA issued a safety announcement that the use of dronedarone had been associated with hepatic failure.

Budiodarone (ATI-2042)

A different strategy to circumvent some of the side effects of amiodarone was chosen in the development of budiodarone (ATI-2042). Amiodarone has a long elimination half-life and this likely aggravates the adverse effects observed (Jafari-Fesharaki and Scheinman 1998). An ester modification of amiodarone gave a compound (budiodarone) with reduced plasma half-life (7 h) and distribution volume relative to amiodarone, but with retained pharmacological action on multiple cardiac ion channels and comparable anti-arrhythmic efficacy (data from ARYx Therapeutics, (Juhasz and Bodor 2000; Morey et al. 2001)). The ester modification renders budiodarone available for rapid elimination following ester cleavage by plasma and tissue esterases. This faster metabolism and elimination may reduce tissue accumulation and toxicity, thereby improving the safety profile of the compound. A proof of concept study in six women with paroxysmal AF has demonstrated that budiodarone significantly reduced the AF burden, defined as the time spent in AF divided by the total recording time (Arya et al. 2009). There was in this study a tendency towards an increase in the number AF fibrillation episodes but this was offset by the decreases in episode duration. Aryx Therapeutics reported that a randomised, double-blind, placebo-controlled phase 2b study on 72 patients with paroxysmal AF has substantiated these findings by demonstrating that budiodarone significantly reduced the time patients spend in AF by up to 83%.

Celivarone

Celivarone is a non-iodinated derivate structurally related to amiodarone, which would suggest better tolerability without risk of hypothyroidism and thyrotoxicosis (Han et al. 2009). As is the case for amiodarone, it is a multi channel blocker with

anti-adrenergic properties and therefore calivarone holds class I, II, III, and IV anti-arrhythmic properties (Gautier et al. 2004). In several animal ex vivo and in vivo models it has been found to prolong both the atrial and ventricular ERP and action potential duration. Celivarone also shows anti-arrhythmic effects in both AF and VF models, with the effects being superior or equipotent to amiodarone or dronedarone (Gautier et al. 2005). Celivarone is developed by Sanofi-Aventis and is currently undergoing clinical trials as an anti-arrhythmic agent.

Novel Drugs Approved for the Treatment of AF

Vernakalant

Vernakalant was in 2010 granted marketing approval in the European Union for the rapid conversion of recent onset AF to sinus rhythm by intravenous infusion. The compound was discovered by Cardiome and developed together with Merck and Astellas in Europe and North American, respectively. Acute intravenous infusion of vernakalant resulted in a significantly higher rate of conversion from AF to sinus rhythm in patients with recent onset AF (3 hours-7 days) as compared to placebo. However, the anti-AF effects were not observed in AF patients with longer duration of AF (8–45 days) (Roy et al. 2008; Pratt et al. 2010). In patients with post cardiac surgery AF (lasting 3–72 h) vernakalant resulted in significantly higher conversion rate as compared to placebo (Kowey et al. 2009). In the AVRO trial intravenous treatment with vernakalant resulted in a significantly larger proportion of recent onset (3–48 h) AF patients converting from AF to sinus rhythm within the first 90 min as compared to amiodarone (Camm et al. 2011). In the clinical trials, vernakalant was found to be well tolerated, but it caused hypotension and a transient prolongation of QTc. Enrolment to the phase 3b study of Vernakalant injection in patients with recent onset symptomatic AF (ACT V) was recently suspended following a single serious case of cardiogenic shock in a patient who received the drug (http://clinicaltrials.gov/ct2/show/NCT00989001?term=act+v&rank=1).

The anti-arrhythmic action of vernakalant is attributed to its multi channel blocking effects on both depolarising and repolarising cardiac currents. It inhibits I_{Na} and its potency is dependent on the stimulation rate and resting membrane potential. It is a more potent blocker at fast rates and depolarised resting membrane potentials (at 20 Hz with a resting membrane potential of −80 mV $IC_{50} = 9$ μM; at 1 Hz with a resting membrane potential of −80 mV $IC_{50} = 107$ μM). Vernakalant is an open state/inactivated state sodium channel blocker, and display fast onset of action when the channel is repeatedly activated, as it would be found in the setting of AF. Vernakalant also displays relative fast dissociation constants (Fedida et al. 2005) which are thought to be important for atrial selectivity (Antzelevitch and Burashnikov 2009). The voltage dependence of the sodium channel block contributes to the atrial selectivity, since more negative resting membrane potentials, as it is found in the ventricles, is needed for full availability of the sodium channels and unbinding of the

drug. Hence the more depolarised resting membrane potential found in the atria will potentiate the sodium blocking properties. Vernakalant also inhibits I_{Kur} ($IC_{50} = 13 \pm 1$) and I_{KACh} ($IC_{50} = 10 \pm 1$), and I_{to} ($IC_{50} = 15 \pm 2$) with higher potency as the stimulation frequency increases. The effective free plasma concentration in patients that were converted by vernakalant was ~5 μM (Roy et al. 2004). Vernakalant also inhibits $K_v1.1$ with an IC_{50} value of 21 μM. This potentially pro-arrhythmic effect is counteracted by the block of the persistent Na^+ current by vernakalant, which limits the APD prolongation and risk of EAD developing (Orth et al. 2006). The combined I_{Na} inhibition and the I_K blocking effects would be expected to result in prolonged atrial refractoriness and slowed atrial conduction. Data published in abstracts have demonstrated that vernakalant holds anti-AF effects in vagally stimulated and atrially tachypaced canine AF models and in atrially tachypaced goats. In both dogs and goats, vernakalant increased the atrial ERP without changes in QT. Atrial predominant effects on effective refractory period where also found in non-human primates (for review see (Billman 2010)). Likewise, when vernakalant was infused to produce a steady state plasma concentration similar to what was found in the human clinical trials, only the atrial ERP was significantly prolonged (Bechard et al. 2011). Human electrophysiological studies confirmed the atrial selectivity of the drug by demonstrating slowing of atrial conduction velocity and prolonged atrial refractoriness and no changes in ventricular ERP or QTc (Dorian et al. 2007), although later larger clinical trials demonstrated transient prolongation of QTc after vernakalant infusion.

Currently, vernakalant is investigated as an oral formulation for maintenance of sinus rhythm following conversion of AF. Cardiome reported that data from a phase 2b study demonstrated that that the 500 mg dosing group significantly reduced the rate of AF relapse as compared to placebo. It was recently announced that Merck has confirmed its plans for development of an oral formulation of vernakalant. So far no phase III data are available.

Conclusion

The current strategy for rhythm control in AF includes the use of class I sodium channel blockers. These are however contraindicated in patients with ischemic and structural heart disease, because they potently slow conduction in the ventricles. The other choice is potassium channel blockers, but these predispose to acquired long QT and increase the risk of torsade de pointes arrhythmias, because they potently prolong ventricular repolarization. Currently the multi ion channel blocker amiodarone is the most effective compound for maintenance of sinus rhythm in AF patients. However, its chronic use is associated with extracardiac toxicity. In comparison, dronedarone has a better safety profile but is less effective in terminating AF (Piccini et al. 2009). Preferably, novel drugs should be devoid of unwanted ventricular effects and extracardiac toxicity as well as displaying improved efficacy. Perhaps this will be achieved by targeting ion channels that

are predominantly expressed in the atria, or by taking advantage of chamber specific electrophysiological differences.

Increased knowledge about the relative importance of atrial and ventricular ion channels has guided the mechanistical understanding of normal cardiac sinus rhythm and pathophysiological arrhythmogenic conditions. It is evident that pharmacological treatment of AF should rely on atrial selectivity but the number of possible atria-selective targets is sparse and has until recently been limited to the channels underlying the currents I_{KACh} and I_{Kur}. Among ion channels being either expressed predominantly in the atria, or being from a functional perspective more important in the atria, Ca^{2+}-activated small conductance K^+ channels (SK channels) are the more recently identified. Inhibition of these channels has proven antiarrhythmic in several acute conditions of AF in rodents but the propensity for these channels to be valuable targets for AF treatment in larger species and in more persistent situations of AF still await to be addressed.

Overall, pre-clinical data certainly points in the direction of interesting possibilities for treatment of AF with minimal side effects using an atria-selective approach. From a clinical perspective this notion also seems to be valid at least for acute conversion of paroxysmal AF. Whether an atria-selective target approach can also be valid for conversion of more sustained AF and reduce the long term burden of AF remains to be seen from further clinical studies.

References

Abbott GW, Sesti F, Splawski I, Buck ME, Lehmann MH, Timothy KW, Keating MT, Goldstein SA (1999) MiRP1 forms IKr potassium channels with HERG and is associated with cardiac arrhythmia. Cell 97:175–187

Allessie MA, Bonke FI, Schopman FJ (1973) Circus movement in rabbit atrial muscle as a mechanism of trachycardia. Circ Res 33:54–62

Allessie MA, Bonke FI, Schopman FJ (1975) The mechanism of supraventricular tachycardia induced by a single premature beat in the isolated left atrium of the rabbit. I. Circus movement as a consequence of unidirectional block of the premature impulse. Recent Adv Stud Cardiac Struct Metab 5:303–308

Allessie MA, Bonke FI, Schopman FJ (1976) Circus movement in rabbit atrial muscle as a mechanism of tachycardia. II. The role of nonuniform recovery of excitability in the occurrence of unidirectional block, as studied with multiple microelectrodes. Circ Res 39:168–177

Allessie MA, Bonke FI, Schopman FJ (1977) Circus movement in rabbit atrial muscle as a mechanism of tachycardia. III. The "leading circle" concept: a new model of circus movement in cardiac tissue without the involvement of an anatomical obstacle. Circ Res 41:9–18

Allessie M, Ausma J, Schotten U (2002) Electrical, contractile and structural remodeling during atrial fibrillation. Cardiovasc Res 54:230–246

Amos GJ, Wettwer E, Metzger F, Li Q, Himmel HM, Ravens U (1996) Differences between outward currents of human atrial and subepicardial ventricular myocytes. J Physiol 491(Pt 1): 31–50

Andersson B, Abi-Gerges N, Carlsson L (2010) The combined ion channel blocker AZD1305 attenuates late Na current and IKr-induced action potential prolongation and repolarization instability. Europace 12:1003–1010

Angelo K, Jespersen T, Grunnet M, Nielsen MS, Klaerke DA, Olesen SP (2002) KCNE5 induces time- and voltage-dependent modulation of the KCNQ1 current. Biophys J 83:1997–2006

Antzelevitch C, Burashnikov A (2009) Atrial-selective sodium channel block as a novel strategy for the management of atrial fibrillation. J Electrocardiol 42:543–548

Antzelevitch C, Belardinelli L, Zygmunt AC, Burashnikov A, Di Diego JM, Fish JM, Cordeiro JM, Thomas G (2004) Electrophysiological effects of ranolazine, a novel antianginal agent with antiarrhythmic properties. Circulation 110:904–910

Antzelevitch C, Pollevick GD, Cordeiro JM, Casis O, Sanguinetti MC, Aizawa Y, Guerchicoff A, Pfeiffer R, Oliva A, Wollnik B, Gelber P, Bonaros EP Jr, Burashnikov E, Wu Y, Sargent JD, Schickel S, Oberheiden R, Bhatia A, Hsu LF, Haissaguerre M, Schimpf R, Borggrefe M, Wolpert C (2007) Loss-of-function mutations in the cardiac calcium channel underlie a new clinical entity characterized by ST-segment elevation, short QT intervals, and sudden cardiac death. Circulation 115:442–449

Antzelevitch C, Burashnikov A, Sicouri S, Belardinelli L (2011) Electrophysiologic basis for the antiarrhythmic actions of ranolazine. Heart Rhythm 8:1281–1290

Armoundas AA, Hobai IA, Tomaselli GF, Winslow RL, O'Rourke B (2003) Role of sodium-calcium exchanger in modulating the action potential of ventricular myocytes from normal and failing hearts. Circ Res 93:46–53

Arya A, Silberbauer J, Teichman SL, Milner P, Sulke N, Camm AJ (2009) A preliminary assessment of the effects of ATI-2042 in subjects with paroxysmal atrial fibrillation using implanted pacemaker methodology. Europace 11:458–464

Attwell D, Cohen I, Eisner D, Ohba M, Ojeda C (1979) The steady state TTX-sensitive ("window") sodium current in cardiac Purkinje fibres. Pflugers Arch 379:137–142

Bachmann A, Gutcher I, Kopp K, Brendel J, Bosch RF, Busch AE, Gogelein H (2001) Characterization of a novel Kv1.5 channel blocker in Xenopus oocytes, CHO cells, human and rat cardiomyocytes. Naunyn Schmiedebergs Arch Pharmacol 364:472–478

Backx PH, Marban E (1993) Background potassium current active during the plateau of the action potential in guinea pig ventricular myocytes. Circ Res 72:890–900

Barfod ET, Moore AL, Lidofsky SD (2001) Cloning and functional expression of a liver isoform of the small conductance Ca2+-activated K+ channel SK3. Am J Physiol Cell Physiol 280:C836–C842

Barhanin J, Lesage F, Guillemare E, Fink M, Lazdunski M, Romey G (1996) K(V)LQT1 and lsK (minK) proteins associate to form the I(Ks) cardiac potassium current. Nature 384:78–80

Bean BP (1985) Two kinds of calcium channels in canine atrial cells. Differences in kinetics, selectivity, and pharmacology. J Gen Physiol 86:1–30

Bechard J, Gibson JK, Killingsworth CR, Wheeler JJ, Schneidkraut MJ, Huang J, Ideker RE, McAfee DA (2011) Vernakalant selectively prolongs atrial refractoriness with no effect on ventricular refractoriness or defibrillation threshold in pigs. J Cardiovasc Pharmacol 57:302–307

Bendahhou S, Marionneau C, Haurogne K, Larroque MM, Derand R, Szuts V, Escande D, Demolombe S, Barhanin J (2005) In vitro molecular interactions and distribution of KCNE family with KCNQ1 in the human heart. Cardiovasc Res 67:529–538

Bennett PB, Yazawa K, Makita N, George AL Jr (1995) Molecular mechanism for an inherited cardiac arrhythmia. Nature 376:683–685

Berkefeld H, Fakler B, Schulte U (2010) Ca2+-activated K+ channels: from protein complexes to function. Physiol Rev 90:1437–1459

Bers DM (2002) Cardiac excitation-contraction coupling. Nature 415:198–205

Bers DM, Perez-Reyes E (1999) Ca channels in cardiac myocytes: structure and function in Ca influx and intracellular Ca release. Cardiovasc Res 42:339–360

Billman GE (2010) Vernakalant, a mixed sodium and potassium ion channel antagonist that blocks K(v)1.5 channels, for the potential treatment of atrial fibrillation. Curr Opin Investig Drugs 11: 1048–1058

Blaauw Y, Gogelein H, Tieleman RG, van Hunnik A, Schotten U, Allessie MA (2004) "Early" class III drugs for the treatment of atrial fibrillation: efficacy and atrial selectivity of AVE0118 in remodeled atria of the goat. Circulation 110:1717–1724

Black IW, Fatkin D, Sagar KB, Khandheria BK, Leung DY, Galloway JM, Feneley MP, Walsh WF, Grimm RA, Stollberger C et al (1994) Exclusion of atrial thrombus by transesophageal echocardiography does not preclude embolism after cardioversion of atrial fibrillation. A multicenter study. Circulation 89:2509–2513

Blass BE, Fensome A, Trybulski E, Magolda R, Gardell SJ, Liu K, Samuel M, Feingold I, Huselton C, Jackson CM, Djandjighian L, Ho D, Hennan J, Janusz JM (2009) Selective Kv1.5 blockers: development of (R)-1-(methylsulfonylamino)-3-[2-(4-methoxyphenyl) ethyl]-4-(4-methoxypheny l)-2-imidazolidinone (KVI-020/WYE-160020) as a potential treatment for atrial arrhythmia. J Med Chem 52:6531–6534

Bond CT, Pessia M, Xia XM, Lagrutta A, Kavanaugh MP, Adelman JP (1994) Cloning and expression of a family of inward rectifier potassium channels. Receptors Channels 2:183–191

Bond CT, Maylie J, Adelman JP (1999) Small-conductance calcium-activated potassium channels. Ann N Y Acad Sci 868:370–378

Bosch RF, Zeng X, Grammer JB, Popovic K, Mewis C, Kuhlkamp V (1999) Ionic mechanisms of electrical remodeling in human atrial fibrillation. Cardiovasc Res 44:121–131

Bosch RF, Scherer CR, Rub N, Wohrl S, Steinmeyer K, Haase H, Busch AE, Seipel L, Kuhlkamp V (2003) Molecular mechanisms of early electrical remodeling: transcriptional downregulation of ion channel subunits reduces I(Ca, L) and I(to) in rapid atrial pacing in rabbits. J Am Coll Cardiol 41:858–869

Boyett MR, Honjo H, Kodama I (2000) The sinoatrial node, a heterogeneous pacemaker structure. Cardiovasc Res 47:658–687

Boyle WA, Nerbonne JM (1992) Two functionally distinct 4-aminopyridine-sensitive outward K+ currents in rat atrial myocytes. J Gen Physiol 100:1041–1067

Brandt MC, Priebe L, Bohle T, Sudkamp M, Beuckelmann DJ (2000) The ultrarapid and the transient outward K(+) current in human atrial fibrillation. Their possible role in postoperative atrial fibrillation. J Mol Cell Cardiol 32:1885–1896

Bredt DS, Wang TL, Cohen NA, Guggino WB, Snyder SH (1995) Cloning and expression of two brain-specific inwardly rectifying potassium channels. Proc Natl Acad Sci U S A 92: 6753–6757

Brown AM, Birnbaumer L (1990) Ionic channels and their regulation by G protein subunits. Annu Rev Physiol 52:197–213

Burashnikov A, Antzelevitch C (2003) Reinduction of atrial fibrillation immediately after termination of the arrhythmia is mediated by late phase 3 early afterdepolarization-induced triggered activity. Circulation 107:2355–2360

Burashnikov A, Antzelevitch C (2010) New developments in atrial antiarrhythmic drug therapy. Nat Rev Cardiol 7:139–148

Burashnikov A, Di Diego JM, Zygmunt AC, Belardinelli L, Antzelevitch C (2007) Atrium-selective sodium channel block as a strategy for suppression of atrial fibrillation: differences in sodium channel inactivation between atria and ventricles and the role of ranolazine. Circulation 116:1449–1457

Burashnikov A, Belardinelli L, Antzelevitch C (2010a) Acute dronedarone is inferior to amiodarone in terminating and preventing atrial fibrillation in canine atria. Heart Rhythm 7: 1273–1279

Burashnikov A, Sicouri S, Di Diego JM, Belardinelli L, Antzelevitch C (2010b) Synergistic effect of the combination of ranolazine and dronedarone to suppress atrial fibrillation. J Am Coll Cardiol 56:1216–1224

Burashnikov A, Zygmunt AC, Di Diego JM, Linhardt G, Carlsson L, Antzelevitch C (2010c) AZD1305 exerts atrial predominant electrophysiological actions and is effective in suppressing atrial fibrillation and preventing its reinduction in the dog. J Cardiovasc Pharmacol 56: 80–90

Burke MA, Mutharasan RK, Ardehali H (2008) The sulfonylurea receptor, an atypical ATP-binding cassette protein, and its regulation of the KATP channel. Circ Res 102:164–176

Camm AJ, Capucci A, Hohnloser SH, Torp-Pedersen C, Van Gelder IC, Mangal B, Beatch G (2011) A randomized active-controlled study comparing the efficacy and safety of vernakalant to amiodarone in recent-onset atrial fibrillation. J Am Coll Cardiol 57:313–321

Carbone E, Lux HD (1987) Kinetics and selectivity of a low-voltage-activated calcium current in chick and rat sensory neurones. J Physiol 386:547–570

Carlsson J, Miketic S, Windeler J, Cuneo A, Haun S, Micus S, Walter S, Tebbe U (2003) Randomized trial of rate-control versus rhythm-control in persistent atrial fibrillation: the Strategies of Treatment of Atrial Fibrillation (STAF) study. J Am Coll Cardiol 41:1690–1696

Carlsson L, Andersson B, Linhardt G, Lofberg L (2009) Assessment of the ion channel-blocking profile of the novel combined ion channel blocker AZD1305 and its proarrhythmic potential versus dofetilide in the methoxamine-sensitized rabbit in vivo. J Cardiovasc Pharmacol 54: 82–89

Carmeliet E (1992) Voltage- and time-dependent block of the delayed K+ current in cardiac myocytes by dofetilide. J Pharmacol Exp Ther 262:809–817

Carvas M, Nascimento BC, Acar M, Nearing BD, Belardinelli L, Verrier RL (2010) Intrapericardial ranolazine prolongs atrial refractory period and markedly reduces atrial fibrillation inducibility in the intact porcine heart. J Cardiovasc Pharmacol 55:286–291

Cha TJ, Ehrlich JR, Chartier D, Qi XY, Xiao L, Nattel S (2006) Kir3-based inward rectifier potassium current: potential role in atrial tachycardia remodeling effects on atrial repolarization and arrhythmias. Circulation 113:1730–1737

Choisy SC, Arberry LA, Hancox JC, James AF (2007) Increased susceptibility to atrial tachyarrhythmia in spontaneously hypertensive rat hearts. Hypertension 49:498–505

Christ T, Boknik P, Wohrl S, Wettwer E, Graf EM, Bosch RF, Knaut M, Schmitz W, Ravens U, Dobrev D (2004) L-type Ca2+ current downregulation in chronic human atrial fibrillation is associated with increased activity of protein phosphatases. Circulation 110:2651–2657

Christ T, Wettwer E, Voigt N, Hala O, Radicke S, Matschke K, Varro A, Dobrev D, Ravens U (2008) Pathology-specific effects of the IKur/Ito/IK, ACh blocker AVE0118 on ion channels in human chronic atrial fibrillation. Br J Pharmacol 154:1619–1630

Comtois P, Kneller J, Nattel S (2005) Of circles and spirals: bridging the gap between the leading circle and spiral wave concepts of cardiac reentry. Europace 7(Suppl 2):10–20

Comtois P, Sakabe M, Vigmond EJ, Munoz M, Texier A, Shiroshita-Takeshita A, Nattel S (2008) Mechanisms of atrial fibrillation termination by rapidly unbinding Na+ channel blockers: insights from mathematical models and experimental correlates. Am J Physiol Heart Circ Physiol 295:H1489–H1504

Conrath CE, Opthof T (2006) Ventricular repolarization: an overview of (patho)physiology, sympathetic effects and genetic aspects. Prog Biophys Mol Biol 92:269–307

Corley SD, Epstein AE, DiMarco JP, Domanski MJ, Geller N, Greene HL, Josephson RA, Kellen JC, Klein RC, Krahn AD, Mickel M, Mitchell LB, Nelson JD, Rosenberg Y, Schron E, Shemanski L, Waldo AL, Wyse DG (2004) Relationships between sinus rhythm, treatment, and survival in the Atrial Fibrillation Follow-Up Investigation of Rhythm Management (AFFIRM) Study. Circulation 109:1509–1513

Dale TJ, Cryan JE, Chen MX, Trezise DJ (2002) Partial apamin sensitivity of human small conductance Ca2+-activated K+ channels stably expressed in Chinese hamster ovary cells. Naunyn Schmiedebergs Arch Pharmacol 366:470–477

Date T, Takahashi A, Iesaka Y, Miyazaki H, Yamane T, Noma K, Nuruiki N, Ishikawa S, Kanae K, Mochizuki S (2002) Effect of low-dose isoproterenol infusion on left atrial appendage function soon after cardioversion of chronic atrial tachyarrhythmias. Int J Cardiol 84:59–67

Davidenko JM, Pertsov AV, Salomonsz R, Baxter W, Jalife J (1992) Stationary and drifting spiral waves of excitation in isolated cardiac muscle. Nature 355:349–351

Davy JM, Herold M, Hoglund C, Timmermans A, Alings A, Radzik D, Van Kempen L (2008) Dronedarone for the control of ventricular rate in permanent atrial fibrillation: the Efficacy and safety of dRonedArone for the cOntrol of ventricular rate during atrial fibrillation (ERATO) study. Am Heart J 156(527):e521–e529

de Haan S, Greiser M, Harks E, Blaauw Y, van Hunnik A, Verheule S, Allessie M, Schotten U (2006) AVE0118, blocker of the transient outward current (I(to)) and ultrarapid delayed rectifier current (I(Kur)), fully restores atrial contractility after cardioversion of atrial fibrillation in the goat. Circulation 114:1234–1242

DeCara JM, Pollak A, Dubrey S, Falk RH (2000) Positive atrial inotropic effect of dofetilide after cardioversion of atrial fibrillation or flutter. Am J Cardiol 86(685–688):A688

DeMaria CD, Soong TW, Alseikhan BA, Alvania RS, Yue DT (2001) Calmodulin bifurcates the local Ca2+ signal that modulates P/Q-type Ca2+ channels. Nature 411:484–489

Demolis JL, Martel C, Funck-Brentano C, Sachse A, Weimann HJ, Jaillon P (1997) Effects of tedisamil, atenolol and their combination on heart and rate-dependent QT interval in healthy volunteers. Br J Clin Pharmacol 44:403–409

Dhar Malhotra J, Chen C, Rivolta I, Abriel H, Malhotra R, Mattei LN, Brosius FC, Kass RS, Isom LL (2001) Characterization of sodium channel alpha- and beta-subunits in rat and mouse cardiac myocytes. Circulation 103:1303–1310

Diness JG, Sorensen US, Nissen JD, Al-Shahib B, Jespersen T, Grunnet M, Hansen RS (2010) Inhibition of small-conductance Ca2+-activated K+ channels terminates and protects against atrial fibrillation. Circ Arrhythm Electrophysiol 3:380–390

Diness JG, Skibsbye L, Jespersen T, Bartels ED, Sorensen US, Hansen RS, Grunnet M (2011) Effects on atrial fibrillation in aged hypertensive rats by Ca(2+)-activated K(+) channel inhibition. Hypertension 57:1129–1135

Dobrev D, Ravens U (2003) Remodeling of cardiomyocyte ion channels in human atrial fibrillation. Basic Res Cardiol 98:137–148

Dobrev D, Friedrich A, Voigt N, Jost N, Wettwer E, Christ T, Knaut M, Ravens U (2005) The G protein-gated potassium current I(K, ACh) is constitutively active in patients with chronic atrial fibrillation. Circulation 112:3697–3706

Dorian P, Pinter A, Mangat I, Korley V, Cvitkovic SS, Beatch GN (2007) The effect of vernakalant (RSD1235), an investigational antiarrhythmic agent, on atrial electrophysiology in humans. J Cardiovasc Pharmacol 50:35–40

Echt DS, Liebson PR, Mitchell LB, Peters RW, Obias-Manno D, Barker AH, Arensberg D, Baker A, Friedman L, Greene HL et al (1991) Mortality and morbidity in patients receiving encainide, flecainide, or placebo. The Cardiac Arrhythmia Suppression Trial. N Engl J Med 324:781–788

Eisner DA, Vaughan-Jones RD (1983) Do calcium-activated potassium channels exist in the heart? Cell Calcium 4:371–386

Ellinor PT, Lunetta KL, Glazer NL, Pfeufer A, Alonso A, Chung MK, Sinner MF, de Bakker PI, Mueller M, Lubitz SA, Fox E, Darbar D, Smith NL, Smith JD, Schnabel RB, Soliman EZ, Rice KM, Van Wagoner DR, Beckmann BM, van Noord C, Wang K, Ehret GB, Rotter JI, Hazen SL, Steinbeck G, Smith AV, Launer LJ, Harris TB, Makino S, Nelis M, Milan DJ, Perz S, Esko T, Kottgen A, Moebus S, Newton-Cheh C, Li M, Mohlenkamp S, Wang TJ, Kao WH, Vasan RS, Nothen MM, MacRae CA, Stricker BH, Hofman A, Uitterlinden AG, Levy D, Boerwinkle E, Metspalu A, Topol EJ, Chakravarti A, Gudnason V, Psaty BM, Roden DM, Meitinger T, Wichmann HE, Witteman JC, Barnard J, Arking DE, Benjamin EJ, Heckbert SR, Kaab S (2010) Common variants in KCNN3 are associated with lone atrial fibrillation. Nat Genet 42:240–244

Epstein AE, Bigger JT Jr, Wyse DG, Romhilt DW, Reynolds-Haertle RA, Hallstrom AP (1991) Events in the Cardiac Arrhythmia Suppression Trial (CAST): mortality in the entire population enrolled. J Am Coll Cardiol 18:14–19

Fakler B, Brandle U, Glowatzki E, Weidemann S, Zenner HP, Ruppersberg JP (1995) Strong voltage-dependent inward rectification of inward rectifier K+ channels is caused by intracellular spermine. Cell 80:149–154

Fatkin D, Kelly RP, Feneley MP (1994) Relations between left atrial appendage blood flow velocity, spontaneous echocardiographic contrast and thromboembolic risk in vivo. J Am Coll Cardiol 23:961–969

Fedida D (2007) Vernakalant (RSD1235): a novel, atrial-selective antifibrillatory agent. Expert Opin Investig Drugs 16:519–532

Fedida D, Orth PM, Chen JY, Lin S, Plouvier B, Jung G, Ezrin AM, Beatch GN (2005) The mechanism of atrial antiarrhythmic action of RSD1235. J Cardiovasc Electrophysiol 16: 1227–1238

Feng J, Xu D, Wang Z, Nattel S (1998) Ultrarapid delayed rectifier current inactivation in human atrial myocytes: properties and consequences. Am J Physiol 275:H1717–H1725

Fermini B, Wang Z, Duan D, Nattel S (1992) Differences in rate dependence of transient outward current in rabbit and human atrium. Am J Physiol 263:H1747–H1754

Findlay I (2004) Physiological modulation of inactivation in L-type Ca2+ channels: one switch. J Physiol 554:275–283

Flagg TP, Kurata HT, Masia R, Caputa G, Magnuson MA, Lefer DJ, Coetzee WA, Nichols CG (2008) Differential structure of atrial and ventricular KATP: atrial KATP channels require SUR1. Circ Res 103:1458–1465

Ford JW, Milnes JT (2008) New drugs targeting the cardiac ultra-rapid delayed-rectifier current (I Kur): rationale, pharmacology and evidence for potential therapeutic value. J Cardiovasc Pharmacol 52:105–120

Fozzard HA, Hanck DA (1996) Structure and function of voltage-dependent sodium channels: comparison of brain II and cardiac isoforms. Physiol Rev 76:887–926

Freestone B, Lip GY (2004) Tedisamil: a new novel antiarrhythmic. Expert Opin Investig Drugs 13:151–160

Fuster V, Ryden LE, Cannom DS, Crijns HJ, Curtis AB, Ellenbogen KA, Halperin JL, Kay GN, Le Huezey JY, Lowe JE, Olsson SB, Prystowsky EN, Tamargo JL, Wann LS (2011) 2011 ACCF/AHA/HRS focused updates incorporated into the ACC/AHA/ESC 2006 Guidelines for the management of patients with atrial fibrillation: a report of the American College of Cardiology Foundation/American Heart Association Task Force on Practice Guidelines developed in partnership with the European Society of Cardiology and in collaboration with the European Heart Rhythm Association and the Heart Rhythm Society. J Am Coll Cardiol 57:e101–e198

Fye WB (2006) Tracing atrial fibrillation–100 years. N Engl J Med 355:1412–1414

Gaborit N, Steenman M, Lamirault G, Le Meur N, Le Bouter S, Lande G, Leger J, Charpentier F, Christ T, Dobrev D, Escande D, Nattel S, Demolombe S (2005) Human atrial ion channel and transporter subunit gene-expression remodeling associated with valvular heart disease and atrial fibrillation. Circulation 112:471–481

Gaspo R, Bosch RF, Bou-Abboud E, Nattel S (1997) Tachycardia-induced changes in Na+ current in a chronic dog model of atrial fibrillation. Circ Res 81:1045–1052

Gauldie J, Hanson JM, Rumjanek FD, Shipolini RA, Vernon CA (1976) The peptide components of bee venom. Eur J Biochem 61:369–376

Gautier P, Guillemare E, Djandjighian L, Marion A, Planchenault J, Bernhart C, Herbert JM, Nisato D (2004) In vivo and in vitro characterization of the novel antiarrhythmic agent SSR149744C: electrophysiological, anti-adrenergic, and anti-angiotensin II effects. J Cardiovasc Pharmacol 44:244–257

Gautier P, Serre M, Cosnier-Pucheu S, Djandjighian L, Roccon A, Herbert JM, Nisato D (2005) In vivo and in vitro antiarrhythmic effects of SSR149744C in animal models of atrial fibrillation and ventricular arrhythmias. J Cardiovasc Pharmacol 45:125–135

Gentles RG, Grant-Young K, Hu S, Huang Y, Poss MA, Andres C, Fiedler T, Knox R, Lodge N, Weaver CD, Harden DG (2008) Initial SAR studies on apamin-displacing 2-aminothiazole blockers of calcium-activated small conductance potassium channels. Bioorg Med Chem Lett 18:5316–5319

Gogelein H, Brendel J, Steinmeyer K, Strubing C, Picard N, Rampe D, Kopp K, Busch AE, Bleich M (2004) Effects of the atrial antiarrhythmic drug AVE0118 on cardiac ion channels. Naunyn Schmiedebergs Arch Pharmacol 370:183–192

Grunnet M, Jespersen T, Rasmussen HB, Ljungstrom T, Jorgensen NK, Olesen SP, Klaerke DA (2002) KCNE4 is an inhibitory subunit to the KCNQ1 channel. J Physiol 542:119–130

Grunnet M, Olesen SP, Klaerke DA, Jespersen T (2005) hKCNE4 inhibits the hKCNQ1 potassium current without affecting the activation kinetics. Biochem Biophys Res Commun 328: 1146–1153

Grunnet M, Strøbæk D, Olesen SP, Christophersen P (2009) KCa1-KCa5 families. In: Kew J, Davies C (eds) Ion channels: from structure to function. Oxford University Press, Oxford, pp 403–424

Guillemare E, Marion A, Nisato D, Gautier P (2000) Inhibitory effects of dronedarone on muscarinic K+ current in guinea pig atrial cells. J Cardiovasc Pharmacol 36:802–805

Guo D, Lu Z (2000) Mechanism of IRK1 channel block by intracellular polyamines. J Gen Physiol 115:799–814

Guo W, Xu H, London B, Nerbonne JM (1999) Molecular basis of transient outward K+ current diversity in mouse ventricular myocytes. J Physiol 521(Pt 3):587–599

Guo W, Li H, Aimond F, Johns DC, Rhodes KJ, Trimmer JS, Nerbonne JM (2002) Role of heteromultimers in the generation of myocardial transient outward K+ currents. Circ Res 90: 586–593

Gurney A, Manoury B (2009) Two-pore potassium channels in the cardiovascular system. Eur Biophys J 38:305–318

Han TS, Williams GR, Vanderpump MP (2009) Benzofuran derivatives and the thyroid. Clin Endocrinol (Oxf) 70:2–13

Hara M, Shvilkin A, Rosen MR, Danilo P Jr, Boyden PA (1999) Steady-state and nonsteady-state action potentials in fibrillating canine atrium: abnormal rate adaptation and its possible mechanisms. Cardiovasc Res 42:455–469

Hashimoto N, Yamashita T, Tsuruzoe N (2008) Characterization of in vivo and in vitro electrophysiological and antiarrhythmic effects of a novel IKACh blocker, NIP-151: a comparison with an IKr-blocker dofetilide. J Cardiovasc Pharmacol 51:162–169

Hasumi H, Matsuda R, Shimamoto K, Hata Y, Kaneko N (2007) K201, a multi-channel blocker, inhibits clofilium-induced torsades de pointes and attenuates an increase in repolarization. Eur J Pharmacol 555:54–60

Heginbotham L, Lu Z, Abramson T, MacKinnon R (1994) Mutations in the K+ channel signature sequence. Biophys J 66:1061–1067

Henry WL, Morganroth J, Pearlman AS, Clark CE, Redwood DR, Itscoitz SB, Epstein SE (1976) Relation between echocardiographically determined left atrial size and atrial fibrillation. Circulation 53:273–279

Hille B (1992) G protein-coupled mechanisms and nervous signaling. Neuron 9:187–195

Hohnloser SH, Kuck KH, Lilienthal J (2000) Rhythm or rate control in atrial fibrillation–Pharmacological Intervention in Atrial Fibrillation (PIAF): a randomised trial. Lancet 356:1789–1794

Hohnloser SH, Dorian P, Straub M, Beckmann K, Kowey P (2004) Safety and efficacy of intravenously administered tedisamil for rapid conversion of recent-onset atrial fibrillation or atrial flutter. J Am Coll Cardiol 44:99–104

Hohnloser SH, Crijns HJ, van Eickels M, Gaudin C, Page RL, Torp-Pedersen C, Connolly SJ (2009) Effect of dronedarone on cardiovascular events in atrial fibrillation. N Engl J Med 360:668–678

Homma N, Amran MS, Nagasawa Y, Hashimoto K (2006) Topics on the Na+/Ca2+ exchanger: involvement of Na+/Ca2+ exchange system in cardiac triggered activity. J Pharmacol Sci 102:17–21

Hondeghem LM, Snyders DJ (1990) Class III antiarrhythmic agents have a lot of potential but a long way to go. Reduced effectiveness and dangers of reverse use dependence. Circulation 81:686–690

Hondeghem LM, Carlsson L, Duker G (2001) Instability and triangulation of the action potential predict serious proarrhythmia, but action potential duration prolongation is antiarrhythmic. Circulation 103:2004–2013

Inoue M, Imanaga I (1993) Masking of A-type K+ channel in guinea pig cardiac cells by extracellular Ca2+. Am J Physiol 264:C1434–C1438

Isomoto S, Kurachi Y (1997) Function, regulation, pharmacology, and molecular structure of ATP-sensitive K+ channels in the cardiovascular system. J Cardiovasc Electrophysiol 8:1431–1446

Jafari-Fesharaki M, Scheinman MM (1998) Adverse effects of amiodarone. Pacing Clin Electrophysiol 21:108–120

Jager H, Adelman JP, Grissmer S (2000) SK2 encodes the apamin-sensitive Ca(2+)-activated K(+) channels in the human leukemic T cell line, Jurkat. FEBS Lett 469:196–202

Jenkins DP, Strobaek D, Hougaard C, Jensen ML, Hummel R, Sorensen US, Christophersen P, Wulff H (2011) Negative gating modulation by (R)-N-(benzimidazol-2-yl)-1,2,3,4-tetrahydro-1-naphthylamine (NS8593) depends on residues in the inner pore vestibule: pharmacological evidence of deep-pore gating of K(Ca)2 channels. Mol Pharmacol 79:899–909

Jespersen T, Grunnet M, Olesen SP (2005) The KCNQ1 potassium channel: from gene to physiological function. Physiology (Bethesda) 20:408–416

Juhasz A, Bodor N (2000) Cardiovascular studies on different classes of soft drugs. Pharmazie 55:228–238

Kaneko N, Matsuda R, Hata Y, Shimamoto K (2009) Pharmacological characteristics and clinical applications of K201. Curr Clin Pharmacol 4:126–131

Kannel WB, Abbott RD, Savage DD, McNamara PM (1983) Coronary heart disease and atrial fibrillation: the Framingham Study. Am Heart J 106:389–396

Kaufman ES, Zimmermann PA, Wang T, Dennish GW 3rd, Barrell PD, Chandler ML, Greene HL (2004) Risk of proarrhythmic events in the Atrial Fibrillation Follow-up Investigation of Rhythm Management (AFFIRM) study: a multivariate analysis. J Am Coll Cardiol 44:1276–1282

Kelly A, Elliott EB, Matsuda R, Kaneko N, Smith GL, Loughrey CM (2011) The effect of K201 on isolated working rabbit heart mechanical function during pharmacologically-induced Ca(2+) overload. Br J Pharmacol, DOI: 10.1111/j.1476-5381.2011.01531.x

Kneller J, Zou R, Vigmond EJ, Wang Z, Leon LJ, Nattel S (2002) Cholinergic atrial fibrillation in a computer model of a two-dimensional sheet of canine atrial cells with realistic ionic properties. Circ Res 90:E73–E87

Kneller J, Kalifa J, Zou R, Zaitsev AV, Warren M, Berenfeld O, Vigmond EJ, Leon LJ, Nattel S, Jalife J (2005) Mechanisms of atrial fibrillation termination by pure sodium channel blockade in an ionically-realistic mathematical model. Circ Res 96:e35–e47

Knobloch K, Brendel J, Peukert S, Rosenstein B, Busch AE, Wirth KJ (2002) Electrophysiological and antiarrhythmic effects of the novel I(Kur) channel blockers, S9947 and S20951, on left vs. right pig atrium in vivo in comparison with the I(Kr) blockers dofetilide, azimilide, d,l-sotalol and ibutilide. Naunyn Schmiedebergs Arch Pharmacol 366:482–487

Kodama I, Kamiya K, Toyama J (1997) Cellular electropharmacology of amiodarone. Cardiovasc Res 35:13–29

Kong W, Po S, Yamagishi T, Ashen MD, Stetten G, Tomaselli GF (1998) Isolation and characterization of the human gene encoding Ito: further diversity by alternative mRNA splicing. Am J Physiol 275:H1963–H1970

Kostin S, Klein G, Szalay Z, Hein S, Bauer EP, Schaper J (2002) Structural correlate of atrial fibrillation in human patients. Cardiovasc Res 54:361–379

Kovoor P, Wickman K, Maguire CT, Pu W, Gehrmann J, Berul CI, Clapham DE (2001) Evaluation of the role of I(KACh) in atrial fibrillation using a mouse knockout model. J Am Coll Cardiol 37:2136–2143

Kowey PR, Dorian P, Mitchell LB, Pratt CM, Roy D, Schwartz PJ, Sadowski J, Sobczyk D, Bochenek A, Toft E (2009) Vernakalant hydrochloride for the rapid conversion of atrial fibrillation after cardiac surgery: a randomized, double-blind, placebo-controlled trial. Circ Arrhythm Electrophysiol 2:652–659

Kubo Y, Baldwin TJ, Jan YN, Jan LY (1993) Primary structure and functional expression of a mouse inward rectifier potassium channel. Nature 362:127–133

Kumar K, Nearing BD, Carvas M, Nascimento BC, Acar M, Belardinelli L, Verrier RL (2009) Ranolazine exerts potent effects on atrial electrical properties and abbreviates atrial fibrillation duration in the intact porcine heart. J Cardiovasc Electrophysiol 20:796–802

Lafuente-Lafuente C, Mouly S, Longas-Tejero MA, Mahe I, Bergmann JF (2006) Antiarrhythmic drugs for maintaining sinus rhythm after cardioversion of atrial fibrillation: a systematic review of randomized controlled trials. Arch Intern Med 166:719–728

Lagrutta A, Wang J, Fermini B, Salata JJ (2006) Novel, potent inhibitors of human Kv1.5 K+ channels and ultrarapidly activating delayed rectifier potassium current. J Pharmacol Exp Ther 317:1054–1063

Larsen AP, Olesen SP, Grunnet M, Jespersen T (2008) Characterization of hERG1a and hERG1b potassium channels-a possible role for hERG1b in the I (Kr) current. Pflugers Arch 456: 1137–1148

Le Heuzey JY, De Ferrari GM, Radzik D, Santini M, Zhu J, Davy JM (2010) A short-term, randomized, double-blind, parallel-group study to evaluate the efficacy and safety of dronedarone versus amiodarone in patients with persistent atrial fibrillation: the DIONYSOS study. J Cardiovasc Electrophysiol 21:597–605

Lee KS (1992) Ibutilide, a new compound with potent class III antiarrhythmic activity, activates a slow inward Na+ current in guinea pig ventricular cells. J Pharmacol Exp Ther 262:99–108

Lee DS, Goodman S, Dean DM, Lenis J, Ma P, Gervais PB, Langer A (2002) Randomized comparison of T-type versus L-type calcium-channel blockade on exercise duration in stable angina: results of the Posicor Reduction of Ischemia During Exercise (PRIDE) trial. Am Heart J 144:60–67

Li D, Fareh S, Leung TK, Nattel S (1999) Promotion of atrial fibrillation by heart failure in dogs: atrial remodeling of a different sort. Circulation 100:87–95

Li D, Melnyk P, Feng J, Wang Z, Petrecca K, Shrier A, Nattel S (2000) Effects of experimental heart failure on atrial cellular and ionic electrophysiology. Circulation 101:2631–2638

Li GR, Lau CP, Shrier A (2002) Heterogeneity of sodium current in atrial vs epicardial ventricular myocytes of adult guinea pig hearts. J Mol Cell Cardiol 34:1185–1194

Li N, Timofeyev V, Tuteja D, Xu D, Lu L, Zhang Q, Zhang Z, Singapuri A, Albert TR, Rajagopal AV, Bond CT, Periasamy M, Adelman J, Chiamvimonvat N (2009) Ablation of a Ca2+-activated K+ channel (SK2 channel) results in action potential prolongation in atrial myocytes and atrial fibrillation. J Physiol 587:1087–1100

Li ML, Li T, Lei M, Tan XQ, Yang Y, Liu TP, Pei J, Zeng XR (2011) [Increased small conductance calcium-activated potassium channel (SK2 channel) current in atrial myocytes of patients with persistent atrial fibrillation]. Zhonghua Xin Xue Guan Bing Za Zhi 39:147–151

Liegeois JF, Mercier F, Graulich A, Graulich-Lorge F, Scuvee-Moreau J, Seutin V (2003) Modulation of small conductance calcium-activated potassium (SK) channels: a new challenge in medicinal chemistry. Curr Med Chem 10:625–647

Lloyd-Jones DM, Wang TJ, Leip EP, Larson MG, Levy D, Vasan RS, D'Agostino RB, Massaro JM, Beiser A, Wolf PA, Benjamin EJ (2004) Lifetime risk for development of atrial fibrillation: the Framingham Heart Study. Circulation 110:1042–1046

London B, Trudeau MC, Newton KP, Beyer AK, Copeland NG, Gilbert DJ, Jenkins NA, Satler CA, Robertson GA (1997) Two isoforms of the mouse ether-a-go-go-related gene coassemble to form channels with properties similar to the rapidly activating component of the cardiac delayed rectifier K+ current. Circ Res 81:870–878

Lopatin AN, Nichols CG (2001) Inward rectifiers in the heart: an update on I(K1). J Mol Cell Cardiol 33:625–638

Loughrey CM, Otani N, Seidler T, Craig MA, Matsuda R, Kaneko N, Smith GL (2007) K201 modulates excitation-contraction coupling and spontaneous Ca2+ release in normal adult rabbit ventricular cardiomyocytes. Cardiovasc Res 76:236–246

Lu L, Zhang Q, Timofeyev V, Zhang Z, Young JN, Shin HS, Knowlton AA, Chiamvimonvat N (2007) Molecular coupling of a Ca2+-activated K+ channel to L-type Ca2+ channels via alpha-actinin2. Circ Res 100:112–120

Machida T, Hashimoto N, Kuwahara I, Ogino Y, Matsuura J, Yamamoto W, Itano Y, Zamma A, Matsumoto R, Kamon J, Kobayashi T, Ishiwata N, Yamashita T, Ogura T, Nakaya H (2011)

Effects of a highly selective acetylcholine-activated K+ channel blocker on experimental atrial fibrillation. Circ Arrhythm Electrophysiol 4:94–102
Manning A, Thisse V, Hodeige D, Richard J, Heyndrickx JP, Chatelain P (1995) SR 33589, a new amiodarone-like antiarrhythmic agent: electrophysiological effects in anesthetized dogs. J Cardiovasc Pharmacol 25:252–261
Marban E, O'Rourke B (1995) Calcium channels: structure, function, and regulation, in cardiac electrophysiology: from cell to bedside. WB Saunders Comp, Philadelphia
Marrouche NF, Reddy RK, Wittkowsky AK, Bardy GH (2000) High-dose bolus lidocaine for chemical cardioversion of atrial fibrillation: a prospective, randomized, double-blind crossover trial. Am Heart J 139:E8–E11
Mason JW (1987) Amiodarone. N Engl J Med 316:455–466
McAllister RE, Noble D (1966) The time and voltage dependence of the slow outward current in cardiac Purkinje fibres. J Physiol 186:632–662
McCrossan ZA, Abbott GW (2004) The MinK-related peptides. Neuropharmacology 47:787–821
McDonald TV, Yu Z, Ming Z, Palma E, Meyers MB, Wang KW, Goldstein SA, Fishman GI (1997) A minK-HERG complex regulates the cardiac potassium current I(Kr). Nature 388:289–292
Medina I, Krapivinsky G, Arnold S, Kovoor P, Krapivinsky L, Clapham DE (2000) A switch mechanism for G beta gamma activation of I(KACh). J Biol Chem 275:29709–29716
Moe GK, Rheinboldt WC, Abildskov JA (1964) A Computer Model of Atrial Fibrillation. Am Heart J 67:200–220
Morey TE, Seubert CN, Raatikainen MJ, Martynyuk AE, Druzgala P, Milner P, Gonzalez MD, Dennis DM (2001) Structure-activity relationships and electrophysiological effects of short-acting amiodarone homologs in guinea pig isolated heart. J Pharmacol Exp Ther 297:260–266
Mori K, Hara Y, Saito T, Masuda Y, Nakaya H (1995) Anticholinergic effects of class III antiarrhythmic drugs in guinea pig atrial cells. Different molecular mechanisms. Circulation 91:2834–2843
Munk AA, Adjemian RA, Zhao J, Ogbaghebriel A, Shrier A (1996) Electrophysiological properties of morphologically distinct cells isolated from the rabbit atrioventricular node. J Physiol 493(Pt 3):801–818
Murdock DK, Kersten M, Kaliebe J, Larrain G (2009) The use of oral ranolazine to convert new or paroxysmal atrial fibrillation: a review of experience with implications for possible "pill in the pocket" approach to atrial fibrillation. Indian Pacing Electrophysiol J 9:260–267
Nagy ZA, Virag L, Toth A, Biliczki P, Acsai K, Banyasz T, Nanasi P, Papp JG, Varro A (2004) Selective inhibition of sodium-calcium exchanger by SEA-0400 decreases early and delayed after depolarization in canine heart. Br J Pharmacol 143:827–831
Nagy N, Szuts V, Horvath Z, Seprenyi G, Farkas AS, Acsai K, Prorok J, Bitay M, Kun A, Pataricza J, Papp JG, Nanasi PP, Varro A, Toth A (2009) Does small-conductance calcium-activated potassium channel contribute to cardiac repolarization? J Mol Cell Cardiol 47:656–663
Namekata I, Tsuruoka N, Tsuneoka Y, Matsuda T, Takahara A, Tanaka Y, Suzuki T, Takahashi T, Iida-Tanaka N, Tanaka H (2011) Blocking effect of NIP-142 on the KCNQ1/KCNE1 channel current expressed in HEK293 cells. Biol Pharm Bull 34:153–155
Nattel S (2002) New ideas about atrial fibrillation 50 years on. Nature 415:219–226
Nattel S (2009) Calcium-activated potassium current: a novel ion channel candidate in atrial fibrillation. J Physiol 587:1385–1386
Nattel S, Carlsson L (2006) Innovative approaches to anti-arrhythmic drug therapy. Nat Rev Drug Discov 5:1034–1049
Nattel S, Shiroshita-Takeshita A, Brundel BJ, Rivard L (2005) Mechanisms of atrial fibrillation: lessons from animal models. Prog Cardiovasc Dis 48:9–28
Nattel S, Maguy A, Le Bouter S, Yeh YH (2007) Arrhythmogenic ion-channel remodeling in the heart: heart failure, myocardial infarction, and atrial fibrillation. Physiol Rev 87:425–456
Nattel S, Burstein B, Dobrev D (2008) Atrial remodeling and atrial fibrillation: mechanisms and implications. Circ Arrhythm Electrophysiol 1:62–73

Nerbonne JM (2000) Molecular basis of functional voltage-gated K+ channel diversity in the mammalian myocardium. J Physiol 525(Pt 2):285–298

Nerbonne JM, Kass RS (2005) Molecular physiology of cardiac repolarization. Physiol Rev 85: 1205–1253

Nilius B, Hess P, Lansman JB, Tsien RW (1985) A novel type of cardiac calcium channel in ventricular cells. Nature 316:443–446

Okishige K, Nishizaki M, Azegami K, Igawa M, Yamawaki N, Aonuma K (2000) Pilsicainide for conversion and maintenance of sinus rhythm in chronic atrial fibrillation: a placebo-controlled, multicenter study. Am Heart J 140:e13

Olson TM, Alekseev AE, Liu XK, Park S, Zingman LV, Bienengraeber M, Sattiraju S, Ballew JD, Jahangir A, Terzic A (2006) Kv1.5 channelopathy due to KCNA5 loss-of-function mutation causes human atrial fibrillation. Hum Mol Genet 15:2185–2191

Opolski G, Torbicki A, Kosior DA, Szulc M, Wozakowska-Kaplon B, Kolodziej P, Achremczyk P (2004) Rate control vs rhythm control in patients with nonvalvular persistent atrial fibrillation: the results of the Polish How to Treat Chronic Atrial Fibrillation (HOT CAFE) Study. Chest 126:476–486

Orth PM, Hesketh JC, Mak CK, Yang Y, Lin S, Beatch GN, Ezrin AM, Fedida D (2006) RSD1235 blocks late INa and suppresses early afterdepolarizations and torsades de pointes induced by class III agents. Cardiovasc Res 70:486–496

Ozgen N, Dun W, Sosunov EA, Anyukhovsky EP, Hirose M, Duffy HS, Boyden PA, Rosen MR (2007) Early electrical remodeling in rabbit pulmonary vein results from trafficking of intracellular SK2 channels to membrane sites. Cardiovasc Res 75:758–769

Pandit SV, Berenfeld O, Anumonwo JM, Zaritski RM, Kneller J, Nattel S, Jalife J (2005) Ionic determinants of functional reentry in a 2-D model of human atrial cells during simulated chronic atrial fibrillation. Biophys J 88:3806–3821

Patel C, Yan GX, Kowey PR (2009) Dronedarone. Circulation 120:636–644

Pedersen OD, Bagger H, Keller N, Marchant B, Kober L, Torp-Pedersen C (2001) Efficacy of dofetilide in the treatment of atrial fibrillation-flutter in patients with reduced left ventricular function: a Danish investigations of arrhythmia and mortality on dofetilide (diamond) substudy. Circulation 104:292–296

Perez-Reyes E (2003) Molecular physiology of low-voltage-activated t-type calcium channels. Physiol Rev 83:117–161

Pertsov AM, Davidenko JM, Salomonsz R, Baxter WT, Jalife J (1993) Spiral waves of excitation underlie reentrant activity in isolated cardiac muscle. Circ Res 72:631–650

Piccini JP, Hasselblad V, Peterson ED, Washam JB, Califf RM, Kong DF (2009) Comparative efficacy of dronedarone and amiodarone for the maintenance of sinus rhythm in patients with atrial fibrillation. J Am Coll Cardiol 54:1089–1095

Pinto JM, Boyden PA (1998) Reduced inward rectifying and increased E-4031-sensitive K+ current density in arrhythmogenic subendocardial purkinje myocytes from the infarcted heart. J Cardiovasc Electrophysiol 9:299–311

Piper DR, Hinz WA, Tallurri CK, Sanguinetti MC, Tristani-Firouzi M (2005) Regional specificity of human ether-a'-go-go-related gene channel activation and inactivation gating. J Biol Chem 280:7206–7217

Polontchouk L, Haefliger JA, Ebelt B, Schaefer T, Stuhlmann D, Mehlhorn U, Kuhn-Regnier F, De Vivie ER, Dhein S (2001) Effects of chronic atrial fibrillation on gap junction distribution in human and rat atria. J Am Coll Cardiol 38:883–891

Pratt CM, Camm AJ, Cooper W, Friedman PL, MacNeil DJ, Moulton KM, Pitt B, Schwartz PJ, Veltri EP, Waldo AL (1998) Mortality in the Survival With ORal D-sotalol (SWORD) trial: why did patients die? Am J Cardiol 81:869–876

Pratt CM, Roy D, Torp-Pedersen C, Wyse DG, Toft E, Juul-Moller S, Retyk E, Drenning DH (2010) Usefulness of vernakalant hydrochloride injection for rapid conversion of atrial fibrillation. Am J Cardiol 106:1277–1283

Pribnow D, Johnson-Pais T, Bond CT, Keen J, Johnson RA, Janowsky A, Silvia C, Thayer M, Maylie J, Adelman JP (1999) Skeletal muscle and small-conductance calcium-activated potassium channels. Muscle Nerve 22:742–750

Radicke S, Cotella D, Graf EM, Ravens U, Wettwer E (2005) Expression and function of dipeptidyl-aminopeptidase-like protein 6 as a putative beta-subunit of human cardiac transient outward current encoded by Kv4.3. J Physiol 565:751–756

Ravens U, Dobrev D (2003) Cardiac sympathetic innervation and control of potassium channel function. J Mol Cell Cardiol 35:137–139

Regan CP, Wallace AA, Cresswell HK, Atkins CL, Lynch JJ Jr (2006) In vivo cardiac electrophysiologic effects of a novel diphenylphosphine oxide IKur blocker, (2-Isopropyl-5-methylcyclohexyl) diphenylphosphine oxide, in rat and nonhuman primate. J Pharmacol Exp Ther 316:727–732

Roden DM (1998) Taking the "idio" out of "idiosyncratic": predicting torsades de pointes. Pacing Clin Electrophysiol 21:1029–1034

Rogart RB, Cribbs LL, Muglia LK, Kephart DD, Kaiser MW (1989) Molecular cloning of a putative tetrodotoxin-resistant rat heart Na+ channel isoform. Proc Natl Acad Sci U S A 86: 8170–8174

Romey G, Hugues M, Schmid-Antomarchi H, Lazdunski M (1984) Apamin: a specific toxin to study a class of Ca2+-dependent K+ channels. J Physiol (Paris) 79:259–264

Ronaszeki A, Alings M, Egstrup K, Gaciong Z, Hranai M, Kiraly C, Sereg M, Figatowski W, Bondarov P, Johansson S, Frison L, Edvardsson N, Berggren A (2011) Pharmacological cardioversion of atrial fibrillation–a double-blind, randomized, placebo-controlled, multicentre, dose-escalation study of AZD1305 given intravenously. Europace 13:1148–1156

Rosa JC, Galanakis D, Ganellin CR, Dunn PM, Jenkinson DH (1998) Bis-quinolinium cyclophanes: 6,10-diaza-3(1,3),8(1,4)-dibenzena-1,5(1,4)- diquinolinacyclodecaphane (UCL 1684), the first nanomolar, non-peptidic blocker of the apamin-sensitive Ca(2+)-activated K+ channel. J Med Chem 41:2–5

Rosati B, Pan Z, Lypen S, Wang HS, Cohen I, Dixon JE, McKinnon D (2001) Regulation of KChIP2 potassium channel beta subunit gene expression underlies the gradient of transient outward current in canine and human ventricle. J Physiol 533:119–125

Roy D, Rowe BH, Stiell IG, Coutu B, Ip JH, Phaneuf D, Lee J, Vidaillet H, Dickinson G, Grant S, Ezrin AM, Beatch GN (2004) A randomized, controlled trial of RSD1235, a novel anti-arrhythmic agent, in the treatment of recent onset atrial fibrillation. J Am Coll Cardiol 44: 2355–2361

Roy D, Pratt CM, Torp-Pedersen C, Wyse DG, Toft E, Juul-Moller S, Nielsen T, Rasmussen SL, Stiell IG, Coutu B, Ip JH, Pritchett EL, Camm AJ (2008) Vernakalant hydrochloride for rapid conversion of atrial fibrillation: a phase 3, randomized, placebo-controlled trial. Circulation 117:1518–1525

Sanders P, Morton JB, Kistler PM, Vohra JK, Kalman JM, Sparks PB (2003) Reversal of atrial mechanical dysfunction after cardioversion of atrial fibrillation: implications for the mechanisms of tachycardia-mediated atrial cardiomyopathy. Circulation 108:1976–1984

Sanguinetti MC, Tristani-Firouzi M (2006) hERG potassium channels and cardiac arrhythmia. Nature 440:463–469

Sanguinetti MC, Curran ME, Zou A, Shen J, Spector PS, Atkinson DL, Keating MT (1996) Coassembly of K(V)LQT1 and minK (IsK) proteins to form cardiac I(Ks) potassium channel. Nature 384:80–83

Satoh T, Zipes DP (1998) Cesium-induced atrial tachycardia degenerating into atrial fibrillation in dogs: atrial torsades de pointes? J Cardiovasc Electrophysiol 9:970–975

Schotten U, de Haan S, Verheule S, Harks EG, Frechen D, Bodewig E, Greiser M, Ram R, Maessen J, Kelm M, Allessie M, Van Wagoner DR (2007) Blockade of atrial-specific K+-currents increases atrial but not ventricular contractility by enhancing reverse mode Na+/Ca2+-exchange. Cardiovasc Res 73:37–47

Schram G, Pourrier M, Melnyk P, Nattel S (2002) Differential distribution of cardiac ion channel expression as a basis for regional specialization in electrical function. Circ Res 90:939–950

Scirica BM, Morrow DA, Hod H, Murphy SA, Belardinelli L, Hedgepeth CM, Molhoek P, Verheugt FW, Gersh BJ, McCabe CH, Braunwald E (2007) Effect of ranolazine, an antianginal agent with novel electrophysiological properties, on the incidence of arrhythmias in patients with non ST-segment elevation acute coronary syndrome: results from the Metabolic Efficiency With Ranolazine for Less Ischemia in Non ST-Elevation Acute Coronary Syndrome Thrombolysis in Myocardial Infarction 36 (MERLIN-TIMI 36) randomized controlled trial. Circulation 116:1647–1652

Shi Y, Ducharme A, Li D, Gaspo R, Nattel S, Tardif JC (2001) Remodeling of atrial dimensions and emptying function in canine models of atrial fibrillation. Cardiovasc Res 52:217–225

Shinagawa K, Shi YF, Tardif JC, Leung TK, Nattel S (2002) Dynamic nature of atrial fibrillation substrate during development and reversal of heart failure in dogs. Circulation 105:2672–2678

Shorofsky SR, January CT (1992) L- and T-type Ca2+ channels in canine cardiac Purkinje cells. Single-channel demonstration of L-type Ca2+ window current. Circ Res 70:456–464

Sicouri S, Burashnikov A, Belardinelli L, Antzelevitch C (2010) Synergistic electrophysiologic and antiarrhythmic effects of the combination of ranolazine and chronic amiodarone in canine atria. Circ Arrhythm Electrophysiol 3:88–95

Sills MN, Xu YC, Baracchini E, Goodman RH, Cooperman SS, Mandel G, Chien KR (1989) Expression of diverse Na+ channel messenger RNAs in rat myocardium. Evidence for a cardiac-specific Na+ channel. J Clin Invest 84:331–336

Singh BN, Connolly SJ, Crijns HJ, Roy D, Kowey PR, Capucci A, Radzik D, Aliot EM, Hohnloser SH (2007) Dronedarone for maintenance of sinus rhythm in atrial fibrillation or flutter. N Engl J Med 357:987–999

Skanes AC, Gray RA, Zuur CL, Jalife J (1998) Effects of postshock atrial pacing on atrial defibrillation outcome in the isolated sheep heart. Circulation 98:64–72

Skibsbye L, Diness JG, Sorensen US, Hansen RS, Grunnet M (2011) The Duration of Pacing-induced Atrial Fibrillation Is Reduced in Vivo by Inhibition of Small Conductance Ca2+-activated K+ Channels. J Cardiovasc Pharmacol 57:672–681

Soldatov NM (1994) Genomic structure of human L-type Ca2+ channel. Genomics 22:77–87

Soltysinska E, Olesen SP, Christ T, Wettwer E, Varro A, Grunnet M, Jespersen T (2009) Transmural expression of ion channels and transporters in human nondiseased and end-stage failing hearts. Pflugers Arch 459:11–23

Sorensen US, Strobaek D, Christophersen P, Hougaard C, Jensen ML, Nielsen EO, Peters D, Teuber L (2008) Synthesis and structure-activity relationship studies of 2-(N-substituted)-aminobenzimidazoles as potent negative gating modulators ofsmall conductance Ca2+-activated K+ channels. J Med Chem 51:7625–7634

Sossalla S, Kallmeyer B, Wagner S, Mazur M, Maurer U, Toischer K, Schmitto JD, Seipelt R, Schondube FA, Hasenfuss G, Belardinelli L, Maier LS (2010) Altered Na(+) currents in atrial fibrillation effects of ranolazine on arrhythmias and contractility in human atrial myocardium. J Am Coll Cardiol 55:2330–2342

Splawski I, Tristani-Firouzi M, Lehmann MH, Sanguinetti MC, Keating MT (1997) Mutations in the hminK gene cause long QT syndrome and suppress IKs function. Nat Genet 17:338–340

Sridhar A, da Cunha DN, Lacombe VA, Zhou Q, Fox JJ, Hamlin RL, Carnes CA (2007) The plateau outward current in canine ventricle, sensitive to 4-aminopyridine, is a constitutive contributor to ventricular repolarization. Br J Pharmacol 152:870–879

Stocker M (2004) Ca(2+)-activated K+ channels: molecular determinants and function of the SK family. Nat Rev Neurosci 5:758–770

Strobaek D, Hougaard C, Johansen TH, Sorensen US, Nielsen EO, Nielsen KS, Taylor RD, Pedarzani P, Christophersen P (2006) Inhibitory gating modulation of small conductance Ca2+-activated K+ channels by the synthetic compound (R)-N-(benzimidazol-2-yl)-1,2,3,4-tetrahydro-1-naphtylamine (NS8593) reduces afterhyperpolarizing current in hippocampal CA1 neurons. Mol Pharmacol 70:1771–1782

Strutz-Seebohm N, Gutcher I, Decher N, Steinmeyer K, Lang F, Seebohm G (2007) Comparison of potent Kv1.5 potassium channel inhibitors reveals the molecular basis for blocking kinetics and binding mode. Cell Physiol Biochem 20:791–800

Sun W, Sarma JS, Singh BN (1999) Electrophysiological effects of dronedarone (SR33589), a noniodinated benzofuran derivative, in the rabbit heart: comparison with amiodarone. Circulation 100:2276–2281

Sun W, Sarma JS, Singh BN (2002) Chronic and acute effects of dronedarone on the action potential of rabbit atrial muscle preparations: comparison with amiodarone. J Cardiovasc Pharmacol 39:677–684

Takahashi N, Morishige K, Jahangir A, Yamada M, Findlay I, Koyama H, Kurachi Y (1994) Molecular cloning and functional expression of cDNA encoding a second class of inward rectifier potassium channels in the mouse brain. J Biol Chem 269:23274–23279

Tamargo J, Caballero R, Gomez R, Valenzuela C, Delpon E (2004) Pharmacology of cardiac potassium channels. Cardiovasc Res 62:9–33

Tanaka H, Hashimoto N (2007) A multiple ion channel blocker, NIP-142, for the treatment of atrial fibrillation. Cardiovasc Drug Rev 25:342–356

Tanaka H, Namekata I, Hamaguchi S, Kawamura T, Masuda H, Tanaka Y, Iida-Tanaka N, Takahara A (2010) Effect of NIP-142 on potassium channel alpha-subunits Kv1.5, Kv4.2 and Kv4.3, and mouse atrial repolarization. Biol Pharm Bull 33:138–141

Toivonen L, Raatikainen P, Walfridsson H, Englund A, Hegbom F, Anfinsen OG, Gjesdal K, Pehrson S, Johansson S, Frison L, Berggren AR, Edvardsson N (2010) A randomized invasive cardiac electrophysiology study of the combined ion channel blocker AZD1305 in patients after catheter ablation of atrial flutter. J Cardiovasc Pharmacol 56:300–308

Topert C, Doring F, Wischmeyer E, Karschin C, Brockhaus J, Ballanyi K, Derst C, Karschin A (1998) Kir2.4: a novel K+ inward rectifier channel associated with motoneurons of cranial nerve nuclei. J Neurosci 18:4096–4105

Touboul P, Brugada J, Capucci A, Crijns HJ, Edvardsson N, Hohnloser SH (2003) Dronedarone for prevention of atrial fibrillation: a dose-ranging study. Eur Heart J 24:1481–1487

Tuteja D, Xu D, Timofeyev V, Lu L, Sharma D, Zhang Z, Xu Y, Nie L, Vazquez AE, Young JN, Glatter KA, Chiamvimonvat N (2005) Differential expression of small-conductance Ca2+-activated K+ channels SK1, SK2, and SK3 in mouse atrial and ventricular myocytes. Am J Physiol Heart Circ Physiol 289:H2714–H2723

Tuteja D, Rafizadeh S, Timofeyev V, Wang S, Zhang Z, Li N, Mateo RK, Singapuri A, Young JN, Knowlton AA, Chiamvimonvat N (2010) Cardiac small conductance Ca2+-activated K+ channel subunits form heteromultimers via the coiled-coil domains in the C termini of the channels. Circ Res 107:851–859

Van Gelder IC, Hagens VE, Bosker HA, Kingma JH, Kamp O, Kingma T, Said SA, Darmanata JI, Timmermans AJ, Tijssen JG, Crijns HJ (2002) A comparison of rate control and rhythm control in patients with recurrent persistent atrial fibrillation. N Engl J Med 347:1834–1840

Van Wagoner DR, Pond AL, McCarthy PM, Trimmer JS, Nerbonne JM (1997) Outward K+ current densities and Kv1.5 expression are reduced in chronic human atrial fibrillation. Circ Res 80:772–781

Vandenberg CA (1987) Inward rectification of a potassium channel in cardiac ventricular cells depends on internal magnesium ions. Proc Natl Acad Sci U S A 84:2560–2564

Venetucci LA, Trafford AW, O'Neill SC, Eisner DA (2007) Na/Ca exchange: regulator of intracellular calcium and source of arrhythmias in the heart. Ann N Y Acad Sci 1099:315–325

Vergara C, Latorre R, Marrion NV, Adelman JP (1998) Calcium-activated potassium channels. Curr Opin Neurobiol 8:321–329

Vick JA, Hassett CC, Shipman WH (1972) Beta Adrenergic and Antiarrhythmic Effect of Apamin, A Component of Bee Venom. Edgewood Arsenal Technical Report EATR 4664:1–13

Voigt N, Maguy A, Yeh YH, Qi X, Ravens U, Dobrev D, Nattel S (2008) Changes in I K, ACh single-channel activity with atrial tachycardia remodelling in canine atrial cardiomyocytes. Cardiovasc Res 77:35–43

Waldo AL, Camm AJ, deRuyter H, Friedman PL, MacNeil DJ, Pauls JF, Pitt B, Pratt CM, Schwartz PJ, Veltri EP (1996) Effect of d-sotalol on mortality in patients with left ventricular dysfunction after recent and remote myocardial infarction. The SWORD Investigators. Survival With Oral d-Sotalol. Lancet 348:7–12

Wang DW, Yazawa K, George AL Jr, Bennett PB (1996) Characterization of human cardiac Na+ channel mutations in the congenital long QT syndrome. Proc Natl Acad Sci U S A 93: 13200–13205

Wang W, Watanabe M, Nakamura T, Kudo Y, Ochi R (1999) Properties and expression of Ca2+-activated K+ channels in H9c2 cells derived from rat ventricle. Am J Physiol 276: H1559–H1566

Wang TJ, Larson MG, Levy D, Vasan RS, Leip EP, Wolf PA, D'Agostino RB, Murabito JM, Kannel WB, Benjamin EJ (2003) Temporal relations of atrial fibrillation and congestive heart failure and their joint influence on mortality: the Framingham Heart Study. Circulation 107:2920–2925

Wann LS, Curtis AB, January CT, Ellenbogen KA, Lowe JE, Estes NA III, Page RL, Ezekowitz MD, Slotwiner DJ, Jackman WM, Stevenson WG, Tracy CM, Fuster V, Ryden LE, Cannom DS, Le Heuzey JY, Crijns HJ, Lowe JE, Curtis AB, Olsson SB, Ellenbogen KA, Prystowsky EN, Halperin JL, Tamargo JL, Kay GN, Wann LS, Jacobs AK, Anderson JL, Albert N, Hochman JS, Buller CE, Kushner FG, Creager MA, Ohman EM, Ettinger SM, Stevenson WG, Guyton RA, Tarkington LG, Halperin JL, Yancy CW (2011) 2011 ACCF/AHA/HRS focused update on the management of patients with atrial fibrillation (updating the 2006 guideline): a report of the American College of Cardiology Foundation/American Heart Association Task Force on Practice Guidelines. Circulation 123:104–123

Watanabe Y, Hara Y, Tamagawa M, Nakaya H (1996) Inhibitory effect of amiodarone on the muscarinic acetylcholine receptor-operated potassium current in guinea pig atrial cells. J Pharmacol Exp Ther 279:617–624

Weatherall KL, Goodchild SJ, Jane DE, Marrion NV (2010) Small conductance calcium-activated potassium channels: from structure to function. Prog Neurobiol 91:242–255

Weerapura M, Nattel S, Chartier D, Caballero R, Hebert TE (2002) A comparison of currents carried by HERG, with and without coexpression of MiRP1, and the native rapid delayed rectifier current. Is MiRP1 the missing link? J Physiol 540:15–27

Weidmann S (1951) Effect of current flow on the membrane potential of cardiac muscle. J Physiol 115:227–236

Wettwer E, Hala O, Christ T, Heubach JF, Dobrev D, Knaut M, Varro A, Ravens U (2004) Role of IKur in controlling action potential shape and contractility in the human atrium: influence of chronic atrial fibrillation. Circulation 110:2299–2306

Wijffels MC, Kirchhof CJ, Dorland R, Allessie MA (1995) Atrial fibrillation begets atrial fibrillation. A study in awake chronically instrumented goats. Circulation 92:1954–1968

Wijffels MC, Dorland R, Mast F, Allessie MA (2000) Widening of the excitable gap during pharmacological cardioversion of atrial fibrillation in the goat: effects of cibenzoline, hydroquinidine, flecainide, and d-sotalol. Circulation 102:260–267

Wirth KJ, Paehler T, Rosenstein B, Knobloch K, Maier T, Frenzel J, Brendel J, Busch AE, Bleich M (2003) Atrial effects of the novel K(+)-channel-blocker AVE0118 in anesthetized pigs. Cardiovasc Res 60:298–306

Wirth KJ, Brendel J, Steinmeyer K, Linz DK, Rutten H, Gogelein H (2007) In vitro and in vivo effects of the atrial selective antiarrhythmic compound AVE1231. J Cardiovasc Pharmacol 49:197–206

Wittekindt OH, Visan V, Tomita H, Imtiaz F, Gargus JJ, Lehmann-Horn F, Grissmer S, Morris-Rosendahl DJ (2004) An apamin- and scyllatoxin-insensitive isoform of the human SK3 channel. Mol Pharmacol 65:788–801

Wolf PA, Abbott RD, Kannel WB (1991) Atrial fibrillation as an independent risk factor for stroke: the Framingham Study. Stroke 22:983–988

Workman AJ, Kane KA, Rankin AC (2001) The contribution of ionic currents to changes in refractoriness of human atrial myocytes associated with chronic atrial fibrillation. Cardiovasc Res 52:226–235

Wulff H, Kolski-Andreaco A, Sankaranarayanan A, Sabatier JM, Shakkottai V (2007) Modulators of small- and intermediate-conductance calcium-activated potassium channels and their therapeutic indications. Curr Med Chem 14:1437–1457

Wyse DG, Waldo AL, DiMarco JP, Domanski MJ, Rosenberg Y, Schron EB, Kellen JC, Greene HL, Mickel MC, Dalquist JE, Corley SD (2002) A comparison of rate control and rhythm control in patients with atrial fibrillation. N Engl J Med 347:1825–1833

Xia XM, Fakler B, Rivard A, Wayman G, Johnson-Pais T, Keen JE, Ishii T, Hirschberg B, Bond CT, Lutsenko S, Maylie J, Adelman JP (1998) Mechanism of calcium gating in small-conductance calcium-activated potassium channels. Nature 395:503–507

Xu H, Guo W, Nerbonne JM (1999) Four kinetically distinct depolarization-activated K+ currents in adult mouse ventricular myocytes. J Gen Physiol 113:661–678

Xu Y, Tuteja D, Zhang Z, Xu D, Zhang Y, Rodriguez J, Nie L, Tuxson HR, Young JN, Glatter KA, Vazquez AE, Yamoah EN, Chiamvimonvat N (2003) Molecular identification and functional roles of a Ca(2+)-activated K+ channel in human and mouse hearts. J Biol Chem 278: 49085–49094

Yagi T, Pu J, Chandra P, Hara M, Danilo P Jr, Rosen MR, Boyden PA (2002) Density and function of inward currents in right atrial cells from chronically fibrillating canine atria. Cardiovasc Res 54:405–415

Yamashita T, Murakawa Y, Ajiki K, Omata M (1997) Incidence of induced atrial fibrillation/flutter in complete atrioventricular block. A concept of 'atrial-malfunctioning' atrio-hisian block. Circulation 95:650–654

Yamawake N, Hirano Y, Sawanobori T, Hiraoka M (1992) Arrhythmogenic effects of isoproterenol-activated Cl- current in guinea-pig ventricular myocytes. J Mol Cell Cardiol 24:1047–1058

Yang Y, Li J, Lin X, Yang Y, Hong K, Wang L, Liu J, Li L, Yan D, Liang D, Xiao J, Jin H, Wu J, Zhang Y, Chen YH (2009) Novel KCNA5 loss-of-function mutations responsible for atrial fibrillation. J Hum Genet 54:277–283

Yang Y, Yang Y, Liang B, Liu J, Li J, Grunnet M, Olesen SP, Rasmussen HB, Ellinor PT, Gao L, Lin X, Li L, Wang L, Xiao J, Liu Y, Liu Y, Zhang S, Liang D, Peng L, Jespersen T, Chen YH (2010) Identification of a Kir3.4 mutation in congenital long QT syndrome. Am J Hum Genet 86:872–880

Yeh YH, Lemola K, Nattel S (2007) Vagal atrial fibrillation. Acta Cardiol Sin 23:1–12

Yu FH, Catterall WA (2003) Overview of the voltage-gated sodium channel family. Genome Biol 4:207

Yu T, Wu RB, Guo HM, Deng CY, Zheng SY, Kuang SJ (2011) [Expression and functional role of small conductance Ca(2+)-activated K(+) channels in human atrial myocytes]. Nan Fang Yi Ke Da Xue Xue Bao 31:490–494

Yue L, Feng J, Gaspo R, Li GR, Wang Z, Nattel S (1997) Ionic remodeling underlying action potential changes in a canine model of atrial fibrillation. Circ Res 81:512–525

Zeng J, Rudy Y (1995) Early afterdepolarizations in cardiac myocytes: mechanism and rate dependence. Biophys J 68:949–964

Zhang Z, Xu Y, Song H, Rodriguez J, Tuteja D, Namkung Y, Shin HS, Chiamvimonvat N (2002) Functional Roles of Ca(v)1.3 (alpha(1D)) calcium channel in sinoatrial nodes: insight gained using gene-targeted null mutant mice. Circ Res 90:981–987

Zhang H, Garratt CJ, Zhu J, Holden AV (2005) Role of up-regulation of IK1 in action potential shortening associated with atrial fibrillation in humans. Cardiovasc Res 66:493–502

Zhang H, Shepherd N, Creazzo TL (2008) Temperature-sensitive TREK currents contribute to setting the resting membrane potential in embryonic atrial myocytes. J Physiol 586:3645–3656

Zimmer T, Bollensdorff C, Haufe V, Birch-Hirschfeld E, Benndorf K (2002) Mouse heart Na+ channels: primary structure and function of two isoforms and alternatively spliced variants. Am J Physiol Heart Circ Physiol 282:H1007–H1017

Zygmunt AC, Goodrow RJ, Weigel CM (1998) INaCa and ICl(Ca) contribute to isoproterenol-induced delayed after depolarizations in midmyocardial cells. Am J Physiol 275: H1979–H1992

Intrinsically Photosensitive Retinal Ganglion Cells

Gary E. Pickard and Patricia J. Sollars

Abstract Intrinsically photosensitive retinal ganglion cells (ipRGCs) respond to light in the absence of all rod and cone photoreceptor input. The existence of these ganglion cell photoreceptors, although predicted from observations scattered over many decades, was not established until it was shown that a novel photopigment, melanopsin, was expressed in retinal ganglion cells of rodents and primates. Phototransduction in mammalian ipRGCs more closely resembles that of invertebrate than vertebrate photoreceptors and appears to be mediated by transient receptor potential channels. In the retina, ipRGCs provide excitatory drive to dopaminergic amacrine cells and ipRGCs are coupled to GABAergic amacrine cells via gap junctions. Several subtypes of ipRGC have been identified in rodents based on their morphology, physiology and expression of molecular markers. ipRGCs convey irradiance information centrally via the optic nerve to influence several functions including photoentrainment of the biological clock located in the hypothalamus, the pupillary light reflex, sleep and perhaps some aspects of vision. In addition, ipRGCs may also contribute irradiance signals that interface directly with the autonomic nervous system to regulate rhythmic gene activity in major organs of the body. Here we review the early work that provided the motivation for searching for a new mammalian photoreceptor, the ground-breaking discoveries, current progress that continues to reveal the unusual properties of these neuron photoreceptors, and directions for future investigation.

Keywords Melanopsin · Circadian rhythms · Suprachiasmatic nucleus · Retina

G.E. Pickard (✉)
School of Veterinary Medicine and Biomedical Sciences, University of Nebraska, Lincoln, NE 68583, USA
e-mail: gpickard2@unl.edu

Rev Physiol Biochem Pharmacol, doi: 10.1007/112_2011_4,

Early Hints of a Third Photoreceptor in the Mammalian Retina

The perception of shapes, color and objects moving in the world begins in the outer retina where light is absorbed by photopigments that are integral membrane apoproteins (opsins) covalently linked to a retinaldehyde chromophore in the rod and cone photoreceptors. The capturing of photons by rod and cone photoreceptors initiates a signaling cascade in which photon capture is converted into an electrical signal. The simplest common pathway these signals take from the eye to the brain is from the photoreceptors to bipolar cells to ganglion cells. Retinal ganglion cells (RGCs) convey the signals centrally as action potentials, transmitted via their axons in the optic nerve, to higher brain regions for integration and the further processing required for conscious visual perception (Fig. 1). Among non-mammalian vertebrates, photoreceptors are also found in locations outside the retina, including the pineal gland and in the brain itself. These extra-ocular photoreceptors mediate tasks not associated directly with visual perception (non-image forming functions such as hormone regulation). However, since the pioneering descriptions of the vertebrate retina by Santiago Ramón y Cajal in the late 1800s, it was believed that the retinal rods and cones were the only photoreceptors in mammals (Cajal 1894).

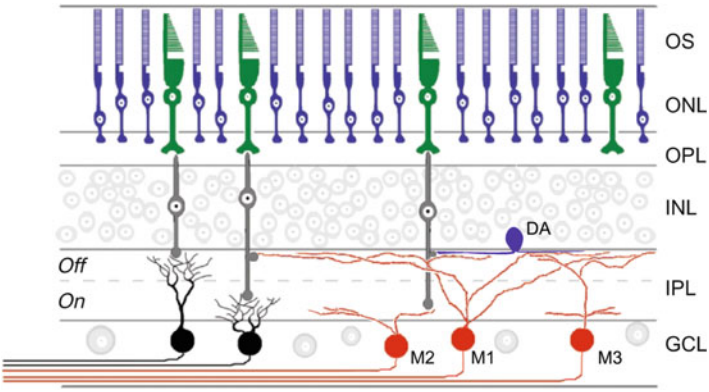

Fig. 1 Schematic vertical section of retina depicting ipRGCs (*red*) and rod and cone photoreceptors. ipRGCs reside in the ganglion cell layer (*GCL*) whereas rods and cones have their cells bodies in the outer nuclear layer (*ONL*). The three morphological types of ipRGC (M1, M2 and M3) are shown. Dendrites of M1 ipRGCs stratify in the distal inner plexiform layer (*IPL*), near the border of the inner nuclear layer (*INL*) in the traditional "OFF" sublamina of the IPL. Dendrites of M2 ipRGCs are confined to the proximal "ON" sublayer of the IPL whereas M3 ipRGCs are bistratified. Conventional RGCs (*black*) receive signals from rods and cones via input from bipolar cells located in the INL. M1 ipRGCs and dopaminergic amacrine cells (*DA*) receive ON bipolar input in the "OFF" sublamina of the IPL via ectopic synapses of ON bipolar cell axons as they pass through the IPL. Conventional RGCs and ipRGCs send axons from the eye to communicate with the brain. M1 ipRGCs also drive excitatory responses in DA presumably by their dendrites that co-stratify in the IPL near the border of the INL. OS, outer segment layer; OPL, outer plexiform layer. Adapted from Berson (2003) and reprinted with permission from Pickard GE, Sollars PJ (2010) Intrinsically photosensitive retinal ganglion cells. Science China Life Sciences 53:58–67

The first suggestion that a non-rod, non-cone photoreceptor might exist in the mammalian retina appeared in 1927. Van Gelder (2008) recalls the story of a young graduate student at Harvard named Clyde E. Keeler, who in 1923 used a wild mouse from several he had caught in his dormitory room, as one of the subjects for an assignment he was given to compare histological sections from the eyes of several different vertebrates. The fact that the histological sections he prepared from the retinas of this mouse were devoid of all rod and cone photoreceptors almost ended his scientific career early, as it was assumed he had done a rather poor job of sectioning the retinal tissue. Keeler, however, convinced that the lack of rods and cones was not a consequence of his histological technique, went on to describe that these mice had actually lost their photoreceptors (Keeler 1924). He next described that, despite having no photoreceptors in the outer retina, the apparently visually blind mice maintained their ability to constrict the iris in response to light stimulation (i.e., the pupillary light reflex) albeit somewhat more slowly than mice with the normal complement of rods and cones. He offered the heretical possibility that "direct stimulation of the internal nuclear or ganglionic cells" by light may have been responsible for the observed behavior of the iris (Keeler 1927). It appeared more likely to others at the time that the mouse iris itself may have been light sensitive and attention to what turns out to have been an important observation, diminished with time.

The Convergence of Retinal Physiology and Internal Time Keeping

Daily rhythms in nature such as the opening and closing of flowers or our patterns of sleep and wakefulness and their association with the perpetual alteration of night and day were perhaps so obvious that their origins were not questioned until the eighteenth century. Jean-Jacques d'Ortous de Marian, a French astronomer, asked if the leaves of the Mimosa plant opened in response to light. He maintained the plants in the dark and noted that the leaves continued to open in the absence of sunlight. Although this is the first description of the endogenous nature of leaf movements, De Marian concluded that the plants must still sense the sun by means other than light (e.g., temperature or humidity) (De Marian 1729). The Swiss botanist Augustin Pyramus de Candolle is credited with the first suggestion of internal timekeeping. He observed that leaf movements persisted under constant light conditions and he concluded from his observations that the rhythm of leaf folding and unfolding must come "from within the plant" (De Candolle 1832). Charles Darwin, in his book on the movements of plants, came to the same conclusion, remarking that "we may conclude that the periodicity of their movements is to a certain extent inherited" (Darwin and Darwin 1880). During the decades that followed the observations made by Keeler, investigators became increasingly aware that not only plants, but all organisms including humans displayed daily rhythms that were generated by an internal time-keeping system or endogenous biological clock (Pittendrigh 1954; Aschoff 1960; Hamner et al. 1962). The first

clear demonstration of this clock-like system in mammals came from a study of the rhythmic behavior of white-footed mice, *Peromyscus leucopus,* housed under constant dim light conditions. Based on his observations, Johnson wrote "this animal has an exceptionally substantial and durable self-winding and self-regulating physiological clock, the mechanism of which remains to be worked out" (Johnson 1939). Richter (1965) sought to determine the clock's physical location in the body and he concluded, after making lesions throughout the brain and removing all major endocrine organs one at a time, that the biological clock was based in the central nervous system and resided in the hypothalamus.

It had also become clear by this time that retinal projections were required for the entrainment of rhythmic behavior of rodents to the day/night cycle; under constant environmental conditions (i.e., constant light or dark) rhythmic behavior "free-runs," expressing the species-typical period of the endogenous circadian (circa "about" and dies "day") clock. After removing the eyes of hundreds of rats, Richter observed that the precise 24 h pattern of rhythmic nocturnal behavior obtained under light:dark conditions free-ran with a circadian period (Richter 1965). The introduction of autoradiographic techniques for demonstrating axonal connections in the central nervous system (Cowan et al. 1972) led to the discovery of a previously unknown retinal projection to the anterior hypothalamus terminating in the suprachiasmatic nucleus (SCN) (Moore and Lenn 1972; Hendrickson et al. 1972). The description of a retinohypothalamic tract (RHT) coupled with the observation that ablation of the SCN abolished behavioral circadian rhythms (Stephan and Zucker 1972) suggested that the SCN was the site of the circadian clock that is normally entrained to the day/night cycle by retinal signals transmitted via the RHT.

Although a direct connection between the retina and the SCN was thus established, it was not known what type of RGC innervated the SCN, whether these cells projected exclusively to the hypothalamus or what their receptive field properties were like. The receptive field properties of SCN-projecting RGCs were determined indirectly by examining the response of SCN neurons to photic stimulation of the retina; SCN neurons had extremely large receptive fields with no "surround" antagonism typical of most RGCs and they responded to stimulus luminance (Groos and Mason 1978, 1980; Meijer et al. 1986). The morphology of SCN-projecting RGCs was first identified by in vivo injection of tracer molecules that were retrogradely transported from the SCN to the retina via the RHT. It was estimated that 1–2% of the total RGC population projected to the SCN and these cells appeared to have a very simple dendritic morphology (Pickard 1980). Although the techniques available at the time precluded a complete morphological description, soma size analysis suggested that more than one type of RGC projected to the SCN (Pickard 1982).

It was also not known at this time whether rod and/or cone photoreceptors conveyed signals to SCN-projecting RGCs. The spectral sensitivity of light stimuli that affect circadian rhythms was first assessed using light-induced phase shifts of rodent circadian activity rhythms as an endpoint. The reported spectral sensitivity

curve generated from light-induced phase shifts had a maximum near 500 nm, similar to the absorption spectrum of rhodopsin, implying rod-generated signals. However, the threshold of the response was unusually high for the rod-dominated rodent retina and the temporal integration of the stimulus was also unusual for a rod-mediated response (Takahashi et al. 1984). Ebihara and Tsuji (1980) and later Foster et al. (1991) used *rd* mice to assess whether rod and/or cone photoreceptors conveyed photoentrainment signals to the SCN. Mice carrying the retinal degeneration mutation (*rd;* the mutation identified by Keeler 1924), are virtually devoid of rod and cone photoreceptors by four weeks of age and do not produce recordable electroretinographic responses or visual evoked potentials (Farber et al. 1994). These investigators reported that adult *rd*/*rd* mice were able to synchronize their circadian activity rhythms to cycles of light and darkness. Similar to Keeler (1927), Ebihara and Tsuji (1980) also suggested that cells other than rods and cones in the retina might be directly light sensitive. However, the universally acknowledged depiction of the organization of the mammalian retina prevailed despite these reports indicating that rodents with severe degeneration of the outer retina remained capable of responding to light (i.e., generating irradiance responses). At the time, the persistent response to light in retinal degenerate mice was widely attributed to the few cone photoreceptor remnants (cone photoreceptors lacking outer segments) that remain in these animals for many months (Dräger and Hubel 1978).

However, many who studied circadian photoentrainment believed that the evidence in support of an unknown "circadian" photoreceptor was compelling and doubted that a few cone photoreceptors lacking outer segments could account for the observed photoentrainment of behavioral rhythms; visual neuroscientists on the other hand, tended to reject the notion that an additional photoreceptor in the mammalian retina had been overlooked throughout 150 years of investigation. To directly test the interpretation that residual cone photoreceptor remnants were responsible for mediating the irradiance responses to light in retinal degenerate animals, transgenic mice were generated lacking all rod and cone photoreceptors. The fact that these animals also retained several irradiance responses including photoentrainment of their circadian locomotor behavior, the pupillary light reflex, and light-induced suppression of nocturnal pineal melatonin secretion provided further strong evidence for the existence of a non-rod, non-cone ocular photoreceptor (Freedman et al. 1999; Lucas et al. 1999) as removal of the eyes eliminates all irradiance responses (Nelson and Zucker 1981). Additional support for a non-rod, non-cone ocular photoreceptor came from reports in rodents and humans describing irradiance responses that had an action spectrum inconsistent with that of any known retinal photoreceptor (Yoshimura and Ebihara 1996; Lucas et al. 2001; Brainard et al. 2001; Thapan et al. 2001). Taken together these data appeared to provide clear evidence for the existence of a non-rod, non-cone photoreceptor in the mammalian retina, although which retinal cells responded to light in the absence of rods and cones and what type of photopigment mediated these responses briefly remained a mystery.

Melanopsin, the Photopigment of Intrinsically Photosensitive Retinal Ganglion Cells

While evidence was accumulating for the existence of a non-rod, non-cone photoreceptor in the mammalian retina, Provencio et al. (1998) were focusing their efforts on identifying the photopigment that might be responsible for the irradiance responses retained in mice lacking rods and cones. But rather than looking in mice or other mammals, these investigators studied frog skin. It was believed that the photoresponse of pigment cells (melanophores) in amphibian skin was mediated by a unique member of the rhodopsin family of G-protein coupled receptors although the exact nature of the opsin in frog skin remained unspecified (Daniolos et al. 1990). Provencio and his co-workers, using cultured dermal melanophores from *Xenopus laevis,* identified the photopigment responsible for the light-induced dispersion of melanosomes. In their ground-breaking paper they described the opsin, named melanopsin, and reported that melanopsin was a member of the opsin family of G-protein coupled receptors sharing the greatest sequence homology to octopus (invertebrate) rhodopsin. Importantly they also reported that melanopsin mRNA was expressed in frog dermal melanophores, in the brain and in the retina, but not in typical retinal photoreceptors (Provencio et al. 1998). These investigators subsequently described the distribution of melanopsin mRNA in the retina of mammals; in both primates and rodents, melanopsin mRNA was expressed not in rod or cone photoreceptors, but rather in the ganglion cell layer, providing the basis for the suggestion that RGCs expressing this novel mammalian opsin were directly photosensitive (Provencio et al. 2000). Gooley et al. (2001) quickly extended these findings by demonstrating that melanopsin was expressed in SCN-projecting RGCs.

SCN-Projecting RGCs Are Intrinsically Photosensitive and Express Melanopsin

The prediction that RGCs were photosensitive was borne out in early 2002 through a set of landmark reports by Berson, Hattar, Yau and colleagues. Berson and coworkers recorded from SCN-projecting RGCs in the rat retina and showed that when these neurons were isolated pharmacologically and physically from all rod and cone synaptic input, they generated action potentials in response to photic stimulation; the ganglion cells were intrinsically photosensitive (Berson et al. 2002). Importantly, they also showed that these intrinsically photosensitive retinal ganglion cells (ipRGCs) expressed melanopsin (Hattar et al. 2002). The discovery of melanopsin by Provencio et al. (1998) and the reports describing ipRGCs in the rodent retina (Berson et al. 2002; Hattar et al. 2002) laid the foundation for what is now an exciting and rapidly growing new subdivision of retinal biology. However, at the time, two key questions remained: (1) was melanopsin truly a photopigment; and (2) was melanopsin required for animals to show irradiance responses such as the pupillary light reflex or entrainment of circadian behavior to the day/night cycle?

The generation of melanopsin knockout mice (*Opn4*$^{-/-}$) answered the second question first. Mice lacking the melanopsin protein, with the ipRGCs otherwise apparently unaffected, retained the ability to entrain to daily cycles of light and darkness and they generated a pupillary light reflex, although several aspects of these irradiances responses were altered (Panda et al. 2002; Ruby et al. 2002; Lucas et al. 2003). Both acute and chronic effects of light on the circadian system were significantly attenuated in melanopsin-deficient mice (Panda et al. 2002; Ruby et al. 2002) and the pupillary light reflex was described as incomplete at high irradiances (Lucas et al. 2003). These unexpected results indicated that classical rod and/or cone photoreceptors and ipRGCs both contribute to irradiance responses. When melanopsin was knocked out in mice lacking functional rods and cones, all tested responses to light were eliminated, confirming a role for melanopsin in irradiance responses to light and also indicating the unlikelihood that any other photoreceptor in the mammalian retina had remained undetected (Panda et al. 2003).

The observation that melanopsin-deficient mice retain the ability to entrain behavioral circadian rhythms to the day/night cycle suggested either that conventional (non-melanopsin) RGCs send afferent fibers to the SCN or that ipRGCs receive synaptic input and relay rod/cone-driven signals to the SCN integrated with their intrinsic photoresponses. The first electron microscopic examination of melanopsin-expressing RGCs provided morphological evidence that ipRGCs receive synaptic input from amacrine cells and bipolar cells (Belenky et al. 2003); in vitro physiological studies of ipRGCs subsequently confirmed that they are driven by rod and/or cone photoreceptor input (Dacey et al. 2005; Perez-Leon et al. 2006; Wong et al. 2007; Schmidt et al. 2008). Moreover, the rod and/or cone photoreceptor-driven input is capable of generating physiological responses in ipRGCs in the absence of melanopsin and the intrinsic photoresponse (Pickard et al. 2009; Schmidt and Kofuji 2010). Thus there is no doubt that ipRGCs are integrated within the conventional signaling pathway in the retina (rod/cone → bipolar cell → RGC). However, the response of ipRGCs to rod/cone generated signals is not homogenous, consistent with the observation that there is considerable variation among ipRGCs in the neurotransmitter receptors they express (see below).

The question of whether conventional RGCs innervate the SCN was addressed initially in double-label studies in rodents. SCN-projecting RGCs were identified using tracer injections into the SCN, and the identified neurons were then assayed by in situ hybridization to determine melanopsin mRNA expression or by immunocytochemical staining of melanopsin protein. In the rat (Gooley et al. 2003) and golden hamster (Morin et al. 2003; Sollars et al. 2003), 80–90% of SCN-projecting RGCs were classified as melanopsin-expressing; in the mouse virtually all (>99%) SCN-projecting RGCs express melanopsin (Baver et al. 2008). Genetic or immunotoxin-induced ablation of melanopsin RGCs in the mouse eliminates these animal's ability to entrain to light/dark cycles, confirming that in this species, rod and/or cone influences on circadian entrainment are mediated via melanopsin expressing ipRGCs which act as a conduit for rod/cone signals to reach the SCN (Göz et al. 2008; Göler et al. 2008; Hatori et al. 2008).

In the rodent retina approximately 2–4% of all RGCs express melanopsin (Sollars et al. 2003; Hattar et al. 2006; Baver et al. 2008; Berson et al. 2010). As indicated above, in the mouse it appears that only melanopsin immunoreactive RGCs send afferent fibers to the SCN whereas this does not appear to be the case in the rat and golden hamster. The dissimilarity in findings among these three different rodents may represent true species differences, but it remains to be demonstrated using physiological techniques that the "non-melanopsin" SCN-projecting RGCs identified in the rat and golden hamster are not intrinsically light sensitive. It is possible that these RGCs either express too little melanopsin to be detected (Baver et al. 2008; Ecker et al. 2010) or express a melanopsin isoform not recognized by the antibodies currently available (Torii et al. 2007; Pires et al. 2009; Davies et al. 2011). The number of "non-melanopsin" RGCs sending afferent fibers to the SCN in the golden hamster and rat is small (i.e., 100–200) making the task of recording from these cells difficult. A complete description of the morphology and dendritic arborization pattern of "non-melanopsin" SCN-projecting RGCs would be useful for comparison to SCN-projecting melanopsin RGCs to ascertain if the "non-melanopsin" neurons projecting to the SCN represent a unique RGC type (Wässle 2004). Although genetic mouse models have played an important role in advancing our understanding of ipRGCs, studies are required on additional species before generalizations regarding RGC input to the SCN can be made.

Melanopsin Is a Photopigment

Evidence confirming the identification of melanopsin as a photopigment was derived from the heterologous expression of melanopsin in several different cell lines. The first data came from purified melanopsin protein harvested from melanopsin transfected COS cells. While it was shown that melanopsin was a photopigment that bound retinaldehyde and was capable of activating a G-protein (Newman et al. 2003), the spectral properties (i.e., maximal absorbance at ≈424 nm) were not consistent with the action spectrum observed by Berson and colleagues for melanopsin-expressing RGCs (≈484 nm) (Berson et al. 2002). Subsequently, the photopigment properties of melanopsin were confirmed after its expression in HEK cells that also expressed transient receptor potential C3 channels (Qiu et al. 2005), Neuro-2a cells (Melyan et al. 2005), and *Xenopus* oocytes (Panda et al. 2005). Together these studies provided convincing evidence that melanopsin was indeed a photopigment. However, one group again reported a melanopsin absorption maximum ≈420 nm (Melyan et al. 2005) whereas the others indicated that expressed melanopsin maximally absorbed light at ≈480 nm (Panda et al. 2005; Qiu et al. 2005), matching more closely the spectral tuning of pharmacologically isolated rat (Berson et al. 2002) and primate (Dacey et al. 2005) ipRGCs. It should be noted that non-mammalian melanopsin also shows peak spectral sensitivity ≈480 nm, in close agreement with mammalian ipRGCs (Koyanagi et al. 2005; Torii et al. 2007; Davies et al. 2011). Thus, it is now

generally agreed that mammalian melanopsin maximally absorbs light at ≈480 nm although direct in vitro spectroscopic analysis of purified mammalian melanopsin is still needed (Bailes and Lucas 2010).

ipRGC Physiological Responses to Light

Several characteristics of the ipRGC response to light set these ganglion cell photoreceptors apart from mammalian rod and cone photoreceptors. In particular, ipRGCs are less sensitive to photic stimulation and their response kinetics are extremely slow compared to that of rods and cones. In addition, the melanopsin phototransduction cascade appears similar to that of many invertebrates, with the result that the polarity of the ipRGC response to light is opposite that of rods and cones, resulting in the generation of action potentials.

ipRGC Response Kinetics

ipRGCs are relatively insensitive to light and their response to light stimulation is extremely sluggish compared to conventional RGCs. Response latency is inversely related to stimulus intensity and under dim light conditions ipRGCs can take many seconds to reach a peak response; the response may also persist for minutes after stimulus termination (Berson et al. 2002; Warren et al. 2003). On the other hand, ganglion cell photoreceptors are similar to rods and cones in that they show adaptation by adjusting their sensitivity according to lighting conditions (Wong et al. 2005). While slow to respond to dim light conditions, ipRGCs appear capable of responding to the capture of a single photon of light (Do et al. 2009). Thus the relatively low sensitivity to light does not appear to be the result of inefficient phototransduction but rather of poor photon catch. It has been estimated that the membrane density of melanopsin is about a thousand times lower than that of photopigments in the outer segments of rod and cone photoreceptors; this relatively low density may account for the poor absorption rate of ipRGCs (Brown and Lucas 2009; Do et al. 2009).

The capture of a single photon in an ipRGC generates a large and prolonged membrane current, greater than that recorded in rod photoreceptors but also 20-fold slower (Chen et al. 1999). It has been suggested that the slow response kinetics of ipRGCs may provide for long temporal integration, which may well suit the primary function of these cells, assessing ambient light levels via irradiance detection (Do et al. 2009). Moreover, since ipRGCs are also synaptically driven by rod and/or cone photoreceptors (Belenky et al. 2003; Dacey et al. 2005; Perez-Leon et al. 2006; Wong et al. 2007; Schmidt et al. 2008), ganglion cell photoreceptors themselves may not require the level of intrinsic sensitivity found in the classic photoreceptors.

It should be noted, however, that brief (1 s) light pulses (DeCoursey 1972; Earnest and Turek 1983) or a short series of extremely brief (2 ms), intense light flashes, which are ineffective as single flashes (van den Pol et al. 1998; Vidal and Morin 2007) can produce significant phase shifts of the circadian clock. Very brief stimuli do not appear to demonstrate the same type of temporal integration associated with light pulses several minutes in duration (Nelson and Takahashi 1999; Vidal and Morin 2007; Morin et al. 2010). The behavioral responses of the circadian system to brief light flashes may represent an integrated response of rod/cone and ganglion cell photoreceptors, although the ability of ipRGCs to generate an intrinsic photoresponse to a 2 ms light flash has not been tested directly. Nevertheless, *rd*/*rd* mice lacking rod and cone photoreceptors show patterns of locomotor activity suppression similar to wild type mice in response to a series of 2 ms light flashes (Morin and Studholme 2011), suggesting that ipRGCs are indeed capable of generating a photoresponse to very brief, intense light flashes.

Photon Capture in ipRGCs Results in Membrane Depolarization

In response to light stimulation, ipRGCs depolarize and generate action potentials, unlike the hyperpolarizing light responses of mammalian rod and cone photoreceptors (Berson et al. 2002; Warren et al. 2003; Hartwick et al. 2007) but similar to the light-inducing depolarizing responses of *Drosophila* and most other invertebrate photoreceptors (Yau and Hardie 2009). Perhaps this invertebrate-like response to light is not surprising since vertebrate melanopsin belongs to the rhabdomeric-opsin subfamily of opsins characteristic of most invertebrates (Isoldi et al. 2005; Nickle and Robinson 2007; Yau and Hardie 2009). Perhaps it should not be a surprise then, that mammalian melanopsin appears to utilize an invertebrate-like phototransduction signaling cascade.

Opsins in mammalian rod and cone ciliary photoreceptors couple to the G_t-protein, transducin, which activates a phosphodiesterase cascade resulting in the closure of cGMP-gated channels and cellular hyperpolarization (Yau and Hardie 2009). Melanopsin in mammalian ipRGCs is believed to be coupled to a G-protein of the G_q family as its cognate G-protein in vivo (Berson 2007; Peirson et al. 2007). In an early study using heterologous expression, melanopsin was shown to activate a G-protein although no further details were provided (Newman et al. 2003). Subsequent studies in other heterologous expression systems suggested a G_q class of G-protein (Panda et al. 2005; Qiu et al. 2005) as did work conducted in *Xenopus* dermal melanophores (Isoldi et al. 2005). Melanopsin and G_q also co-localize in amphioxus rhabdomeric photoreceptors (Koyanagi et al. 2005). However, the identity of the native G-protein employed by mammalian ipRGCs and the downstream cascade triggered by its activation still remain uncertain. There is some evidence supporting a role for $G_{q/11}$ which would activate the effecter enzyme phospholipase C, resulting in depolarization, an invertebrate-like phototransduction cascade (Graham et al. 2008).

The membrane channel that carries the initial inward current following the apparent activation of phospholipase C in ipRGCs has also not yet been conclusively identified. Involvement of mammalian homologues of the transient receptor potential (TRP) channels in *Drosophila* photoreceptors, termed TRP canonical (TRPC) channels, is supported by several lines of evidence including pharmacological blockade of light responses and identification of TRPC channel protein and/or mRNA in RGCs expressing melanopsin. Of the seven members of the subfamily of TRPC subunits that combine to form tetrameric channels (Hoffman et al. 2002), TRPC3, TRPC6, and/or TRPC7 have all been implicated as the TRPC channel mediating the initial depolarization in ipRGCs (Warren et al. 2006; Hartwick et al. 2007; Sekaran et al. 2007; Graham et al. 2008). However, in vitro recordings from ipRGCs in mouse lines lacking expression of functional TRPC3, TRPC6 or TRPC7 subunits indicate that light-evoked depolarization persist largely unchanged (Perez-Leighton et al. 2011). These results indicate that TRPC3, TRPC6, or TRPC7 homomeric channels do not mediate melanopsin-evoked depolarization in ipRGCs, but the possibility remains that these subunits may form heteromultimeric assemblies (Perez-Leighton et al. 2011). The demonstration that ectopic expression of melanopsin in conventional RGCs confers intrinsic photosensitivity to these cells (Lin et al. 2008) suggests that the channels gated by melanopsin may be widespread among ganglion cells. In addition, although one study reported that melanopsin activates diacylglycerol-sensitive TRPC channels in ipRGCs (Warren et al. 2006) another study failed to observe reduction of light-evoked currents in ipRGCs exposed to diacylglycerol analogs (Graham et al. 2008). The future development of more selective TRPC channel blockers and knockout mouse lines in which a combination of TRPC channels is eliminated will aid in determining the specific membrane channels mediating phototransduction in mammalian ipRGCs.

In *Drosophila,* light stimulates Ca^{2+} entry via a TRP channel that has an usually high Ca^{2+} selectivity (P_{Ca}:$P_{Na} > 50$:1) and there is minimal light-induced Ca^{2+} release from internal stores (Yau and Hardie 2009). As in *Drosophila* rhabdomeric photoreceptors, light stimulates an increase in intracellular calcium in mammalian ipRGCs (Sekaran et al. 2003; Hartwick et al. 2007). A small percentage of the light-evoked rise in somal intracellular Ca^{2+} appears to result from Ca^{2+} entry via the cation channel that carries the initial inward current (e.g., TRPC channel) (Hartwick et al. 2007). In HEK cells expressing human melanopsin, the light-triggered rise in intracellular Ca^{2+} results from the release of Ca^{2+} from intracellular stores (Kumbalasiri et al. 2007). However in primary cultures of native rat ipRGCs, Ca^{2+} release from internal stores does not significantly contribute to the light-evoked rise in intracellular Ca^{2+} (Hartwick et al. 2007), similar to *Drosophlia*. Approximately 90% of the light-triggered rise in intracellular Ca^{2+} in isolated rat ipRGCs maintained in primary culture is associated with the opening of L-type voltage-gated calcium channels and the rise in intracellular Ca^{2+} is highly correlated with action potential firing (Hartwick et al. 2007). The current model of ipRGC phototransduction and the light-evoked rise in intracellular Ca^{2+} is summarized in Fig. 2.

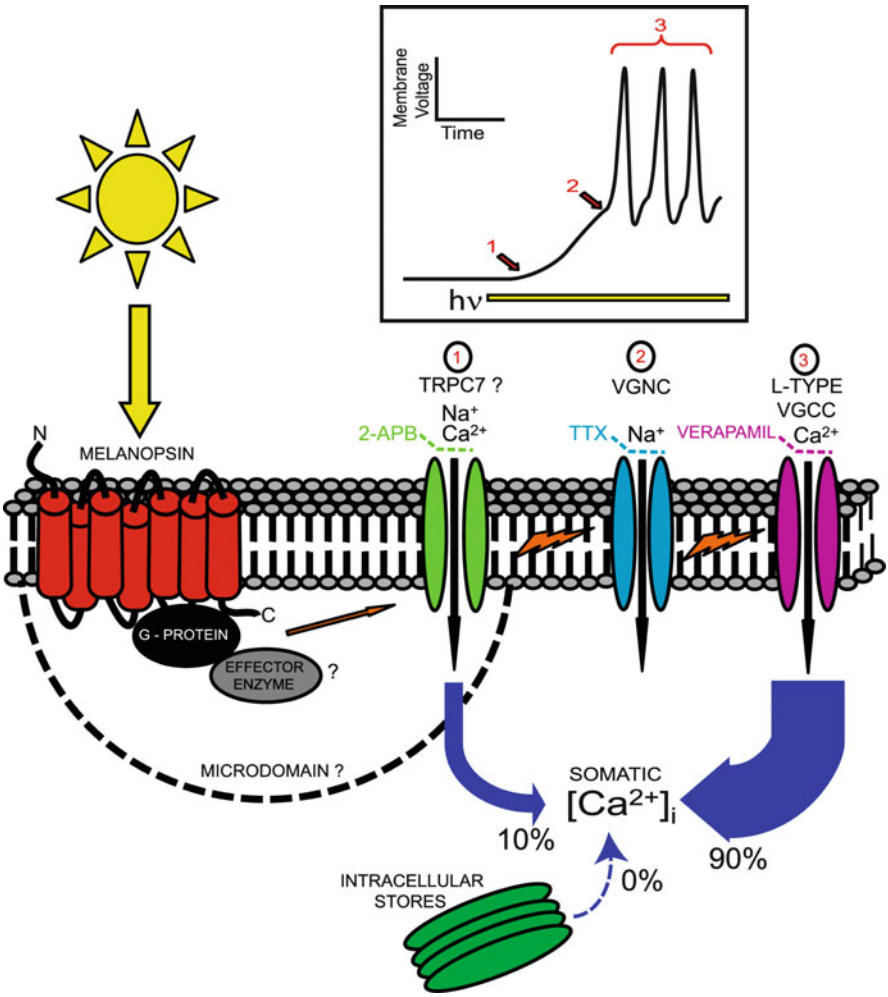

Fig. 2 Schematic overview of phototransduction and light-evoked Ca^{2+} influx in mammalian ipRGCs. After light stimulation of melanopsin photopigment in the plasma membrane, a signaling cascade is initiated that leads to the opening of the light-gated ion channel and membrane depolarization (labeled 1). The details of this cascade remain unclear, although there is evidence that it is G-protein dependent (Warren et al. 2006) with G_q a likely candidate and phospholipase C as the effector enzyme (Graham et al. 2008). The current model suggests a heteromeric TRPC channel is the light-gated ion channel that may include TRPC6 and TRPC7 subunits (Hartwick et al. 2007; Perez-Leighton et al. 2011). The ion flux through this 2-APB-sensitive channel depolarizes (denoted with a lightning bolt in the membrane) the membrane potential, resulting in the activation of voltaged-gated Na^+ channels (VGNCs; labeled 2). The Na^+ flux through TTX-sensitive VGNCs during action potential firing further depolarizes the membrane, leading to the activation of verapamil-sensitive L-type voltage-gated calcium channels (VGCCs) (labeled 3). The relative timing for the opening of these three channel types is illustrated in the boxed drawing that depicts the changes in membrane voltage induced by light exposure in a typical ipRGC. Although Ca^{2+} influx through the initial light-gated ion channel contributes to increased somatic

Chromophore Recycling and Bistability

Another aspect of the ipRGC response to light that appears similar to invertebrate rhabdomeric type photoreceptors is that of photopigment regeneration. The visual pigment consists of two components: an apoprotein moiety, the opsin, and the chromophore, 11-*cis*-retinal, a vitamin A derivative. Light isomerizes 11-*cis*-retinal to all-*trans*-retinal which results in rapid conformational changes in the opsin initiating the phototransduction cascade. After all-*trans*-retinal is reduced to all-*trans*-retinol in mammalian rod and cone photoreceptors, it exits the cell where it is converted in the overlying retinal pigment epithelium (RPE) back to 11-*cis*-retinal by RPE65, a retinyl isomerohydrolase for return to the photoreceptors (Yau and Hardie 2009). Müller cells are intrinsic glia that span the entire width of the mammalian retina and are derived from the same set of progenitors as the retinal neurons. They serve a variety of roles in the mammalian retina, including providing a barrier for substances moving into and out of the retina, and they play a vital role in retinal metabolism. Müller glial cells also recycle 11-*cis*-retinal using a slightly different mechanism than the RPE. These glial cells appear to serve only cone photoreceptors (Wang et al. 2009; Wang and Kefalov 2009) although their role in chromophore recycling from ipRGCs has not been examined.

Unlike vertebrate rod and cone ciliary photoreceptors, the invertebrate rhabdomeric photopigment regenerating system has been considered independent of other cells or tissue. Invertebrate photopigments remain bound to the opsin moiety and are re-isomerized by light of a longer wavelength than that which causes the initial photoactivation; these photopigments are thus considered bistable (Yau and Hardie 2009). It would seem highly unlikely that ipRGCs in the mammalian retina utilize the RPE to recycle 11-*cis*-retinal in vivo since ipRGCs are located in the inner retina, quite removed from the RPE. Moreover, native ipRGCs respond to prolonged light exposure when maintained in vitro in isolation from other retinal cells including Müller glial cells (Hartwick et al. 2007) suggesting either that ipRGCs can convert all-*trans*-retinal back to 11-*cis*-retinal autonomously or that native ipRGCs contain more 11-*cis*-retinal than can be bleached under those conditions. Thus melanopsin would appear to be a prime candidate for a vertebrate bistable photopigment, similar to those of invertebrates. Indeed, using heterologously expressed cephalochordate melanopsin, Koyanagi and colleagues unambiguously demonstrated that melanopsin functions as a bistable pigment in vitro acting as both a photopigment and a photoisomerase (Koyanagi et al. 2005). In zebrafish, in which five isoforms of melanopsin are expressed, some forms of melanopsin

Fig. 2 (continued) $[Ca^{2+}]_i$ during light stimulation, most of the Ca^{2+} signal is the result of the depolarization-induced opening of VGCCs (Hartwick et al. 2007). The presence of a membrane-associated microdomain that prevents some of the Ca^{2+} flux through the light-gated channel from reaching the somatic cytoplasam is also possible. The contribution of intracellular Ca^{2+} stores to light-evoked elevations in mammalian ipRGC $[Ca^{2+}]_i$ is negligible. Figure reprinted with permission from Hartwick et al. (2007)

display invertebrate-like bistability and remain within the opsin binding pocket, while in other forms of melanopsin, the 11-*cis*-retinal is isomerized and then released from the opsin similar to classic rod and cone photopigments (Davies et al. 2011). It remains to be directly demonstrated that melanopsin in mammalian ipRGCs functions as a bistable photopigment in vivo.

This question has been addressed, first by Fu and colleagues using a mouse model deficient in 11-*cis*-retinaldehyde synthesis. These experiments firmly established that melanopsin in mouse ipRGCs detects light with a vitamin A-based chromophore and they also suggested that melanopsin may be bistable (Fu et al. 2005b). Cooper and his coworkers have also addressed the issue of melanopsin's bistability in vivo using an indirect approach by recording single-unit activity in the mouse SCN in response to light stimulation of different wavelengths. They observed that pre-stimulation of the animal with long-wavelength light (e.g., 620 nm) enhanced the responses of SCN neurons to 480 nm light stimulation, consistent with long wavelength light causing re-isomerization and melanopsin being bistable (Mure et al. 2007). Similarly, these authors examined the pupillary light reflex in humans and reported that prior exposure to long wavelength light increases while short wavelength light decreases the amplitude of pupil constriction, again consistent with the interpretation of a bistable photopigment (Mure et al. 2009). Surprisingly however, little long-wavelength photic potentiation was observed when mouse ipRGCs were recorded in vitro using a multielectrode array (Mawad and Van Gelder 2008). The reasons for these differences are not apparent (Cooper and Mure 2008; Van Gelder and Mawad 2008). However, whether or not melanopsin is able to regenerate 11-*cis*-retinal through sequential photon absorption, it has also been reported that melanopsin uses a light-independent retinoid regeneration mechanism (Walker et al. 2008). Similarly, an enzymatic chromophore regeneration mechanism has also been described in *Drosophlia* despite the presence of a bistable photopigment (Wang et al. 2010). Studies using mice lacking outer retinal function may help to determine if long wavelength enhancement of melanopsin-mediated behaviors in vivo is mediated by long wavelength cone input to ipRGCs. Examination of individual native ipRGCs maintained in vitro (Hartwick et al. 2007) may also contribute to determining whether mammalian melanopsin is truly a bistable photopigment.

Multiple ipRGC Subtypes with Widespread Axonal Projections

The existence of a non-rod, non-cone ocular photoreceptor was originally suspected based primarily on the observation that mice lacking rods and cones synchronized their circadian locomotor activity to the day/night cycle by the daily phase resetting of their endogenous circadian clock (Ebihara and Tsuji 1980; Foster et al. 1991). As described above, the SCN circadian oscillator regulates this behavior and the SCN receives direct input from the retina (Moore and Lenn 1972; Hendrickson et al. 1972; Pickard 1982). Thus it was logical to first examine SCN-projecting RGCs for

melanopsin expression (Gooley et al. 2001) and intrinsic photosensitivity (Berson et al. 2002; Hattar et al. 2002). However, in their description of the efferent projections of melanopsin-expressing RGCs, Hattar et al. (2002) indicated that ipRGCs innervated not only the SCN but other brain regions as well (Hattar et al. 2002). Following these initial observations it has become clear that there are multiple ipRGC subtypes that send their axons to many areas in the brain and perhaps even back into the retina.

ipRGCs Targets in the Brain

It was known for some time before the discovery of ipRGCs that RGC axons terminating in the SCN arose as collateral branches of optic axons (Millhouse 1977) that continued on to the intergeniculate leaflet (IGL) of the thalamus (Pickard 1985), that the IGL projected to the SCN via the geniculohypothalamic tract (GHT) (Swanson et al. 1974; Pickard 1982) and that this indirect retinal input to the SCN modulated circadian behavior (Harrington and Rusak 1986; Pickard et al. 1987; Pickard 1989). Using a reporter mouse in which the melanopsin *opn4* gene was replaced with the *tau-lacZ* gene, Hattar and colleagues described melanopsin RGC projections to the IGL in addition to the SCN, consistent with these earlier reports (Hattar et al. 2002). The *tau-lacZ* gene codes for a protein consisting of the β-galactosidase enzyme fused to a signal sequence from tau to promote axonal transport of the reporter enzyme thus enabling visualization of melanopsin axons throughout the brain (Hattar et al. 2002). Using this reporter mouse, melanopsin-expressing RGCs were also described projecting to the olivary pretectal nucleus (OPN) (Hattar et al. 2002), the region of the midbrain that regulates the pupillary light reflex, and subsequently these projections were shown also to arise as collateral branches of RGCs innervating the SCN in the rat (Gooley et al. 2003) and golden hamster (Morin et al. 2003). Moreover, melanopsin RGCs were reported to terminate in several sites in the rat hypothalamus in addition to the SCN, including the ventral subparaventricular zone (vSPZ) dorsocaudal to the SCN and the ventrolateral preoptic nucleus (VLPO) lateral to the SCN (Gooley et al. 2003). As more detailed examinations were performed in the mouse, more central targets of melanopsin RGCs were revealed including the medial amygdala, lateral habenula, superior colliculus and periaqueductal gray (Hattar et al. 2006). Melanopsin projections to the superior colliculus were also described in the hamster (Morin et al. 2003) but not in the rat (Gooley et al. 2003). It is interesting to note that the dorsal raphe nucleus in the midbrain receives retinal afferent fibers but these do not appear to originate from ipRGCs (Luan et al. 2011). Figure 3 provides an overview of ipRGC projections.

Conspicuously lacking among the central targets of melanopsin-expressing RGCs revealed by β-galactosidase axonal labeling in the tau-lacZ mouse was a significant projection to the dorsal lateral geniculate nucleus (dLGN), the thalamic relay to the primary visual cortex mediating visual perception

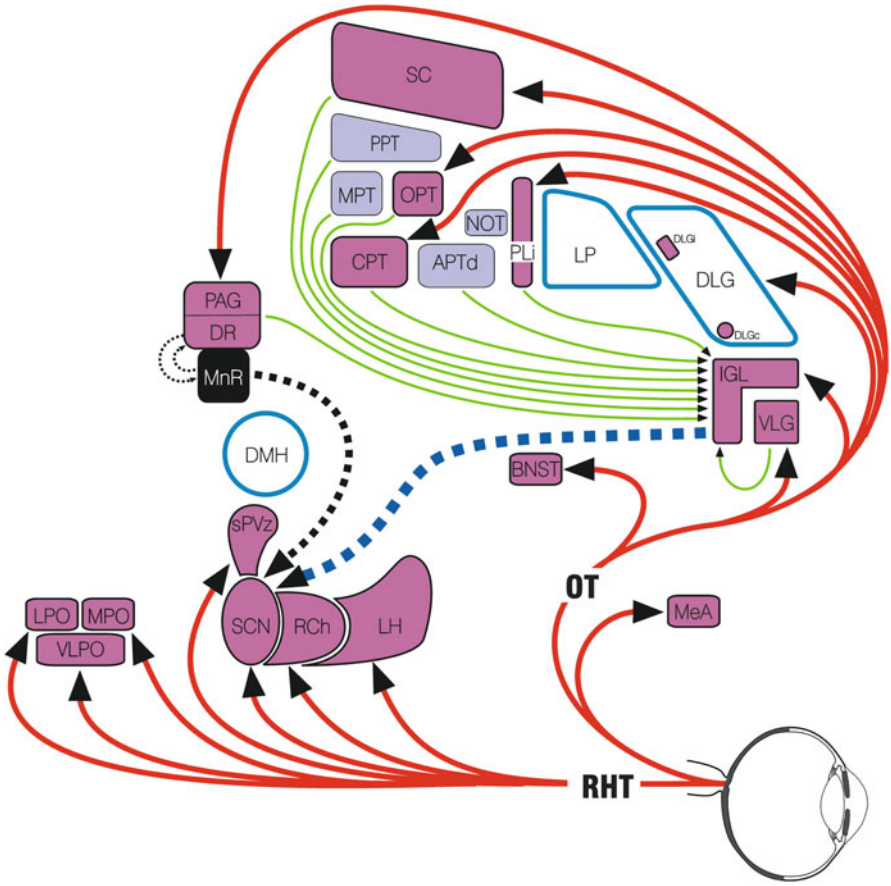

Fig. 3 Schematic representation of fore- and midbrain projections of the rodent retina, with special emphasis on targets of the ipRGCs (*purple regions*; *thick red lines*). Except for the median raphe nucleus (MnR), all other brain regions illustrated are retinorecipient but not necessarily from ipRGCs. *Thick*, *broken blue line* = geniculohypothalamic tract (*GHT*). *Medium*, *broken black line* = 5HT projection from MnR to SCN. *Thin*, *solid green lines* – non-visual projections to IGL. *Thin broken black lines* = reciprocal connections between MnR and DR. DLGi and DLGc – ipRGC projections to the ipsilateral and contralateral dorsal lateral geniculate nucleus, respectively. *APTd* anterior pretectal nucleus dorsal division; *BNST* bed nucleus of the stria terminalis; *CPT* commissural pretectal nucleus; *DLG* dorsal lateral geniculate nucleus; *DMH* dorsomedial hypothalamic nucleus; *DR* dorsal raphe nucleus; *IGL* intergeniculate leaflet; *LH* lateral hypothalamic area; *LPO* lateral preoptic area; *LP* lateral posterior thalamic thalamic nucleus; *MeA* medial amygdaloid nucleus; *MnR* median raphe nucleus; *MPO* medial preoptic area; *MPT* medial pretectal nucleus; *NOT* nucleus of the optic tract; *OPT* olivary pretectal nucleus; *OT* optic tract; *PAG* periaqueductal gray; *PLi* posterior limitans thalamic nucleus; *PPT* posterior pretectal nucleus; *Rch* retrochiasmatic area; *RHT* retinohypothalamic tract; *SC* superior colliculus; *SCN* suprachiasmatic nucleus; *sPVz* subparaventricular zone; *VLG* ventral lateral geniculate nucleus; *VLPO* ventral lateral preoptic nucleus. Based on (Morin et al. 1992; Morin and Blanchard 1997, 1998; Hattar et al. 2002; Gooley et al. 2003; Horowitz et al. 2004; Hattar et al. 2006; Ecker et al. 2010). Adapted from Morin LP, (in press) Circadian visual systems of mammals. In: How animals see the world, Lazareva OF, Shimizu T, Wasserman EA (eds), Chapter 21, pp. 389-415, Oxford University Press. Figure generously provided by L.P. Morin (Stony Brook University)

(Hattar et al. 2002, 2006). Although it is understandable that a photoreceptive system conveying irradiance information centrally might not send signals to the primary visual system mediating conscious visual perception, the absence of β-galactosidase labeled axons projecting to the dLGN in the mouse stood in contrast to work in the primate where melanopsin RGCs were retrogradely labeled after tracer injection into the dLGN (Dacey et al. 2005). The apparent species difference between rodent and primate regarding melanopsin afferents to the dLGN is now recognized to be the result of an under-representation of the melanopsin afferent fibers in the tau-lacZ reporter mouse. For reasons not well understood, the β-galactosidase reporter protein is expressed at detectable levels only in ≈50% of the melanopsin RGCs in the adult tau-lacZ mouse retina (Baver et al. 2008). Using a new *Opn4*-reporter mouse line in which all melanopsin RGCs appear to express the reporter protein, Hattar and colleagues have described widespread melanopsin RGC axonal projections that include a substantial innervation in the dLGN (Ecker et al. 2010).

A substantial projection of ipRGCs to the lateral geniculate body indicates that the apparent dichotomy of "image-forming" and "non-image forming" visual systems, often used to contrast ipRGCs from the rod and cone photoreceptors of the primary visual system (Fu et al. 2005a; Peirson et al. 2009) is perhaps in need of revision, since even at the level of the retina the "visual" rod and cone photoreceptors communicate with the "non-visual" ipRGCs. The role of ipRGC input to the dLGN is still unclear although Dacey and colleagues have suggested that dLGN-projecting ipRGCs in the primate might play a role in the conscious perception of brightness (Dacey et al. 2005). This hypothesis is supported by a report describing non-image-forming responses of two visually blind subjects, one a 56 year old female with autosomal-dominant cone-rod dystrophy and the other an 87 year old male patient with retinitis pigmentosa. In each case, the patient's circadian system appeared to be entrained to the day/night cycle and an intact pupillary light reflex was elicited but only when light exposure was extended to 10 s duration (brief light exposure was ineffective), apparently mediated by ipRGCs (Zaida et al. 2007) and reminiscent of the light-induced iris constriction described by Keeler (1927) in his blind mice. One subject was also reported to be able to correctly identify the presence of a 481 nm test light but was unable to detect light at shorter or longer wavelengths. This unprecedented luminance awareness without conscious visual perception was described by the patient as "brightness" (Zaida et al. 2007). These intriguing findings are clearly in need of further investigation.

A role for melanopsin-based phototransduction in pattern vision in the absence of rods and cones was recently reported. Ecker and co-workers (2010) used a mouse strain in which rod and cone phototransduction had been genetically silenced by disruption of the genes encoding rod α transducin (*Gnat1*) and cone-specific α3 cyclic nucleotide gated channel subunit (*Cnga3*) ($Gnat1^{-/-}$; $Cnga3^{-/-}$ double knockouts) leaving only ipRGCs as functional photoreceptors. The dKO mice were able to discriminate grating stimuli from equiluminant gray and had measurable visual acuity implying a role for ipRGCs in dLGN-mediated visual perception

(Ecker et al. 2010). However, these findings have come under question because it appears that the method used to silence rod and cone phototransduction in this mouse strain may not have been completely successful; these mice apparently retain significant and widespread outer retinal photoreception based on a Gnat1-independent phototransduction mechanism downstream of rod opsin (Allen et al. 2010). Thus the role of ipRGCs in pattern vision remains unclear.

ipRGC Intraretinal Signaling

ipRGCs send irradiance signals centrally via the optic nerve and in addition, these novel ganglion cell photoreceptors also send signals to other cells in the retina via both synaptic and non-synaptic mechanisms. ipRGCs provide light-evoked excitatory signals to dopaminergic amacrine cells and they are coupled to GABAergic amacrine cells via gap junctions.

ipRGCs Provide Excitatory Drive to Dopaminergic Amacrine Cells

Dopaminergic amacrine cells reside in the INL, receive bipolar cell input and release dopamine through volume transmission, influencing visual signaling by all major classes of retinal neurons, from photoreceptors to ganglion cells. However, the mechanism by which light regulates dopaminergic amacrine cell activity has remained poorly understood.

Dopaminergic amacrine cells release dopamine in response to flickering light and steady background illumination, as well as during prolonged darkness (Witkovsky 2004). It was demonstrated that this functional heterogeneity was reflected at the cellular level by physiologically distinct subpopulations of dopaminergic amacrine cells which show transient, sustained, and null responses to light (Zhang et al. 2007). ON-transient dopaminergic amacrine cells receive ON-bipolar cell input, perhaps via ectopic ON-bipolar cell synapses in the outer sublayer of the IPL (Dumitrescu et al. 2009) whereas input from bipolar cells is not required for the excitatory light responses of ON-sustained dopaminergic amacrine cells (Zhang et al. 2008). Surprisingly, ON-sustained dopaminergic amacrine cells receive excitatory (glutamatergic) drive from ipRGCs (Zhang et al. 2008, 2010), perhaps where their processes are in direct contact with ipRGC dendrites in the IPL near the border of the INL. ON-transient dopaminergic amacrine cell responses to light are absent in rd^{-}/rd^{-} mice lacking rods and cones, consistent with the interpretation that photoreceptors acting via bipolar cells provide signals to these cells (Zhang et al. 2008). Conversely, when recordings were made in dopaminergic amacrine cells in melanopsin knockout mice, none of the 35 cells examined that responded to light stimulation showed ON-sustained responses, consistent with the previous findings indicating that this subtype of dopaminergic amacrine cell is driven only by ipRGCs (Zhang et al. 2010). This unprecedented ganglion cell signaling within the retina provides a novel basis for light-evoked restructuring of retinal circuits

via dopaminergic amacrine cells and indicates that information flow in the retina is truly bi-directional.

Although dendrites of melanopsin RGCs are in contact with dopaminergic amacrine cell processes in the IPL near the border of the INL (Ostergaard et al 2007; Viney et al. 2007; Vugler et al. 2007; Zhang et al. 2008), there is no direct evidence that ipRGC signals to dopaminergic amacrine cells occur via their dendrites. Another possible mechanism by which ipRGCs might communicate with dopaminergic neurons is via ipRGC axon collaterals that loop back into the INL to synapse on dopaminergic amacrine cells. RGCs sending axon collaterals into the IPL have been described in cat (Dacey 1985), monkey (Usai et al. 1991) and human retina (Peterson and Dacey 1998); in human retina ≈2% the RGCs examined had intraretinal axon collaterals that terminated in the outer half of the IPL and arose from RGCs with sparsely branched monostratified dendritic trees that aborized in the ON sublayer of the IPL (Peterson and Dacey 1998). In the cat retina, a small number of varicose processes in the IPL stain for one of the isoforms of the vesicular glutamate transporter (VGLUT2) and it was suggested that these may represent RGC axon collaterals (Fyk-Kolodziej et al. 2004); ipRGCs use glutamate as a neurotransmitter and express VGLUT2 (Johnson et al. 2007; Engelund et al. 2010). A preliminary report indicates that indeed some ipRGCs may send axon collaterals into the IPL (Joo et al. 2011).

ipRGCs Are Coupled to GABAergic Amacrine Cells via Gap Junctions

In addition to regulating the activity of ON-sustained dopaminergic amacrine cells in the retina, it was reported that ipRGCs also influence the activity of other cells in the ganglion cell layer of the retina via electrical synapses or gap junctions (Sekaran et al. 2003, 2005). These investigators examined light-evoked increases in intracellular Ca^{2+} in cells in the ganglion cell layer and concluded that the light-responsive units formed an extensive network that could be uncoupled by application of the gap junction blocker carbenoxolone (Sekaran et al. 2003, 2005). However, Bramley et al. (2011) have reported that carbenoxolone blocks the light-evoked rise in intracellular Ca^{2+} in isolated rat ipRGCs by blocking voltage-gated calcium channels; similar effects of carbenoxolone on voltage-gated calcium channels have been described for isolated amphibian cone photoreceptors (Vessey et al. 2004). The direct action of carbenoxolone on light-evoked Ca^{2+} responses in ipRGCs would have led Sekaran et al. (2003, 2005) to greatly overestimate the extent of coupling between ipRGCs and other cells in the ganglion cell layer of the retina. This is not to say that ipRGCs do not form electrical synapses with other cells. Neurobiotin tracer injections into individual ipRGCs revealed coupling to an average of ≈8 widefield GABAergic amacrine cells located in the ganglion cell layer; no homologous tracer coupling to ipRGCs or heterologous coupling to other ganglion cells was observed (Müller et al. 2010). Neither the connexins that mediate coupling between ipRGCs and GABAergic amacrine cells nor the function of this electrical coupling between ipRGCs and displaced amacrine cells is currently known.

Different Types of ipRGC Have Different Central Targets

There are multiple types of ganglion cell in the mammalian retina. Based on morphological criteria such as soma size, the level of dendritic stratification in the inner plexiform layer (IPL), the extent of the dendritic field and the complexity of dendritic branching, conventional ganglion cells have been grouped into many types or clusters (Rockhill et al. 2002; Kong et al. 2005). Physiologically, ganglion cells can be classified simply as belonging to one of three types; those that respond to increments in light (ON cells), those that respond to decrements in light (OFF cells), and those that respond to the initiation and termination of a stimulus (ON-OFF cells). ON cells have their dendritic processes confined to the lower part of the IPL, the ON substratum, where they typically receive input from ON bipolar cells; OFF cells have their dendrites limited to the upper stratum of the IPL, the OFF sublayer, and receive input from OFF bipolar cells. Ganglion cells with bistratified dendritic arborizations in both the lower and upper layers of the IPL are ON-OFF cells (Famiglietti and Kolb 1976; Nelson et al. 1978).

In their original report of SCN-projecting ipRGCs in the rat, Berson et al. (2002) described these cells as sparsely branching and stratifying almost exclusively in the OFF sublayer of the IPL, near the border of the inner nuclear layer (INL). In the primate retina, two types of monostratified ipRGCs were described that send their dendrites to either the inner or the outer sublayers of the IPL although both types generated sustained ON responses to light stimulation recorded in vitro (Dacey et al. 2005). It was very unusual to find ganglion cells with dendrites in the OFF sublayer of the IPL generating ON responses to light (see below). When Baver et al. (2008) retrogradely labeled SCN-projecting RGCs in the tau-lacZ reporter mouse and examined cells for melanopsin, they found that the vast majority (80%) of SCN-projecting ipRGCs deployed their dendrites to the OFF sublamina of the IPL near the INL border and these cells were termed M1 cells. The remainder of ipRGCs projecting to the SCN sent their dendrites to the ON sublayer of the IPL; these cells were termed M2 (Baver et al. 2008). These two plexuses of melanopsin dendrites in the inner and outer IPL of the mouse had been described previously (Provencio et al. 2002). In addition, the melanopsin immunostaining of M1 ipRGCs usually appeared more intense than the staining of the M2 cells suggesting that M1 ipRGCs expressed more melanopsin protein.

M1 and M2 ipRGCs also project to the OPN in approximately equal proportions, but they terminate in different regions of the OPN; M1 ipRGCs innervate the outer shell region of the OPN where projection neurons that innervate the pre-autonomic Edinger-Westphal nucleus reside (Baver et al. 2008). M2 ipRGCs send their axons to innervate the OPN central core (Baver et al. 2008; Ecker et al. 2010). In addition to sending their dendrites to different regions of the IPL, M2 ipRGCs are generally considered to have a more complex dendritic arborization pattern and are approximately one log unit less sensitive to light compared to M1 cells (Schmidt et al. 2008; Schmidt and Kofuji 2009; Schmidt et al. 2011). The lower intrinsic sensitivity to light would be consistent with the suggested lower level of

melanopsin expression in these cells (Baver et al. 2008). Although M2 ipRGCs may generate a smaller intrinsic response to light, the rod/cone mediated synaptic input plays a greater role in shaping the integrated light-evoked responses and the resting membrane properties of M2 cells than M1 cells (Schmidt and Kofuji 2010).

Both M1 and M2 ipRGCs receive excitatory input via the ON bipolar pathway (Pickard et al. 2009; Schmidt and Kofuji 2010). The anatomical basis for this very unusual ON physiological input to M1 ipRGCs with dendrites in the OFF sublayer of the IPL appears to be mediated by ectopic synapses onto M1 ipRGCs from ON-bipolar cells as their axons pass through the OFF layer of the IPL (Fig. 1) (Dumitrescu et al. 2009; Hoshi et al. 2009). This arrangement has been described as an accessory ON sublayer in the outer IPL (Dumitrescu et al. 2009). In addition to the different morphological and physiological characteristics between M1 and M2 ipRGCs described above, very recently it has been reported that M1 cells can be further discriminated into two subgroups based on a molecular marker, the transcription factor Brn3b, with Brn3b-negative M1 cells projecting to the SCN and Brn3b-positive cells innervating the shell of the OPN (Chen et al. 2011). It remains to be determined if there are also physiological differences between these subgroups of M1 ipRGCs.

In addition to M1 and M2 ipRGCs, an M3 ipRGC has been described with dendrites located in both the ON and OFF sublayers of the IPL (Warren et al. 2003; Viney et al. 2007; Schmidt et al. 2008). M3 ipRGCs form a morphologically heterogeneous population with physiological properties similar to those of M2 cells (Schmidt and Kofuji 2011). It remains unclear whether M3 cells represent a distinct ipRGC subtype (Berson et al. 2010). Using a Cre/loxP system, two additional subtypes of ipRGC have been reported; both cell types (M4 and M5) have dendrites that stratisfy in the ON sublayer of the IPL (Ecker et al. 2010). The morphology of M4 and M5 cells are distinct from the other ipRGCs and although they display a very weak intrinsic light response, no melanopsin can be detected in these cells using immunocytochemical techniques (Ecker et al. 2010). The central targets of M3 cells are unknown and it has been suggested that M4 and M5 cells project to the dLGN, superior colliculus and OPN core (see Schmidt et al. 2011). The specific physiological roles played by ipRGC subtypes remains to be determined and it is unclear what role the extremely weak intrinsic light response of M4 and M5 ipRGCs plays in the integrated light-evoked response of these cells. It is interesting to note that in the tiger salamander retina, all ipRGCs are ON ganglion cells and all ON RGCs appear to be intrinsically photosensitive (Rajaraman 2012).

ipRGC Input to the Ventrolateral Preoptic Nucleus

A series of papers reported that ipRGC input to the ventral lateral preoptic nucleus (VLPO) can induce sleep. The VLPO is a region of the hypothalamus involved in sleep homeostasis; VLPO neurons are active during sleep (Gaus et al. 2002). It was previously established that the VLPO receives ipRGC input (Gooley et al. 2003; Hattar et al. 2006) and it was well known that light can influence sleep, promoting

alertness in day-active species and sleep in night-active species. Light presented to mice during the dark period activates neurons in the VLPO and induces sleep. These effects are still present, albeit reduced, in melanopsin knockout mice, indicating that rods and cones also participate in the effects of light on sleep (Altimus et al. 2008; Lupi et al. 2008; Tsai et al. 2009) although a recent report indicates that some melanopsin KO mice exhibit light-induced photosomnolence whereas other do not (Morin and Studholme 2011). The specific subtype of ipRGC innervating the VLPO is currently unknown.

ipRGC Input to the SCN and Seasonal Affective Disorder

The SCN receives a dense serotonergic input that arises from the mesencephalic median raphe nucleus. Selective destruction of serotonergic input to the SCN amplifies circadian behavioral responses to light (Smale et al. 1990; Morin and Blanchard 1991). One site of serotonin's action in the SCN is at 5-HT_{1B} receptors on ipRGC terminals; activation of these presynaptic inhibitory receptors modulates the response of the SCN to photic input (Pickard et al. 1996, 1999). Moreover, 5-HT_{1B} receptor knockout mice maintained under short-day (winter-like) conditions exhibit a delayed phase relationship to the day/night cycle (Sollars et al. 2006) resembling the phase delay demonstrated by people suffering from recurrent winter depression or seasonal affective disorder (SAD) (Lewy et al. 1987; Terman and Terman 2005). Recently Provencio and colleagues described a missense variant of the melanopsin gene in SAD patients (Roecklein et al. 2009). It is likely that many factors contribute to the etiology of SAD, and these may well include reduced sensitivity to light that may result from abnormalities in phototransduction in ipRGCs (Roecklein et al. 2009) and/or abnormalities in 5-HT neurotransmission in the SCN (Sollars et al. 2006).

Alterations in the phase angle of entrainment to the day/night cycle are associated with alterations in the amplitude of the diurnal rhythm of plasma corticosterone secreted from the adrenal cortex; a blunted cortisol rhythm has been reported in SAD patients (Avery et al. 1997). The reduction in corticosterone secretion may result from an altered phase relationship between the adrenal gland's innate circadian rhythm in steroid biosynthesis to the day/night cycle (Oster et al. 2006; Son et al. 2008). Although it is widely accepted that photic input to the hypothalamus is mediated via the RHT to the SCN (see Ishida et al. 2005), it is possible that ipRGC projections to the hypothalamus caudal to the SCN such as the vSPZ (Pickard and Silverman 1981; Gooley et al. 2003; Hattar et al. 2006) may provide direct photic input to hypothalamic neurons that regulate the autonomic outflow to the major organs of the body. Corticosterone is a potent transcriptional regulator and the daily rhythm of corticosterone secretion affects rhythmic gene expression in the brain and many organs of the body (Balsalobre et al. 2000; Lamont et al. 2005). It will be interesting to determine if ipRGCs send photic signals to hypothalamic regions outside the SCN to regulate descending autonomic

circuits that entrain the adrenal clock and thereby contribute to the regulation of corticosterone secretion.

ipRGCs and Retinal Disease

It has been known for several decades that monosodium-L-glutamate (MSG) administered during the neonatal period selectively destroys amacrine, bipolar and ganglion cells in the inner retina resulting in atrophy of the optic nerves and impaired vision in rodents, although the rod and cone photoreceptors are unaffected (Olney 1969). Nemeroff et al. (1977) reported that MSG-treated rats with severe optic nerve atrophy nevertheless showed normal light-induced reduction in serotonin-N-acetyl-transferase activity in the pineal. This result indicated that despite the optic nerve atrophy, sufficient photic signals reached the SCN (or other hypothalamic nuclei) to regulate the well-known descending autonomic circuits to the pineal. Pickard et al. (1982) subsequently examined photic entrainment of circadian activity rhythms and the central projections of the surviving RGCs in MSG-treated golden hamsters and showed that the RHT was affected very little although the primary visual pathways to the thalamus were markedly reduced. These observations suggested that the RGCs that innervated the SCN were resistant to glutamate-induced degeneration (Pickard et al. 1982). It was later estimated that ≈90% of all RGCs were destroyed by MSG treatment whereas retinal input to the SCN was reduced by only ≈30% (Chambille and Serviere 1993). Among the small subpopulation of RGCs in which the immediate-early gene *c-fos* can be induced by light, only about one third are affected by MSG treatment, whereas >90% of RGCs in which light does not evoke Fos are destroyed by MSG (Chambille 1998). The vast majority of RGCs expressing Fos after light stimulation project to the SCN (Hannibal et al. 2007) and these would appear to be M1 ipRGCs (Pickard et al. 2009). Collectively these data suggest that a major portion of the RGCs that innervate the SCN survive neonatal glutamate-induced toxicity.

The mechanism(s) whereby M1 ipRGCs might be protected in vivo against glutamate toxicity are unknown although the response of ipRGCs to glutamate application in vitro appears to be more heterogeneous (Pickard, Hartwick and Sollars, unpublished observations) than that described for conventional RGCs in culture (Hartwick et al. 2008). The diverse response of ipRGCs to glutamate application most likely results from the heterogeneous expression of glutamate receptors and their subunits among ipRGCs although little is currently known about the glutamate receptor subtypes expressed by different ipRGCs (Jakobs et al. 2007). Similarly, the responses of cultured ipRGCs to the inhibitory neurotransmitter glycine are not homogenous (Wiles et al. 2011) giving further evidence that different ipRGC subtypes may have distinct neurotransmitter receptor profiles.

Glaucoma, characterized by RGC degeneration and damage to the optic nerves, is a leading cause of blindness worldwide. Several different animal models of glaucoma have been investigated to determine if melanopsin RGCs are injury-resistant.

Melanopsin-expressing RGCs were found to be selectively spared compared to conventional RGCs in a rat model of chronic ocular hypertension induced by laser photocoagulation of the episcleral and limbal veins of the eye with resultant elevated intraocular pressure (IOP) (Li et al. 2006, 2008). In a different rat model of episcleral vein cauterization, melanopsin-expression RGCs were not apparently spared (Drouyer et al. 2008; Wang et al. 2008) and functional deficits in irradiance responses were reported (Drouyer et al. 2008). In a rat glaucoma model of chronic ocular hypertension induced by weekly injections of chondroitin sulfate into the anterior chamber, melanopsin-expressing RGCs were also found to be equally susceptible to the deleterious effects of ocular hypertension and functional deficits in irradiance responses were also described (de Zavalia et al. 2011). In a model of inherited glaucoma (mouse strain DBA/2J) in which IOP is elevated, melanopsin-expressing RGCs are not selectively spared (Jakobs et al. 2005). Patients with early-stage glaucoma show no deficits in ipRGC function determined by the postillumination pupil response whereas in people with advanced glaucoma, ipRGC function was reduced (Feigl et al 2011). Conversely, axotomized melanopsin-expressing RGCs show enhanced survival compared to conventional RGCs in the mouse (Robinson and Madison 2004). Melanopsin-expressing RGCs were also substantially unaffected in patients with genetically determined neurodegenerative optic neuropathies that selectively affect RGCs due to mitochondrial dysfunction (i.e., Leber hereditary optic neuropathy and dominant optic atrophy) (La Morgia et al. 2010). Taken together, the data suggest that melanopsin-expressing ipRGCs are relatively resistant to several pathological situations although the mechanism(s) that protect the cells under these particular conditions are unknown.

The Future

Since the discovery of ipRGCs less than a decade ago, a remarkable amount of information has been gathered to document the idiosyncrasies of these neuronal photoreceptors and the diverse array of connections and apparent functions these cells subserve. It is clear that much work remains to be done, for although many questions have already been addressed, few answers seem definitive, particularly with regard to the basic phototransduction cascade. The development of novel drugs that selectively inhibit melanopsin phototransduction will help answer some of these questions. Novel applications of the melanopsin phototransduction mechanism in cell lines, such as light-inducible transcription for drug delivery (Ye et al. 2011) are sure to become more numerous. Still, as the mere existence of ipRGCs eluded notice during the first century and a half of active retinal research, it is a near certainty that future research on the structure and function of ipRGCs will shed unexpected new light on most currently held notions of retinal organization.

Acknowledgment Supported by grants from the National Institutes of Health; National Institute of Neurological Disorders and Stroke R01 NS035615 and National Eye Institute R01 EY017809.

References

Allen AE, Cameron MA, Brown TM et al (2010) Visual responses in mice lacking critical components of all known retinal phototransduction cascades. PLoS ONE 5:e15063

Altimus CM, Güler AD, Villa KL et al (2008) Rods-cones and melanopsin detect light and dark to modulate sleep independent of image formation. Proc Natl Acad Sci USA 105:19998–20003

Aschoff J (1960) Exogenous and endogenous components in circadian rhythms. Cold Spring Harbor Symp on Quan Biol 25:11–28

Avery DH, Dahl K, Savage MV et al (1997) Circadian temperature and cortisol rhythms during a constant routine are phase-delayed in hypersomnic winter depression. Biol Psychiatry 41:1109–1123

Bailes HJ, Lucas RJ (2010) Melanopsin and inner retinal photoreception. Cell Mol Life Sci 67:99–111

Balsalobre A, Brown SA, Marcacci L et al (2000) Resetting of circadian time in peripheral tissues by glucocorticoid signaling. Science 289:2344–2347

Baver SB, Pickard GE, Sollars PJ et al (2008) Two types of melanopsin retinal ganglion cell differentially innervate the hypothalamic suprachiasmatic nucleus and the olivary pretectal nucleus. Eur J Neurosci 27:1763–1770

Belenky MA, Smeraski CA, Provencio I et al (2003) Melanopsin retinal ganglion cells receive bipolar and amacrine cell synapses. J Comp Neurol 460:380–393

Berson DM (2003) Strange vision: ganglion cells as circadian photoreceptors. Trends Neurosci 26:314–320

Berson DM (2007) Phototransduction in ganglion-cell photoreceptors. Pflügers Arch 454:849–855

Berson DM, Dunn FA, Takao M (2002) Phototransduction by retinal ganglion cells that set the circadian clock. Science 295:1070–1073

Berson DM, Castrucci AM, Provencio I (2010) Morphology and mosaics of melanopsin-expressing retinal ganglion cell types in mice. J Comp Neurol 518:2405–2422

Brainard GC, Hanifin JP, Rollag MD et al (2001) Human melatonin regulation is not mediated by the three cone photopic visual system. J Clin Endocrinol Met 86:433–436

Bramley JR, Wiles EM, Sollars PJ et al (2011) Carbenoxolone blocks the light-evoked rise in intracellular calcium in isolated melanopsin ganglion cell photoreceptors. PLoS ONE 6:e22721

Brown TM, Lucas RJ (2009) Melanopsin phototransduction: great excitement over a poor catch. Curr Biol 19:R256–R257

Cajal S Ramón y (1894) Les Nouvelles Ideés sur la Structure du Système Nerveux chez l'Homme et chez les Vértebrés. Reinwald, Paris

Chambille I (1998) Retinal ganglion cells expressing the FOS protein after light stimulation in the Syrian hamster are relatively insensitive to neonatal treatment with monosodium glutamate. J Comp Neurol 392:458–467

Chambille I, Serviere J (1993) Neurotoxic effects of neonatal injections of monosodium L-glutamate (L-MSG) on the retinal ganglion cell layer of the golden hamster: anatomical and functional consequences on the circadian system. J Comp Neurol 338:67–82

Chen CK, Burns ME, Spencer M et al (1999) Abnormal photoresponses and light-induced apoptosis in rods lacking rhodopsin kinase. Proc Natl Acad Sci USA 96:3718–3722

Chen SK, Badea TC, Hattar S (2011) Photoentrainment and pupillary light reflex are mediated by distinct populations of ipRGCs. Nature 476:92–95

Cooper HM, Mure LS (2008) Expected and unexpected properties of melanopsin signaling. J Biol Rhythms 23:392–393
Cowan WM, Gottlieb DI, Hendrickson AE et al (1972) The autoradiographic demonstration of axonal connection in the central nervous system. Brain Res 37:21–51
Dacey DM (1985) Wide-spreading terminal axons in the inner plexiform layer of the cat's retina: evidence for intrinsic axon collaterals of ganglion cells. J Comp Neurol 242:247–262
Dacey DM, Lioa H-W, Peterson BB et al (2005) Melanopsin-expressing ganglion cells in primate retina signal colour and irradiance and project to the LGN. Nature 433:749–754
Daniolos A, Lerner AB, Lerner MR (1990) Action of light on frog pigment cells in culture. Pigment Cell Res 3:38–43
Darwin C, Darwin F (1880) The power of movements in plants. John Murray, London
Davies WIL, Zheng L, Hughes S et al (2011) Functional diversity of melanopsins and their global expression in the teleost retina. Cell Mol Life Sci (in press)
De Candolle A (1832) Physiologie vegetale, ou Exposition des forces et des fonctions vitals des vegetaux, Bechet jeune, Paris
De Mairan M (1729) Observation botanique. Historie de l'Academie Royale des Sciences, Paris:1
DeCoursey PJ (1972) LD ratios and the entrainment of circadian activity in a nocturnal and diurnal rodent. J Comp Physiol 78:221–235
de Zavalia N, Plano SA, Fernandez DC et al (2011) Effect of experimental glaucoma on the non-image forming visual system. J Neurochem 117:904–914
Do MT, Kang SH, Xue T et al (2009) Photon capture and signaling by melanopsin retinal ganglion cells. Nature 457:281–287
Dräger UC, Hubel DH (1978) Studies of visual function and its decay in mice with hereditary retinal degeneration. J Comp Neurol 180:85–114
Drouyer E, Dkhissi-Benyahya O, Chiquet C et al (2008) Glaucoma alters the circadian timing system. PLoS ONE 3:e3931
Dumitrescu ON, Pucci FG, Wong KY et al (2009) Ectopic retinal ON bipolar cell synapses in the OFF inner plexiform layer: contacts with dopaminergic amacrine cells and melanopsin ganglion cells. J Comp Neurol 517:226–244
Earnest DJ, Turek FW (1983) Effect of one-second light pulses on testicular function and locomotor activity in the golden hamster. Biol Reprod 28:557–565
Ebihara S, Tsuji K (1980) Entrainment of the circadian activity rhythm to the light dark cycle: effective light intensity for a Zeitgeber in the retinal degenerate C3H mouse and normal C57BL mouse. Physiol Behav 24:523–527
Ecker J, Dumitrescu ON, Wong KY et al (2010) Melanopsin-expressing retinal ganglion-cell photoreceptors: cellular diversity and role in pattern vision. Neuron 67:49–60
Engelund A, Fahrenkrug J, Harrison A et al (2010) Vesicular glutamate transporter 2 (VGLUT2) is co-stored with PACAP in projections from the rat melanopsin-containing retinal ganglion cells. Cell Tiss Res 340:243–255
Famiglietti EV, Kolb H (1976) Structural basis for on- and off-center responses in retinal ganglion cells. Science 194:193–195
Farber DB, Flannery JG, Bowes-Rickman C (1994) The rd mouse story: Seventy years of research on an animal model of inherited retinal degeneration. Prog Retinal Eye Res 13:31–64
Feigl B, Mattes D, Thomas R et al (2011) Intrinsically photosensitive (melanopsin) retinal ganglion cell function in glaucoma. Invest Ophthalmol Vis Sci 52:4362–4367
Foster RG, Provencio I, Hudson D et al (1991) Circadian photoreception in the retinally degenerate mouse (*rd*/*rd*). J Comp Physiol A 169:39–50
Freedman MS, Lucas RJ, Soni B et al (1999) Regulation of mammalian circadian behavior by non-rod, non-cone, ocular photoreceptors. Science 284:502–504
Fu Y, Liao H-W, Do MTH et al (2005a) Non-image-forming ocular photoreception in vertebrates. Curr Opin Neurobiol 15:415–422
Fu Y, Zhong H, Wang M-H H et al (2005b) Intrinsically photosensitive retinal ganglion cells detect light with a vitamin A-based photopigment, melanopsin. Proc Natl Acad Sci USA 102:10339–10344

Fyk-Kolodziej B, Dzhagaryan A, Qin P et al (2004) Immunocytochemical localization of three vesicular glutamate transporters in the cat retina. J Comp Neurol 475:518–530
Gaus SE, Strecker RE, Tate BA et al (2002) Ventrolateral preoptic nucleus contains sleep-active, galaninergic neurons in multiple mammalian species. Neurosci 115:285–294
Gooley JJ, Lu J, Chou TC et al (2001) Melanopsin in cells of origin of the retinohypothalamic tract. Nat Neurosci 4:1165
Gooley JJ, Lu J, Fischer D et al (2003) A broad role for melanopsin in nonvisual photoreception. J Neurosci 23:7093–7106
Göz D, Studholme K, Lappi DA et al (2008) Targeted destruction of photosensitive retinal ganglion cells with a saporin conjugate alters the effects of light on mouse circadian rhythms. PLoS ONE 3:e3153
Graham DM, Wong KY, Shapiro P et al (2008) Melanopsin ganglion cells use a membrane-associated rhabdomeric phototransduction cascade. J Neurophysiol 99:2522–2532
Groos GA, Mason R (1978) Maintained discharge of rat suprachiasmatic neurons at different adaptation levels. Neurosci Lett 8:59–64
Groos GA, Mason R (1980) The visual properties of rat and cat suprachiasmatic neurons. J Comp Physiol 135:349–356
Güler AD, Ecker JL, Lall GS et al (2008) Melanopsin cells are the principal conduits for rod-cone input to non-image-forming vision. Nature 453:102–105
Hamner KC, Finn JC, Sirohi GS, Hoshizaki T, Carpenter BH (1962) The biological clock at the south pole. Nature 195:476–480
Hannibal J, Georg B, Fahrenkrug J (2007) Melanopsin changes in neonatal albino rat independent of rods and cones. NeuroReport 18:81–85
Harrington ME, Rusak B (1986) Lesions of the thalamic intergeniculate leaflet alter hamster circadian rhythms. J Biol Rhythms 1:309–325
Hartwick ATE, Bramley JR, Yu J et al (2007) Light-evoked calcium responses of isolated melanopsin-expressing retinal ganglion cells. J Neurosci 27:13468–13480
Hartwick ATE, Hamilton CM, Baldridge WH (2008) Glutamatergic calcium dynamics and deregulation of rat retinal ganglion cells. J Physiol 586:3425–3446
Hatori M, Le H, Vollmers C et al (2008) Inducible ablation of melanopsin-expressing retinal ganglion cells reveals their central role in non-image forming visual responses. PLoS ONE 3:e2451
Hattar S, Liao HW, Takao M et al (2002) Melanopsin-containing retinal ganglion cells: architecture, projections, and intrinsic photosensitivity. Science 295:1065–1070
Hattar S, Kumar M, Park A et al (2006) Central projections of melanopsin-expressing retinal ganglion cells in the mouse. J Comp Neurol 497:326–349
Hendrickson AE, Wagoner N, Cowan WM (1972) An autoradioradiographic and electron microscopic study of retinohypothalamic connections. Z Zellforsch 135:1–26
Hoffman T, Schaefer M, Schultz G et al (2002) Subunit composition of mammalian transient receptor potential channels in living cells. Proc Natl Acad Sci USA 99:7461–7466
Horowitz SS, Blanchard J, Morin LP (2004) Intergeniculate leaflet and ventral lateral geniculate nucleus afferent connections: An anatomical substrate for functional input from the vestibulovisuomotor system. J Comp Neurol 474:227–245
Hoshi H, Liu W-L, Massey SC et al (2009) ON inputs to the OFF layer: bipolar cells that break the stratification rules of the retina. J Neurosci 29:8875–8883
Ishida A, Mutoh T, Ueyama T et al (2005) Light activates the adrenal gland: timing of gene expression and glucocorticoid release. Cell Metab 2:297–307
Isoldi MC, Rollag MD, Castrucci AM et al (2005) Rhabdomeric phototransduction initiated by the vertebrate photopigment melanopsin. Proc Natl Acad Sci USA 102:1217–1221
Jakobs TC, Ben Y, Masland RH (2007) Expression of mRNA for glutamate receptor subunits distinguishes the major classes of retinal neurons, but is less specific for individual cell types. Mol Vis 13:933–948
Jakobs TC, Libby RT, Ben Y et al (2005) Retinal ganglion cell degeneration is topological but not cell type specific in DBA/2J mice. J Cell Biol 171:313–325

Johnson J, Fremeau RT, Duncan JL et al (2007) Vesicular glutamate transporter 1 is required for photoreceptor synaptic signaling but not for intrinsic visual functions. J Neurosci 27: 7245–7255
Johnson MS (1939) Effect of continuous light on periodic spontaneous activity of white-footed mice (Peromyscus). J Exper Zool 82:315–328
Joo HR, Hattar S, Chen SK (2011) Anatomy and targeting of sparsely labeled M1 ipRGC using the inducible Cre/LoxP system. Soc Neurosci 174.04
Keeler CE (1924) The inheritance of a retinal abnormality in white mice. Proc Natl Acad Sci USA 10:329–333
Keeler CE (1927) Iris movements in blind mice. Am J Physiol 81:107–112
Kong J-H, Fish DR, Rockhill RL et al (2005) Diversity of ganglion cells in the mouse retina: unsupervised morphological classification and its limits. J Comp Neurol 489:293–310
Koyanagi M, Kubokawa K, Tsukamoto H et al (2005) Cephalochordate melanopsin: evolutionary linkage between invertebrate visual cells and vertebrate photosensitive retinal ganglion cells. Curr Biol 15:1065–1069
Kumbalasiri T, Rollag MD, Isoldi MC et al (2007) Melanopsin triggers the release of internal calcium stores in response to light. Photochem Photobiol 83:273–279
La Morgia C, Ross-Cisneros FN, Sadun AA et al (2010) Melanopsin retinal ganglion cells are resistant to neurodegeneration in mitochrondrial optic neuropathies. Brain 133:2426–2438
Lamont EW, Robinson B, Stewart J et al (2005) The central and basolateral nuclei of the amygdala exhibit opposite diurnal rhythms of expression of the clock protein Period2. Proc Natl Acad Sci USA 102:4180–4184
Lazareva OF, Shimizu T, Wasserman EA (2011) How animals see the world. Oxford University Press (in press)
Lewy AJ, Sack RL, Miller S et al (1987) Antidepressant and circadian phase-shifting effects of light. Science 235:352–354
Li RS, Chen BY, Tay DK et al (2006) Melanopsin-expressing retinal ganglion cells are more injury-resistant in a chronic ocular hypertension model. Invest Ophthalmol Vis Sci 47: 2951–2958
Li SY, Yau SY, Chen BY et al (2008) Enhanced survival of melanopsin-expressing retinal ganglion cells after injury is associated with the PI3 K/Akt pathway. Cell Mol Neurobiol 28:1095–1107
Lin B, Koizumi A, Tanaka N et al (2008) Restoration of visual function in retinal degeneration mice by ectopic expression of melanopsin. Proc Natl Acad Sci USA 105:16009–16014
Luan L, Ren C, Lau BW-M et al (2011) Y-like retinal ganglion cells innervate the dorsal raphe nucleus in the Mongolian gerbil (Meriones unguiculatus). PLoS ONE 6:e18938
Lucas RJ, Freedman MS, Munoz M et al (1999) Regulation of mammalian pineal by non-rod, non-cone, ocular photoreceptors. Science 284:505–507
Lucas RJ, Douglas RH, Foster RG (2001) Characterization of an ocular photopigment capable of driving pupillary constriction in mice. Nat Neurosci 4:621–626
Lucas RJ, Hattar S, Takao M et al (2003) Diminished papillary light reflex at high irradiances in melanopsin-knockout mice. Science 299:245–247
Lupi D, Oster H, Thompson S et al (2008) The acute light-induction of sleep is mediated by OPN-4based photoreception. Nat Neurosci 11:1068–1073
Mawad K, Van Gelder RN (2008) Absence of long-wavelength photic potentiation of murine intrinsically photosensitive retinal ganglion cell firing in vitro. J Biol Rhythms 23:387–391
Meijer JH, Groos GA, Rusak B (1986) Luminance coding in a circadian pacemaker: the suprachiasmatic nucleus of the rat and hamster. Brain Res 382:109–118
Melyan Z, Tarttelin EE, Bellingham et al (2005) Addition of human melanopsin renders mammalian cells photoresponsive. Nature 433:741–745
Millhouse OE (1977) Optic chiasm collaterals afferent to the suprachiasmatic nucleus. Brain Res 137:351–355
Moore RY, Lenn NJ (1972) A retinohypothalamic projection in the rat. J Comp Neurol 146:1–14

Morin LP, Blanchard J (1991) Depletion of brain serotonin by 5,7-DHT modifies hamster circadian rhythm response to light. Brain Res 566:173–185
Morin LP, Blanchard J (1997) Neuropeptide Y and enkephalin immunoreactivity in retinorecipient nuclei of the hamster pretectum and thalamus. Vis Neurosci 14:765–777
Morin LP, Blanchard J (1998) Interconnections among nuclei of the subcortical visual shell: the intergeniculate leaflet is a major constituent of the hamster subcortical visual system. J Comp Neurol 396:288–309
Morin LP, Studholme KM (2011) Separation of function for classical and ganglion cell photoreceptors with respect to circadian rhythm entrainment and induction of photosomnolence. Neurosci (in press)
Morin LP, Blanchard J, Moore RY (1992) Intergeniculate leaflet and suprachiasmatic nucleus organization and connections in the golden hamster. Vis Neurosci 8:219–230
Morin LP, Blanchard JH, Provencio I (2003) Retinal ganglion cell projections to the hamster suprachiasmatic nucleus, intergeniculate leaflet, and visual midbrain: bifurcation and melanopsin immunoreactivity. J Comp Neurol 465:401–416
Morin LP, Lituma PJ, Studholme KM (2010) Two components of nocturnal locomotor suppression by light. J Biol Rhythms 25:197–207
Müller LPS, Do MTH, Yau KW et al (2010) Tracer coupling of intrinsically photosensitive retinal ganglion cells to amacrine cells in the mouse retina. J Comp Neurol 518:4813–4824
Mure LS, Rieux C, Hattar S et al (2007) Melanopsin-dependent nonvisual responses: evidence for photopigment bistability in vivo. J Biol Rhythms 22:411–424
Mure LS, Cornut P-L, Rieux C et al (2009) Melanopsin bistability: a fly's eye technology in the human retina. PLoS ONE 4:e5991
Nelson DE, Takahashi JS (1999) Integration and saturation within the circadian photic entrainment pathway of hamsters. Am J Physiol 46:R1351–R1361
Nelson RJ, Zucker I (1981) Absence of extraocular photoreception in diurnal and nocturnal rodents exposed to direct sunlight. J Comp Biochem Physiol 69A:145–148
Nelson R, Famiglietti EV, Kolb H (1978) Intracellular staining reveals different levels of stratification for on- and off-center ganglion cells in cat retina. J Neurophysiol 41:472–483
Nemeroff CB, Konkol RJ, Bissette G et al (1977) Analysis of the disruption in hypothalamic-pituitary regulation in rats treated neonatally with monosodium L-glutamate (MSG): evidence for involvement of tuberoinfundibular cholinergic and dopaminergic systems in neuroendocrine regulation. Endocrinol 101:613–622
Newman LA, Walker MT, Brown RL et al (2003) Melanopsin forms a functional short-wavelength photopigment. Biochem 42:12734–12738
Nickle B, Robinson PR (2007) The opsins of the vertebrate retina: insights from structural, biochemical, and evolutionary studies. Cell Mol Life Sci 64:2917–2932
Olney JW (1969) Glutamate induced retinal degeneration in neonatal mice. Electron microscopy of the acutely evolving lesion. J Neuropathol Exp Neurol 28:455–474
Oster H, Damerow S, Kiessling S et al (2006) The circadian rhythm of glucocorticoids is regulated by a gating mechanism residing in the adrenal cortical clock. Cell Metab 4:163–173
Ostergaard J, Hannibal J, Fahrenkrug J (2007) Synaptic contact between melanopsin-containing retinal ganglion cells and rod bipolar cells. Invest Ophthalmol Vis Sci 48:3812–3820
Panda S, Sato TK, Castrucci AM et al (2002) Melanopsin (Opn4) requirement for normal light-induced circadian phase shifting. Science 298:2213–2216
Panda S, Provencio I, Tu DC et al (2003) Melanopsin is required for non-image-forming photic responses in blind mice. Science 301:525–527
Panda S, Nayak SK, Campo B et al (2005) Illumination of the melanopsin signaling pathway. Science 307:600–604
Peirson SN, Oster H, Jones SL et al (2007) Microarry analysis and functional genomics identify novel components of melanopsin signaling. Curr Biol 17:1363–1372
Peirson SN, Halford S, Foster RG (2009) The evolution of irradiance detection: melanopsin and the non-visual opsins. Phil Trans R Soc B 364:2849–2865

Perez-Leighton CE, Schmidt TM, Abramowitz J et al (2011) Intrinsic phototransduction persists in melanopsin-expressing ganglion cells lacking diacylglycerol-sensitive TRPC subunits. Eur J Neurosci 33:856–867

Perez-Leon JA, Warren EJ, Allen CN et al (2006) Synaptic inputs to retinal ganglion cells that set the circadian clock. Eur J Neurosci 24:1117–1123

Peterson BB, Dacey DM (1998) Morphology of human retinal ganglion cells with intraretinal axon collaterals. Vis Neurosci 15:377–387

Pickard GE (1980) Morphological characteristics of retinal ganglion cells projecting to the suprachiasmatic nucleus: a horseradish peroxidase study. Brain Res 183:458–465

Pickard GE (1982) The afferent connections of the suprachiasmatic nucleus of the golden hamster with emphasis on the retinohypothalamic projection. J Comp Neurol 211:65–83

Pickard GE (1985) Bifurcating axons of retinal ganglion cells terminate in the hypothalamic suprachiasmatic nucleus and the intergeniculate leaflet of the thalamus. Neurosci Lett 55:211–217

Pickard GE (1989) Entrainment of the circadian rhythm of wheel running activity is phase shifted by ablation of the intergeniculate leaflet. Brain Res 494:151–154

Pickard GE, Silverman AJ (1981) Direct retinal projections to the hypothalamus, piriform cortex and accessory optic nuclei in the golden hamster as demonstrated by a sensitive anterograde horseradish peroxidase technique. J Comp Neurol 196:155–172

Pickard GE, Turek FW, Lamperti AA et al (1982) The effect of neonatally administered monosodium glutamate (MSG) on the development of retinofugal projections and entrainment of circadian locomotor activity. Behav Neural Biol 34:433–444

Pickard GE, Ralph M, Menaker M (1987) The intergeniculate leaflet partially mediates the effects of light on circadian rhythms. J Biol Rhythms 2:35–56

Pickard GE, Weber TE, Scott PA et al (1996) $5HT_{1B}$ receptor agonists inhibit light-induced phase shifts of the circadian activity rhythm and expression of the immediate-early gene c-fos in the suprachiasmatic nucleus. J Neurosci 16:8208–8220

Pickard GE, Smith BN, Belenky M et al (1999) $5HT_{1B}$ receptor-mediated presynaptic inhibition of retinal input to the suprachiasmatic nucleus. J Neurosci 19:4034–4045

Pickard GE, Baver SB, Ogilvie MD et al (2009) Light-induced Fos expression in intrinsically photosensitive retinal ganglion cells in melanopsin knockout ($Opn4^{-/-}$) mice. PLoS ONE 4:e4984

Pires SS, Hughes S, Turton M et al (2009) Differential expression of two distinct functional isoforms of melanopsin *(Opn4)* in the mammalian retina. J Neurosci 29:12332–12342

Pittendrigh CS (1954) On temperature independence in the clock-system controlling emergence time in *Drosophlia*. Proc Natl Acad Sci USA 40:1018–1029

Provencio I, Jiang G, de Grip WJ et al (1998) Melanopsin: an opsin in melanophores, brain and eye. Proc Natl Acad Sci USA 95:340–345

Provencio I, Rodriguez IR, Jiang G et al (2000) A novel human opsin in the inner retina. J Neurosci 20:600–605

Provencio I, Rollag MD, Castrucci AM (2002) Photoreceptive net in the mammalian retina. Nature 415:493

Qiu X, Kumbalasiri T, Carlson SM et al (2005) Induction of photosensitivity by heterologous expression of melanopsin. Nature 433:745–749

Rajaraman K (2012) ON ganglion cells are intrinsically photosensitive in the tiger salamander retina. J Comp Neurol 520:100–200

Richter CP (1965) Biological clocks in medicine and psychiatry. Charles C Thomas, Springfield

Robinson GA, Madison RD (2004) Axotomized mouse retinal ganglion cells containing melanopsin show enhanced survival, but not enhanced axon regrowth into a peripheral nerve graft. Vis Res 44:2667–2674

Rockhill RL, Daly FJ, MacNeil MA et al (2002) The diversity of ganglion cells in a mammalian retina. J Neurosci 22:3831–3843

Roecklein KA, Rohan KJ, Duncan WC et al (2009) A missense variant (P10L) of the melanopsin *(OPN4)* gene in seasonal affective disorder. J Affect Disorders 114:279–285

Ruby NF, Brennan TJ, Xie X et al (2002) Role of melanopsin in circadian responses to light. Science 298:2211–2213
Schmidt TM, Kofuji P (2009) Functional and morphological differences among intrinsically photosensitive retinal ganglion cells. J Neurosci 29:476–482
Schmidt TM, Kofuji P (2010) Differential cone pathway influence on intrinsically photosensitive retinal ganglion cells subtypes. J Neurosci 30:16262–16271
Schmidt TM, Kofuji P (2011) Structure and function of bistratified intrinsically photosensitive retinal ganglion cells in the mouse. J Comp Neurol 519:1492–1504
Schmidt TM, Taniguchi K, Kofuji P (2008) Intrinsic and extrinsic light responses in melanopsin-expressing cells during development. J Neurophysiol 100:371–384
Schmidt TM, Chen SK, Hattar S (2011) Intrinsically photosensitive retinal ganglion cells: many subtypes, diverse functions. Trends Neurosci 34:572–580
Sekaran S, Foster RG, Lucas RJ et al (2003) Calcium imaging reveals a network of intrinsically light-sensitive inner-retinal neurons. Curr Biol 13:1290–1298
Sekaran S, Lupi D, Jones CJ et al (2005) Melanopsin-dependent photoreception provides earliest light detection in the mammalian retina. Curr Biol 15:1099–1107
Sekaran S, Lall GS, Ralphs KL et al (2007) 2-aminoethoxydiphenylborane is an acute inhibitor of directly photosensitive retinal ganglion cell activity in vitro and in vivo. J Neurosci 27:3981–3986
Smale L, Michels KM, Moore RY et al (1990) Destruction of the hamster serotonergic system by 5,7-DHT: effects on circadian rhythm phase, entrainment and response to triazolam. Brain Res 515:9–19
Sollars PJ, Smeraski CA, Kaufman JD et al (2003) Melanopsin and non-melanopsin expressing retinal ganglion cells innervate the hypothalamic suprachiasmatic nucleus. Vis Neurosci 20:601–610
Sollars PJ, Ogilvie MD, Simpson AM et al (2006) Photic entrainment is altered in the 5-HT_{1B} receptor knockout mouse. J Biol Rhythms 21:21–32
Son GH, Chung S, Hk C et al (2008) Adrenal peripheral clock controls the autonomous circadian rhythm of glucocorticoid by causing rhythmic steroid production. Proc Natl Acad Sci USA 105:20970–20975
Stephan FK, Zucker I (1972) Circadian rhythms in drinking behavior and locomotor activity of rats are eliminated by hypothalamic lesions. Proc Natl Acad Sci USA 69:1583–1586
Swanson LW, Cowan WM, Jones EG (1974) An autoradioradiographic study of the efferent connections of the ventral lateral geniculate nucleus in the albino rat and cat. J Comp Neurol 156:143–163
Takahashi JS, DeCoursey PJ, Bauman L et al (1984) Spectral sensitivity of a novel photoreceptive system mediating entrainment of mammalian circadian rhytms. Nature 308:186–188
Terman M, Terman JS (2005) Light therapy. In: Kryger MH, Roth T, Dement WC (eds) Principles and practice of sleep medicine, 4th edn. Elsevier, Philadelphia, pp 1424–1442
Thapan K, Arendt J, Skene DJ (2001) An action spectrum for melatonin suppression: evidence for a novel non-rod, non-cone photoreceptor system in humans. J Physiol 535:261–267
Torii M, Kojima D, Okano T et al (2007) Two isoforms of chicken melanopsins show blue light sensitivity. FEBS Lett 581:5327–5331
Tsai JW, Hannibal J, Hagiwara G et al (2009) Melanopsin as a sleep modulator: circadian gating of direct effects of light on sleep and altered sleep homeostasis in *Opn4*$^{-/-}$ mice. PLoS Biol 7:e1000125
Usai C, Ratto GM, Bisti S (1991) Two systems of branching axons in monkey's retina. J Comp Neurol 308:149–161
Van den Pol AN, Cao V, Heller HC (1998) Circadian system of mice integrates brief light stimuli. Am J Physiol 275:R654–R657
Van Gelder RN (2008) Non-visual photoreception: sensing light without sight. Curr Biol 18: R38–R39
Van Gelder RN, Mawad K (2008) Illuminating the mysteries of melanopsin and circadian photoreception. J Biol Rhythms 23:394–395

Vessey JP, Lalonde MR, Mizan HA (2004) Carbenoxolone inhibition of voltage-gated Ca channels and synaptic transmission in the retina. J Neurophysiol 92:1252–1256
Vidal L, Morin LP (2007) Absence of normal photic integration in the circadian visual system: response to millisecond light flashes. J Neurosci 27:3375–3382
Viney TJ, Balint K, Hillier D et al (2007) Local retinal circuits of melanopsin-containing ganglion cells identified by transsynaptic viral tracing. Curr Biol 17:981–988
Vugler AA, Redgrave P, Semo M et al (2007) Dopamine neurons form a discrete plexus with melanopsin cells in normal and degenerating retina. Exp Neurol 205:26–35
Walker MT, Brown RL, Cronin TW et al (2008) Photochemistry of retinal chromophore in mouse melanopsin. Proc Natl Acad Sci USA 105:8861–8865
Wang JS, Kefalov VJ (2009) An alternative pathway mediates the mouse and human cone visual cycle. Curr Biol 19:1665–1669
Wang HZ, Lu QJ, Wang NL (2008) Loss of melanopsin-containing retinal ganglion cells in a rat glaucoma model. Chin Med J 121:1015–1019
Wang JS, Estevez ME, Cornwall MC et al (2009) Intra-retinal visual cycle required for rapid and complete cone dark adaptation. Nat Neurosci 12:295–302
Wang X, Wang T, Jiao Y et al (2010) Requirement for an enzymatic visual cycle in *Drosophlia*. Curr Biol 20:93–102
Warren EJ, Allen CN, Brown RL et al (2003) Intrinsic light responses of retinal ganglion cells projecting to the circadian system. Eur J Neurosci 17:1727–1735
Warren EJ, Allen CN, Brown RL et al (2006) The light-activated signaling pathway in SCN-projecting rat retinal ganglion cells. Eur J Neurosci 23:2477–2487
Wässle H (2004) Parallel processing in the mammalian retina. Nat Rev Neurosci 5:747–757
Wiles EM, Sollars PJ, Pickard GE (2011) Intrinsically photosensitive retinal ganglion cells isolated from neonatal rat retina are depolarized by glycine. Soc Neurosci 602.14
Witkovsky P (2004) Dopamine and retinal function. Doc Ophthalmol 108:17–40
Wong KY, Dunn FA, Berson DM (2005) Photoreceptor adaptation in intrinsically photosensitive retinal ganglion cells. Neuron 48:1001–1010
Wong KY, Dunn FA, Graham DM et al (2007) Synapic influences on rat ganglion-cell photoreceptors. J Physiol 582:279–296
Yau K-W, Hardie RC (2009) Phototransduction motifs and variations. Cell 139:247–264
Ye H, Baba MD, Peng RW et al (2011) A synthetic optogenetic transcription device enhances blood-glucose homeostasis in mice. Science 332:1565–1568
Yoshimura T, Ebihara S (1996) Spectral sensitivity of photoreceptors mediating phase-shifts of circadian rhythms in retinally degenerate CBA/J (rd/rd) and normal CBA/N (+/+) mice. J Comp Physiol 178:797–802
Zaida F, Hull JT, Peirson SN et al (2007) Short-wavelenfth light sensitivity of circadian, pupillary, and visual awareness in humans lacking an outer retina. Curr Biol 17:2122–2128
Zhang DQ, Zhou TR, McMahon DG (2007) Functional heterogeneity of retinal dopaminergic neurons underlying their multiple roles in vision. J Neurosci 27:692–699
Zhang DQ, Wong KY, Sollars PJ et al (2008) Intraretinal signaling by ganglion cell photoreceptors do dopaminergic amacrine neurons. Proc Natl Acad Sci USA 105:14181–14186
Zhang DQ, Sollars PJ, Pickard GE (2010) Signaling by ganglion cell photoreceptors to dopaminergic amacrine cells requires the photopigment melanopsin and AMP-type glutamate receptors. ARVO #1206

Quantifying and Modeling the Temperature-Dependent Gating of TRP Channels

Thomas Voets

Abstract The ability to sense environmental temperatures and to avoid noxious heat or cold is crucial for the survival of all organisms. In mammals, sensory neurons from dorsal root and trigeminal ganglia convey thermal information from the skin, mouth and nose to the central nervous system. Recent evidence has established that thermoTRPs, a subset of the TRP superfamily of cation channels, act as primary temperature sensors in cold- and heat-sensitive neurons. The gating of these thermoTRPs exhibits strong temperature dependence, leading to steep changes in inward current upon heating or cooling. The origin of this striking temperature sensitivity remains incompletely understood. In this review, I propose criteria that define a thermoTRP, analyse the usefulness and limitations of the commonly used parameters *thermal threshold* and Q_{10}, provide an overview of possible thermodynamic principles and gating schemes for thermosensitive TRP channels, and perform a meta-analysis of published work on the molecular basis of the heat sensitivity in TRPV1. This review may form a useful reference for the analysis and interpretation of further biophysical and structure-function studies dissecting the molecular basis of thermosensitivity in TRP channels.

1 Introduction

1.1 Thermosensation in Mammals

Temperature sensing (or thermosensing) is arguably the most elementary sense. We all know the intense pain when touching or ingesting noxiously cold or hot

T. Voets
Laboratory of Ion Channel Research and TRP Research Platform Leuven (TRPLe), KU Leuven, Herestraat 49 bus 802, 3000 Leuven, Belgium
e-mail: thomas.voets@med.kuleuven.be

Rev Physiol Biochem Pharmacol, doi: 10.1007/112_2011_5,

substances, which initiates a rapid avoidance reflex and helps preventing serious, potentially fatal injury. Moreover, we are generally well capable of estimating the ambient temperature, and, on average, feel most at ease at an ambient temperature of around 26°C (Grivel and Candas 1991). Ambient temperatures that deviate too much from the preferred temperature region initiate a variety human actions, all aimed at increasing comfort and minimizing the energy expenditure required to maintain the core body temperature around 37°C (Romanovsky 2007; Morrison and Nakamura 2011).

Temperature sensing depends on sensory neurons that have their cell bodies in trigeminal (TG) and dorsal root ganglia (DRG) and extend sensory nerve endings into skin and mucosa (Basbaum et al. 2009). The membrane surrounding these nerve endings contains a variety of ion channels. These include background and voltage-gated K^+ channels that ensure a negative voltage over the membrane under resting conditions; voltage-gated Na^+ channels that are required for the generation of action potentials; and different types of Ca^{2+} and/or Na^+-permeable cation channels that open in response to sensory stimuli, resulting in membrane depolarization and, when a certain threshold is crossed, action potential initiation (Talavera et al. 2008; Basbaum et al. 2009). These action potentials are then propagated along the sensory neuron, ultimately leading to synaptic transmission toward second-order neurons in the dorsal horn (DRG) or sensory nucleus in the brain (TG). Members of the transient receptor potential (TRP) superfamily have been identified as highly temperature-sensitive non-selective cation channels acting as primary temperature sensors in thermosensitive neurons (Caterina et al. 2000; Davis et al. 2000; Lee et al. 2005; Moqrich et al. 2005; Bandell et al. 2007; Bautista et al. 2007; Caterina 2007; Colburn et al. 2007; Dhaka et al. 2007; Talavera et al. 2008; Basbaum et al. 2009; Vriens et al. 2011).

1.2 A Definition of ThermoTRPs

What defines a thermoTRP? Since all chemical and biochemical reactions are temperature-dependent, some TRP channels must be somehow "extraordinary" in their thermosensitivity to deserve the label thermoTRP. I propose that a thermoTRP exhibits the following biophysical and functional characteristics:

(1) Steep temperature dependence
To function as a thermosensor, a thermoTRP must generate robust depolarizing currents in response to a change in temperature. The temperature-sensitivity of (inward) currents mediated by thermoTRPs has often been quantified in terms of a Q_{10}-value, which can be calculated as the relative increase in current amplitude at a specific voltage when temperature increases by 10 degrees, i.e. as $Q_{10} = I_{T+10}/I_T$. As an admittedly arbitrary criterion I propose that a TRP

channel must exhibit a minimal Q_{10} value of ≥ 5 (or ≤ 0.2, in case of a cold-activated channel) for inward current in a relevant temperature range to classify as a thermoTRP.

(2) Expression in relevant cell types
Under healthy conditions, deeper structures of the body are kept at a relatively constant core body temperature of ~37°C. Only cells in skin, eyes, mouth, oesophagus and upper airways are exposed to external thermal variations of more than a few degrees on a regular basis (Romanovsky 2007). To act as thermosensors, a thermoTRP should be functionally expressed at sites that experience significant changes in temperature, such as in skin keratinocytes, sensory nerve endings, oral mucosa or taste cells.

(3) Underlie thermosensitivity of a physiological process
All known temperature-sensitive TRP channels are not only activated by changes in temperature but also by other chemical and/or physical stimuli. In many cases, it remains to be established whether the temperature-sensitivity is relevant, or just an epiphenomenon of little or no physiological relevance. I propose that, for a TRP channel to classify as a thermoTRP, there must be *in vivo* evidence that its temperature dependence underlies the thermosensitivity of a (patho)physiological process.

According to the current TRP channel literature, at least 11 mammalian TRP channels exhibit steep temperature dependence in accordance with criterion (1), namely TRPV1, TRPV2, TRPV3, TRPV4, TRPM2, TRPM3, TRPM4 and TRPM5, which are activated upon warming, and TRPM8,TRPA1 and TRPC5, which are activated upon cooling (Caterina et al. 1997, 1999; McKemy et al. 2002; Peier et al. 2002a, b; Smith et al. 2002; Watanabe et al. 2002; Xu et al. 2002; Chung et al. 2003; Story et al. 2003; Talavera et al. 2005; Togashi et al. 2006; Karashima et al. 2009; Vriens et al. 2011; Zimmermann et al. 2011). However, based on criteria (2) and (3), several of these channels do not (yet) fully merit the title of thermoTRP. For example, TRPV2 is activated by noxious heat and expressed in sensory neurons (Caterina et al. 1999); yet, there is no convincing evidence that TRPV2 is involved in heat sensing (Park et al. 2011). Likewise, TRPM2 is activated by heat, and it has even been shown to modulate the temperature sensitivity of insulin release from pancreatic islets (Togashi et al. 2006); yet, there is no evidence that pancreatic islets exhibit TRPM2-dependent, temperature-sensitive insulin release *in vivo*. The heat-activated TRPM4 is ubiquitously expressed, but as yet there are no indications that it may modulate thermosensitivity of a physiological process. Even the contribution to innocuous and noxious heat sensing of TRPV3 and TRPV4, which both have been widely described as thermosensors involved in warmth sensation in skin keratinocytes (Lee et al. 2005; Moqrich et al. 2005), has been recently questioned (Huang et al. 2011). On the other hand, it is unclear from the literature whether temperature sensitivity has been systematically tested for all TRP channels. Thus, ongoing research in this field may cause the list of thermoTRPs to further grow (or shrink).

2 Parametrizing ThermoTRPs: Q_{10} and Thermal Threshold?

As a yardstick for quantitative comparison, many studies have used the Q_{10} and thermal threshold (T_{thres}) values to parameterize the responses of TRP channels to cold and heat, and to pinpoint the effects of channel modulation and mutagenesis on thermosensivity.

A widely used procedure to determine Q_{10} and T_{thres} is illustrated in Fig. 1. Figure 1a shows a hypothetical whole-cell patch-clamp recording at fixed voltage (e.g. −70 mV) from a cell expressing a heat-activated thermoTRP stimulated with a temperature ramp from 20 to 50°C (scaling up the current amplitudes by ~3 orders of magnitude may provide a simulation of a typical Xenopus laevis two-electrode voltage-clamp experiment). The whole-cell current ($I_{whole\text{-}cell}$) is the sum of the current mediated by thermoTRP channels ($I_{thermoTRP}$; Fig. 1b) and a background current ($I_{background}$), which consists of the non-cellular leak current through the seal between pipette and membrane, and of any background current present in cell membrane (Fig. 1c). $I_{thermoTRP}$ was assumed to have a high thermosensitivity ($Q_{10,thermoTRP} = 30$), and an amplitude of 2 nA at 50°C, which is in the middle of the range of published data for TRPV1. In contrast, $I_{background}$ was assumed to have a low thermosensitivity ($Q_{10,background} = 1.4$), a typical value for ionic diffusion, and an amplitude of 70 pA at 50°C (which corresponds to a seal resistance of 1 GΩ, quite a good seal quality at this elevated temperature). Figure 1d show a different representation of these data, relating the logarithm of $I_{whole\text{-}cell}$ to the reciprocal of the temperature in Kelvin, as in an Arrhenius plot (bottom X-axis). In this representation, the Q_{10} values of $I_{thermoTRP}$ and $I_{background}$ can be determined from the slope (m) of the tangent lines to the low and high temperature parts of this plot:

$$Q_{10} = 10^{-\frac{10m}{T^2}} \tag{1}$$

T_{thres} has been defined as the temperature at which these tangent lines intersect, yielding ~39°C in this example (Fig. 1d).

Although the value of T_{thres} might give an indication about the temperature range in which the channel could play a physiological role, this parameter appears to be a poor and sometimes even misleading descriptor of the actual temperature sensitivity of the channel. Firstly, thermal activation of thermoTRPs is not governed by a single characteristic thermal threshold. Instead, activating changes in temperature result in a steep but gradual increase in channel open probability, from undetectable to detectable levels. This is comparable to strongly voltage-gated K^+, Na^+, Ca^{2+}, or H^+ channels, whose open probability increases steeply with voltage, without exhibiting a single voltage threshold. Interestingly, as many thermoTRPs are also voltage-gated, T_{thres} values will change depending on the voltage at which they were determined measured. Thus, the use of T_{thres} gives the false impression that activation of thermoTRPs is an all-or-nothing event.

Secondly, T_{thres} is very sensitive to factors that are not related to the gating and temperature dependence of the thermoTRP under study. In particular, T_{thres}

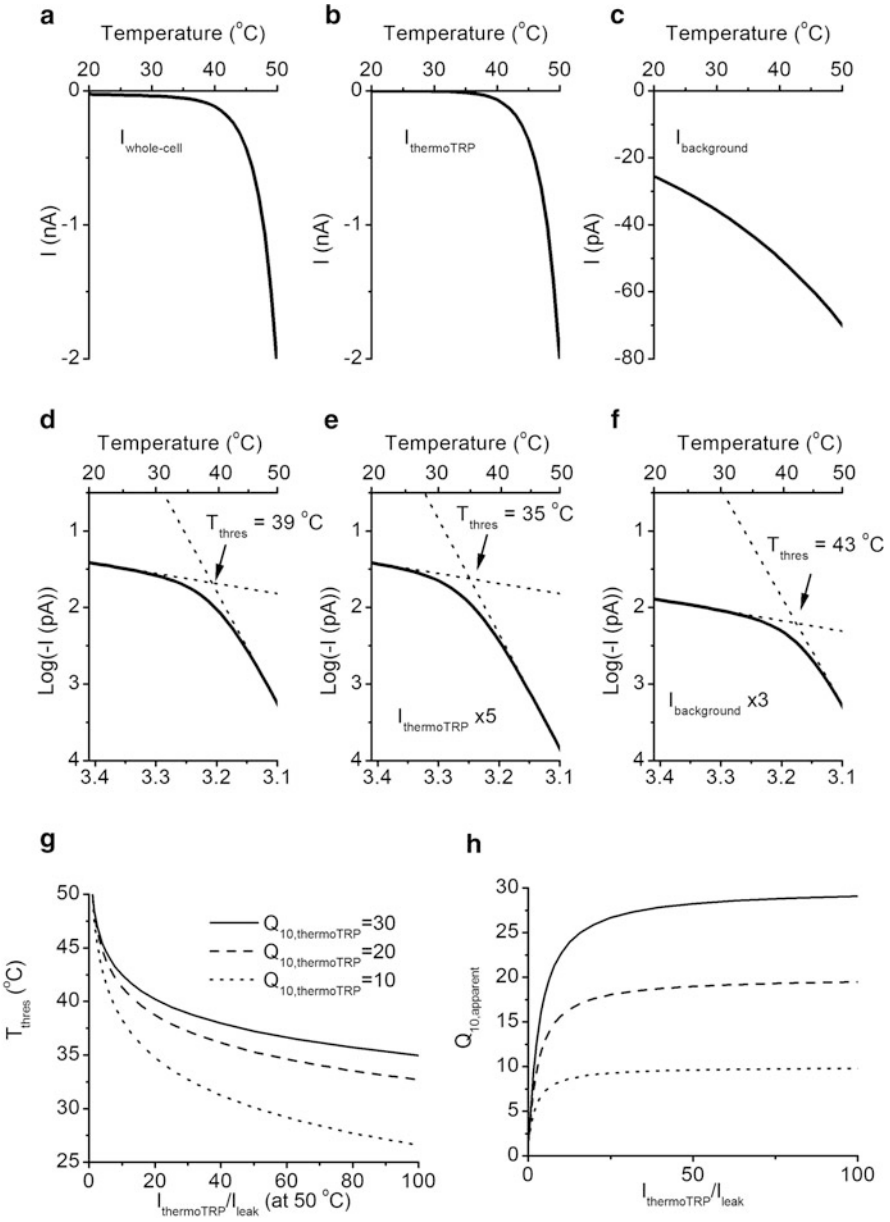

Fig. 1 (**a–c**) Simulation of whole-cell current in a cell expressing a heat-activated thermoTRP, consisting of a thermoTRP-mediated current and a background current. (**d–f**) Arrhenius plots corresponding to the current in panel (**a**), as well as to instances where the thermoTRP-mediated current or the background current are increased. (**g**) Dependence of T_{thres} and apparent Q_{10} on the relative amplitude of thermoTRP-mediated and background current and on the temperature sensitivity of the thermoTRP. See text for more details

is very sensitive to changes in the relative amplitude of $I_{thermoTRP}$ compared to $I_{background}$ (Fig. 1e–g). As illustrated in Fig. 1e, increasing the amplitude of $I_{thermoTRP}$ leads to a significant reduction in T_{thres} (Fig. 1e), whereas an increase in $I_{background}$ shifts T_{thres} to higher temperatures (Fig. 1f). Figure 1g shows the actual relationship between T_{thres} and $I_{thermoTRP}/I_{background}$ (at 50°C) for $Q_{10,thermoTRP}$ varying from 10 to 30. It can be appreciated that moderate variations in the expression levels of the thermoTRP under study, which are inherent to overexpression studies, or in the amplitudes of the background and leak currents, which is inherent to the patch-clamp technique, lead to significant changes in T_{thres}. These changes are more pronounced for lower $Q_{10,thermoTRP}$ values. Thus, overall, T_{thres} has no clear relation to the thermosensitivity of the thermoTRP under study, and can change greatly without changes to the actual thermosensitive gating process.

Given these considerations, the use of T_{thres} to describe and compare the temperature-sensitivity of different thermoTRPs should be discouraged. Nonetheless, the TRP channel literature provides ample examples of the misconceptions that can arise from the use of thermal threshold. For example, based on initial studies describing the heat activation of TRPV1 in oocytes, many later studies have taken a T_{thres} of 43°C for this channel for granted. Moreover, based on this 43-°C threshold value, the potential roles of TRPV1 in thermosensitive processes that take place at normal body temperature have been widely discarded. In contrast, the finding that TRPV1-antagonists cause hyperthermia provides strong evidence that this channel is involved in thermosensation at ~37°C. T_{thres} has also been used to compare and evaluate the effects of mutations and signaling pathways on the thermosensitivity of TRP channels. Based on the above, it is clear that such an approach is only valid when both TRP channel expression levels and $I_{background}$ are kept constant. Arguably, these conditions are not readily met in typical patch-clamp or *Xenopus laevis* oocyte studies.

$Q_{10,thermoTRP}$ can be used to determine whether a channel classifies as a thermoTRP (see above) and may provide relevant thermodynamic information on temperature dependence of channel gating (see below). However, also here some caution is warranted. Firstly, the apparent Q_{10} ($Q_{10,apparent}$) estimated from the slope of plots as illustrated in Fig. 1d only provide a good estimate of the actual $Q_{10,thermoTRP}$ when $I_{thermoTRP} \gg I_{background}$. Indeed, it can be shown that

$$\log Q_{10,apparent} = \frac{I_{thermoTRP} \times \log Q_{10,thermoTRP} + I_{background} \times \log Q_{10,background}}{I_{thermoTRP} + I_{background}} \tag{2}$$

implying that $Q_{10,apparent}$ varies with $I_{thermoTRP}/I_{background}$ (Fig. 1g). Rearrangement of Equation (2) yields the following expression for $Q_{10,thermoTRP}$

$$Q_{10,thermoTRP} = 10^{\left(1+\frac{I_{background}}{I_{thermoTRP}}\right)\times \log Q_{10,apparent} - \frac{I_{background}}{I_{thermoTRP}} \times \log Q_{10,background}} \tag{3}$$

which can be readily applied whenever $I_{background}$ can be estimated, e.g. by application of a blocker of the thermoTRP current or by extrapolation. A short survey of the literature indicates that $Q_{10,apparent}$ is regularly determined under conditions where $I_{thermoTRP}/I_{background} \leq 10$, which, according to Equation (2), leads to significantly erroneous estimates of $Q_{10,thermoTRP}$. This analysis also provides an explanation for the fact that reported Q_{10} values for thermoTRPs can vary by almost one order of magnitude, even within a single study.

Secondly, Q_{10} values derived from whole-cell current recordings reflect the combined thermal sensitivity of the gating and the permeation of the thermoTRP under study: $Q_{10,thermoTRP} = Q_{10,gating} \times Q_{10,permeation}$. Accurate values for $Q_{10,permeation}$ of some TRP and other channels have been obtained based on temperature-induced changes in single-channel conductance, yielding values in the range between 1.3 and 2. Thus, it is advisable correct for effects on permeation when describing the thermal sensitivity of TRP channel gating, according to:

$$Q_{10,gating} = Q_{10,thermoTRP}/Q_{10,permeation}. \tag{4}$$

Overall, these theoretical considerations indicate that T_{thres} and uncorrected Q_{10} cannot be considered as robust descriptors of the gating of thermoTRPs. Moreover, real-life factors such as current noise, uncorrected amplifier off-set, uncompensated series resistance, speed of the temperature changes and leak-subtraction protocols can lead to further spurious changes in estimates of T_{thres} and Q_{10}. To understand the mechanisms of temperature-dependent gating and its modulation by site-directed mutagenesis, ligands, phosphorylation and more, there is a clear need for parameters that are both more robust and more informative. This may be achieved by analysing the experimentally derived gating properties of thermoTRPs using mathematical models that describe the temperature-dependent transitions between closed and open states of the channel in terms of thermodynamically relevant parameters.

3 Basic Characteristic of Prototype ThermoTRPs: TRPM8 and TRPV1

As the gating behavior of the heat-activated TRPV1 and the cold-activated TRPM8 has been studied in most detail, these will be used in this work as the two thermoTRP prototypes. Figure 2a–d show typical steady-state whole-cell currents for these two channels at different voltages and temperatures, such as they can be readily measured upon overexpression in cell lines such as HEK293, COS or CHO. Qualitatively and quantitatively highly similar recordings can be found in published work from different groups (Caterina et al. 1997; McKemy et al. 2002; Peier et al. 2002a; Brauchi et al. 2004, 2006; Voets et al. 2004; Rohacs et al. 2005; Bandell et al. 2006; Matta and Ahern 2007; Voets et al. 2007; Grandl et al. 2010; Mahieu

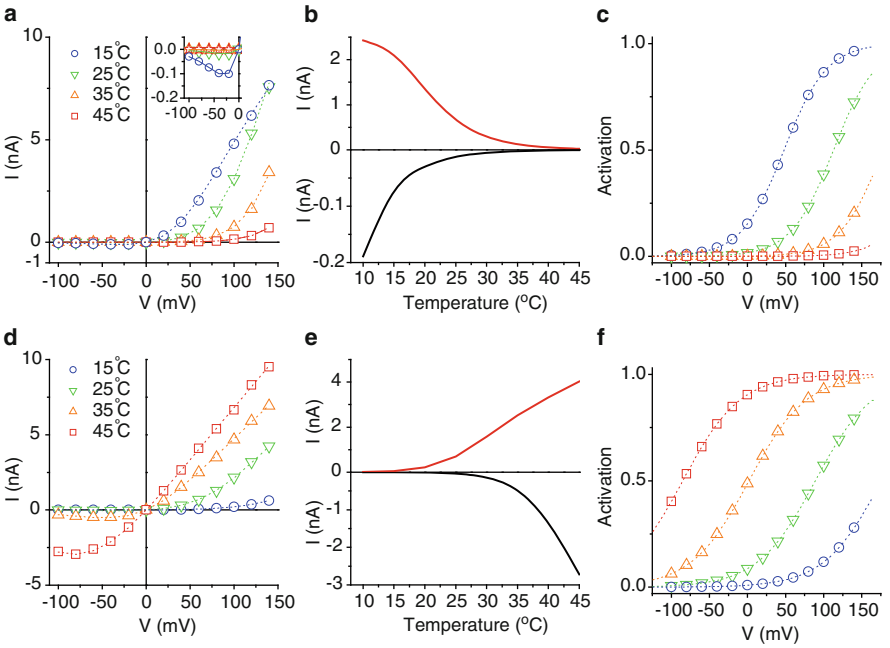

Fig. 2 Properties of steady-state whole-cell currents mediated by TRPM8 (*top*) and TRPV1 (*bottom*). (**a**, **d**) Steady-state whole-cell currents at the end of voltage-steps to the indicated voltages at temperatures ranging from 15 to 45°C. (**b**, **e**) Temperature-dependence of currents measured at +70 mV (*red traces*) and −70 mV (*black traces*). (**c**, **f**) Voltage-dependent activation curves, determined from steady-state currents as in panels (**a**) and (**d**)

et al. 2010). Importantly, the temperature dependence of these two channels is preserved in cell-free membrane patches and even in artificial bilayers (Tominaga et al. 1998; Voets et al. 2004; Zakharian et al. 2010), indicating that temperature sensitivity is not dependent on cellular signaling pathways but rather represents an intrinsic property of these channels.

A first characteristic is the outward rectification of the steady-state current-voltage relations of both channels (Fig. 2a, d). As the single channel conductance of TRPM8 and TRPV1 is virtually voltage-independent, the rectification reflects the fact that these channels are voltage-gated and activated upon depolarization. A second characteristic is the voltage-dependence of the temperature sensitivity of both channels (Fig. 2b, e).During gradual cooling, activation of TRPM8 at depolarized potentials precedes that at negative potentials. Likewise, outward TRPV1 currents can be measured at lower temperatures than inward currents. Based on these data, it has been postulated that temperature-dependent activation of these and other thermoTRPs can be described – at least partly – as graded, temperature-dependent shifts of their voltage-dependent activation curves, as illustrated in Fig. 2c, f.

It should be noted that most – if not all – thermoTRPs can also be activated by chemical ligands, such as menthol (TRPM8) or capsaicin (TRPV1). Recent

research indicates that, as illustrated for TRPM8, a functional thermoTRP channel can have four independent and energetically equivalent ligand binding sites (Janssens and Voets 2011). For simplicity, we focus in the remainder of this review solely on the temperature-dependent gating of thermoTRPs.

4 Models of Thermosensitive Gating

Below, an overview is provided of different potential gating schemes that can be envisaged to model the biophysical properties illustrated in Fig. 3.

4.1 Linear Models

4.1.1 The Two-State Model

A two-state model represents the simplest possible gating scheme for any regulated channel (Fig. 3). The equilibrium between the open (O) and closed (C) state of the channel can be the described by the equilibrium constant K:

$$\mathrm{K} = \frac{\mathrm{O}}{\mathrm{C}} = \exp\left(\frac{-\Delta H + T\Delta S + zFV}{RT}\right) \tag{5}$$

where ΔH is the difference in enthalpy (in J mol^{-1}) and ΔS the difference in entropy (in J mol^{-1} K^{-1}) between the O and C state, z the gating charge (which equals 0 in the case of a voltage-independent channel), V the transmembrane voltage, F the Faraday constant and R the universal gas constant. The channel's open probability is then given by:

$$P_{open} = \frac{O}{O+C} = \frac{1}{1+\frac{1}{K}} = \frac{1}{1+\exp\left(\frac{\Delta H - T\Delta S - zFV}{RT}\right)}. \tag{6}$$

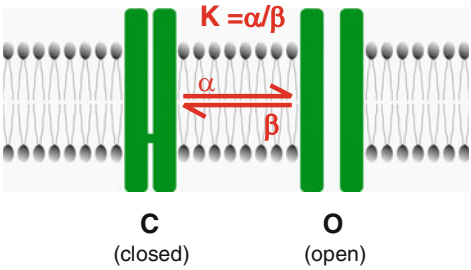

Fig. 3 Graphical representation of the two-state model

P_{open} changes with temperature according to:

$$\frac{dP_{open}}{dT} = \left(\frac{1}{1+\exp\left(\frac{\Delta H - T\Delta S - zFV}{RT}\right)}\right)^2 \times \exp\left(\frac{\Delta H - T\Delta S - zFV}{RT}\right) \times \frac{(\Delta H - zFV)}{RT^2} \tag{7}$$

assuming that ΔH, ΔS and z do not change with temperature. It follows that a channel is heat-activated (i.e. $dP_{open}/dT > 0$) when (ΔH-zFV) > 0 and cold-activated when (ΔH-zFV) < 0 (Nilius et al. 2005). Equation (7) can be rearranged to obtain the theoretical slope of the Arrhenius plot:

$$\left(\frac{d\log P_{open}}{d(1/T)}\right) = -\frac{1}{\ln 10} \times \frac{1}{1+\exp\left(\frac{-\Delta H + T\Delta S + zFV}{RT}\right)} \times \frac{(\Delta H - zFV)}{R}. \tag{8}$$

This yield the following equation for $Q_{10,\text{gating}}$:

$$Q_{10,gating} = 10^{\frac{10}{\ln 10} \times \frac{1}{1+\exp\left(\frac{-\Delta H + T\Delta S + zFV}{RT}\right)} \times \frac{(\Delta H - zFV)}{RT^2}}. \tag{9}$$

$Q_{10,\text{gating}}$ is maximal at low open probabilities (i.e. when ΔH-TΔS-zFV ≫ 0), where

$$Q_{10,gating} \approx 10^{4.34 \times \frac{(\Delta H - zFV)}{RT^2}}. \tag{10}$$

This implies that ΔH can be readily estimated when $Q_{10,\text{gating}}$ has been accurately determined at low P_{open}:

$$\Delta H = \frac{RT^2}{4.34} \log Q_{10,gating} + zFV. \tag{11}$$

For example, in the case of a heat-activated thermoTRP with a $Q_{10,\text{gating}}$ of 30 measured at −70 mV and 40°C, and with z = 0.7, this yields a ΔH of +240 kJ/mol (+57 kcal/mol).

In the case of thermoTRPs that are both temperature- and voltage-dependent, as is the case for TRPM8, TRPV1 and several other thermoTRPs, Equation (6) can be rewritten as

$$P_{open} = \frac{1}{1+\exp\left(\frac{zF}{RT}(V_{1/2} - V)\right)} \tag{12}$$

where $V_{1/2}$ represents the voltage for half-maximal activation. $V_{1/2}$ changes linearly with temperature according to:

$$V_{1/2} = \frac{1}{zF}(\Delta H - T\Delta S). \tag{13}$$

Thus, ΔS and ΔH can be readily derived from the slope and the intercept of a linear fit to experimentally derived $V_{1/2}$ values in function of temperature.

In some cases, it is also possible to experimentally determine the temperature dependence of the kinetics of the transition between the two states. This can be achieved by measuring the mono-exponential time constant (τ) of current relaxation following a step-wise change in temperature or voltage. For the two-state model, τ is related to the opening rate (α), closing rate (β) and steady-state probability:

$$\alpha = \frac{P_{open}}{\tau} \text{ and } \beta = \frac{1 - P_{open}}{\tau}. \tag{14}$$

Following Eyring rate theory, α and β depend on temperature and voltage according to:

$$\alpha = \frac{k_b T}{h} \cdot e^{\frac{-\Delta H_{open} + T\Delta S_{open} + \delta zFV}{RT}} \text{ and } \beta = \frac{k_b T}{h} \cdot e^{\frac{-\Delta H_{close} + T\Delta S_{close} - (1-\delta)zFV}{RT}} \tag{15}$$

where ΔH_{open} and ΔH_{close} represent the enthalpies and ΔS_{open} and ΔS_{close} the entropies associated with channel opening and closing, δ the fraction of the gating charge moved in the outward direction, k_b the Boltzmann constant (1.38×10^{-23} J/K) and h the Planck constant (6.63×10^{-34} J/s). Experimentally derived values for α and β can be represented as an Arrhenius plot (ln(α) and ln(β) in function of (1/T)) and fitted with a linear function, which allows easy determination of ΔH_{open}, ΔH_{close}, ΔS_{open} and ΔS_{close} given that:

$$\begin{aligned} \ln \alpha &= \left(\ln \frac{kT}{h} + \frac{\Delta S_{open}}{R} \right) - \frac{\Delta H_{open} - \delta zFV}{R} \times \left(\frac{1}{\mathrm{T}} \right) \\ \ln \beta &= \left(\ln \frac{kT}{h} + \frac{\Delta S_{close}}{R} \right) - \frac{\Delta H_{close} + (1-\delta)zFV}{R} \times \left(\frac{1}{\mathrm{T}} \right). \end{aligned} \tag{16}$$

Note that $\Delta H = \Delta H_{open} - \Delta H_{close}$ and $\Delta S = \Delta S_{open} - \Delta S_{close}$.

To a large extent, the results obtained for TRPV1 and TRPM8 agree well with the predictions of this two-state model in the temperature range between 10°C and 45°C (Voets et al. 2004, 2005). For example, as predicted by Equation (13), there is a quasi linear relation between $V_{1/2}$ and T, and the slope of this relation increases when z is reduced due voltage sensor mutations in TRPM8 (Voets et al. 2007). Likewise, current relaxation time courses for TRPM8 and TRPV1 in response to a sudden change in voltage or temperature are relatively well described by a mono-exponential function (Voets et al. 2004; Yao et al. 2011), and the Arrhenius plots for α and β are linear in the tested temperature range (Voets et al. 2004). This approach has allowed determination and comparison of values for ΔH_{open}, ΔH_{close}, ΔS_{open} and ΔS_{close} for different cold- and heat-activated thermoTRPs, which allows quite accurate simulation of the temperature-dependent kinetics and steady-state behavior of these channels (Voets et al. 2004; Talavera et al. 2005; Karashima et al. 2009; Vriens et al. 2011).

Recently, Clapham and Miller put forward the hypothesis that gating of thermoTRPs is accompanied by large changes in molar heat capacity (ΔC_p), in the range between 8 and 20 kJ mol^{-1} K^{-1} (2–5 kcal mol^{-1} K^{-1}) (Clapham and Miller 2011). Following the laws of thermodynamics, ΔC_p determines how ΔH and ΔS change with temperature, according to:

$$\Delta H(T) = \Delta H_0 + \Delta C_p(T - T_0) = \left(\Delta H_0 - \Delta C_p T_0\right) + \Delta C_p T \tag{17}$$

and

$$\Delta S(T) = \Delta S_0 + \Delta C_p \ln(T/T_0) = \left(\Delta S_0 - \Delta C_p \ln T_0\right) + \Delta C_p \ln T \tag{18}$$

where ΔH_0 and ΔS_0 represent the difference in enthalpy and entropy between the closed and open channel at temperature T_0. For example, if we consider 0–60°C as the physiologically relevant temperature range in which thermoTRPs operate and $T_0 = 0$°C (273 K), then the maximal relative change in ΔH and ΔS in this temperature range is given by:

$$\frac{\Delta H(60°C)}{\Delta H(0°C)} = 1 + \frac{60K \times \Delta C_p}{\Delta H_0} \tag{19}$$

and

$$\frac{\Delta S(60°C)}{\Delta S(0°C)} = 1 + \frac{0.198 \times \Delta C_p}{\Delta S_0}. \tag{20}$$

Whenever $|\Delta H_0| \gg |60\ \text{K} \times \Delta C_p|$ and $|\Delta S_0| \gg |0.198 \times \Delta C_p|$, ΔH and ΔS can be considered constant and Equations (7–13) are valid. However, if $|60\ \text{K} \times \Delta C_p|$ is large compared to $|\Delta H_0|$, the difference in enthalpy between the closed and open channel varies significantly in the relevant temperature range and Equations (7–13) are no longer accurate. Importantly, from Equation (17) it also follows that ΔH equals zero and changes sign at temperature $T_{\Delta H=0}$:

$$T_{\Delta H=0} = T_0 - \frac{\Delta H_0}{\Delta C_p}. \tag{21}$$

At this temperature, the channel switches between a heat-activated ($\Delta H > 0$) and a cold-activated ($\Delta H < 0$) mode. Based on this, Clapham and Miller postulate that every thermoTRP is both heat- and cold-activated. Figure 4 illustrates the effect of varying values of ΔC_p on the temperature dependence of ΔH, ΔS and P_{open} for a generic thermoTRP.

Although intriguing, the published data on thermoTRPs do not provide any evidence that gating of thermoTRPs is accompanied by large changes in molar heat capacity. In contrast, several studies have shown a quasi-linear relation between ln(K) and 1/T (Equation (5)) or between $V_{1/2}$ and temperature

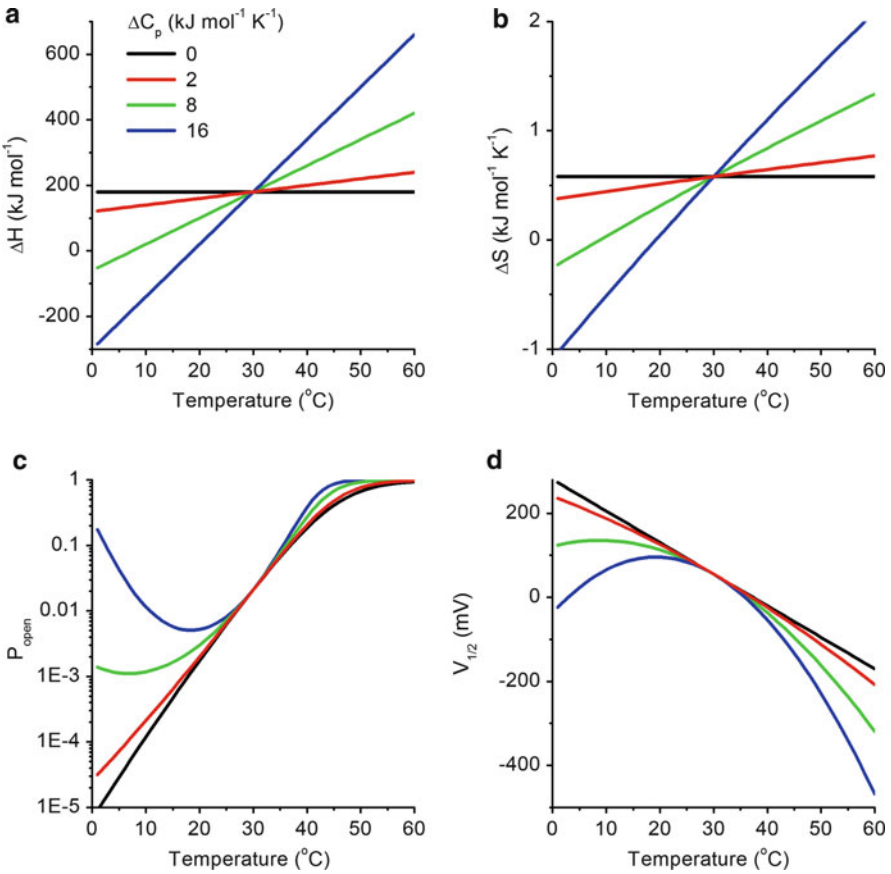

Fig. 4 Effect of ΔC_p on ΔH (**a**), ΔS (**b**), P_{open} (**c**) and $V_{1/2}$ (**d**) for the two-state model. Values of ΔS_0, ΔH_0 and T_0 were chosen such that $\Delta H = 180\,kJ\,mol^{-1}$ and $\Delta S = 0.58\,kJ\,mol^{-1}\,K^{-1}$ at 30°C in all cases and $z = 0.8$ (similar to published values for TRPV1)

(Equation (13)) for different thermoTRP in the physiological temperature range, indicating that ΔH is relatively constant. Moreover, there are no examples in the literature of thermoTRPs that switch between a heat-activated and a cold-activated mode, despite the fact that many have been tested across the entire physiological temperature range. Therefore, in the absence of such experimental evidence (or better: direct calorimetric measurements of ΔC_p), the assumption of constant ΔH and ΔS in the physiological temperature range remains valid.

4.1.2 Multistate Linear Models

Based on kinetic analyses of whole-cell or single-channel recordings, linear models with more than one closed and/or open states have been proposed for certain TRP

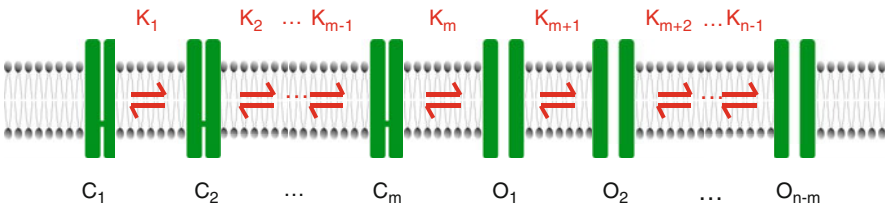

Fig. 5 Graphical representation of the general multistate linear model

channels (Grandl et al. 2010; Yao et al. 2011). In general, for a linear model with n states (Fig. 5), there are n − 1 equilibrium constants (K_1 to K_{n-1}), each of which depends on temperature and voltage as in Equation (5):

$$K_i = \exp\left(\frac{-\Delta H_i + T\Delta S_i + z_i FV}{RT}\right). \tag{22}$$

With m closed and n − m open states, the open probability is given by:

$$\begin{aligned} P_{open} &= \frac{1}{1 + \frac{1+K_1+K_1\times K_2+\ldots+K_1\times K_2\times\ldots\times K_{m-1}}{K_1\times K_2\times\ldots\times K_m+K_1\times K_2\times\ldots\times K_m\times K_{m+1}+\ldots+K_1\times K_2\times\ldots\times K_{n-1}}} \\ &= \frac{1}{1 + \frac{\sum_{i=0}^{m-1}\prod_{j=1}^{i} K_j}{\sum_{i=m}^{n-1}\prod_{j=1}^{i} K_j}}. \end{aligned} \tag{23}$$

The general equation for the temperature-induced changes in P_{open} (dP_{open}/dT) for such linear models is impractically complex. However, assuming that all transitions towards the *n*th state are heat-activated (i.e. $\Delta H_i > 0$ for all transitions), all equilibrium constants will be $\ll 1$ at increasingly low temperatures, where Equation (23) simplifies to

$$P_{open} \approx K_1 \times K_2 \times \ldots \times K_m = \exp\left(\frac{-\sum_{i=1}^{m}\Delta H_i + T\sum_{i=1}^{m}\Delta S_i + \sum_{i=1}^{m} z_i FV}{RT}\right). \tag{24}$$

Under such conditions, the limiting $Q_{10,\text{gating}}$ is given by

$$Q_{10,gating} \approx 10^{4.34\times\frac{\left(\sum_{i=1}^{m}\Delta H_i - \sum_{i=1}^{m} z_i FV\right)}{RT^2}} = \prod_{i=1}^{m} Q_{10,i} \tag{25}$$

where $Q_{10,i}$ represents the temperature sensitivity of the *i*th transition. Thus, the total change in enthalpy leading to channel opening can be obtained by determining

asymptotic $Q_{10,\text{gating}}$ at low P_{open}, similar to the limiting slope method that has been widely used to determine the total gating charge of voltage-gated channels (Almers 1978). A similar analysis applies to a cold-activated channel at increasingly high temperatures, in case all transitions are cold-activated.

It has been postulated that the high temperature-sensitivity of certain thermoTRPs may be generated by sequential mildly temperature-sensitive transitions between multiple open states. In particular, it was stated that the temperature sensitivity of the overall open probability (i.e. $Q_{10,\text{gating}}$) is the product of the temperature dependencies of individual sequential gating transitions between multiple open states (Grandl et al. 2010). However, the above analysis indicates that this postulate is not generally applicable. Instead, the overall temperature sensitivity represents the combined temperature dependencies of individual sequential gating transitions leading to the first main open state, rather than the combined temperature dependence of transitions between open states.

4.2 Allosteric Models

The linear models described above do not make any assumptions about the molecular basis of the changes in enthalpy and entropy that occur when the channel transits between the different states. In principle, these changes may occur all over the channel protein (and even in associated molecules). However, it can be envisaged that specific domains of the channel act as thermosensing modules that change from a resting to an activated state in function of temperature and thereby modulate channel gating (Brauchi et al. 2004; Latorre et al. 2007). Several possible models can be employed to describe the gating of thermoTRPs containing one or more such thermosensing modules. Such models have been termed "allosteric" (from the Greek αλλος = other, and στερεος = object), to emphasize that the thermosensing occurs at a site other than the active site of the channel, being the pore. For a discussion on the use and misuse of the term allosteric, I refer the reader to the excellent treatise by Colquhoun (1998).

4.2.1 The Monod–Wyman–Changeux-Type Allosteric Model

The Monod–Wyman–Changeux (MWC) allosteric model was originally developed to describe the cooperative binding of oxygen to hemoglobin, a tetrameric protein with four oxygen-binding sites (Monod et al. 1965). In the MWC model it is assumed that the *n* subunits (four, in the case of hemoglobin) undergo a concerted transition from a *tense* (T) to a *relaxed* (R) state; subunits in the R state have a higher affinity for ligand than in the T state, and, consequently, ligand binding changes the equilibrium of the protein in favor of the R state (Monod et al. 1965).

This MWC model can be adapted for a thermoTRP with *n* thermosensing modules, where the C and O states of the channel are the equivalents of the T and

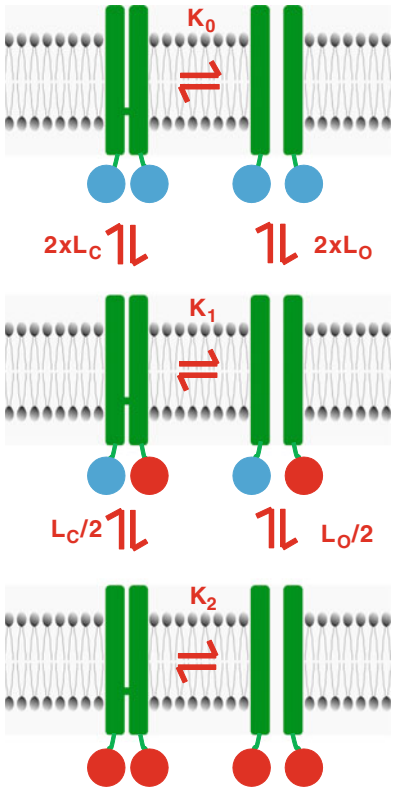

Fig. 6 Graphical representation of the MWC model for a channel with two thermosensing modules. *Blue* and *red circles* represent thermosensing modules in the resting and active state, respectively

R states (Fig. 6). Each thermosensing module can be in either the resting or the active conformation, analogous to the free and ligand-bound state of the binding sites in the original MWC model. In this scheme, a channel has n + 1 closed and n + 1 open states, denoted as C_0–C_n and O_0–O_n, where the subscript indicates the number of thermosensing modules in the active conformation. The equilibrium between two closed states is given by:

$$\frac{C_i}{C_{i-1}} = \frac{(n+1-i)}{i} L_C \tag{26}$$

and

$$L_C = \exp\left(\frac{-\Delta H_C + T\Delta S_C}{RT}\right) \tag{27}$$

where L_C determines the equilibrium between the resting and active conformation of a thermosensing module in a closed channel, which depends on ΔH_C, the difference in enthalpy, and ΔS_C, the difference in entropy between these states. Note that $\Delta H_C > 0$ for a heat-activated and $\Delta H_C < 0$ for a cold-activated module.

When all thermosensing modules are in the resting state, the equilibrium between the closed (C_0) and open (O_0) state is given by:

$$K_0 = \frac{O_0}{C_0} = \exp\left(\frac{-\Delta H_0 + T\Delta S_0 + zFV}{RT}\right). \tag{28}$$

With the assumption that the thermosensitive elements are concentrated in the thermosensing modules, it can be stated that

$$\left|\frac{dK_0}{dT}\right| << \left|\frac{dL_C}{dT}\right| \tag{29}$$

which implies that $|\Delta H_C| \gg |\Delta H_0|$.

If we further assume that the *n* thermosensing units are independent and equivalent, and that activation of each thermosensing unit changes the enthalpic difference between the closed and open state by a factor $\Delta\Delta H/n$, we obtain that:

$$K_i = \frac{O_i}{C_i} = K_0 \exp\left(\frac{-i(\Delta\Delta H - T\Delta\Delta S)}{nRT}\right). \tag{30}$$

Note that

$$\exp\left(\frac{-i(\Delta\Delta H - T\Delta\Delta S)}{nRT}\right) > 1 \tag{31}$$

since we assume that activated thermosensing modules promote channel opening. It follows that

$$\frac{O_i}{O_{i-1}} = \frac{(n+1-i)}{i} L_O \tag{32}$$

where

$$L_O = L_C \exp\left(\frac{-(\Delta\Delta H + T\Delta\Delta S)}{nRT}\right). \tag{33}$$

The probability that the channel is in one of the n + 1 open states is given by

$$P_{open} = \frac{1}{1 + \frac{(1+L_C)^n}{K_0(1+L_O)^n}}. \tag{34}$$

In case of a voltage-gated channel, this equation can be rewritten as

$$P_{open} = \frac{1}{1 + \exp\left(\frac{V_{1/2} - V}{s}\right)} \tag{35}$$

where $V_{1/2}$ is given by

$$V_{1/2} = \frac{1}{zF}(\Delta H_0 - T\Delta S_0) + \frac{nRT}{zF} \ln \frac{1 + L_C}{1 + L_O}. \tag{36}$$

First, consider the temperature range where $L_C \ll 1$ and $L_O \ll 1$, i.e. when $-\Delta H_C + T\Delta S_C \ll 0$ and $(\Delta H_C + \Delta\Delta H) + T(\Delta S_C + \Delta SS) \ll 0$. In this temperature region, the thermosensing modules are mainly in the resting form, and gating can be approximated using a two-state model in which the channel shuttles exclusively between states C_0 and O_0, with open probability:

$$P_{open} \approx \frac{1}{1 + \frac{1}{K_0}}. \tag{37}$$

In case of a voltage-gated channel, the voltage for half-maximal activation is then given by:

$$V_{1/2} \approx \frac{1}{zF}(\Delta H_0 - T\Delta S_0). \tag{38}$$

Next, consider the temperature range where $L_C \gg 1$ and $L_O \gg 1$, i.e. when $-\Delta H_C + T\Delta S_C \gg 0$ and $-(\Delta H_C + \Delta\Delta H) + T(\Delta S_C + \Delta SS) \gg 0$. In this temperature region, the thermosensing modules are mainly in the active form, and gating can be approximated using a two-state model in which the channel shuttles exclusively between states C_n and O_n, and open probability is given by:

$$P_{open} \approx \frac{1}{1 + \frac{1}{K_n}} \tag{39}$$

with

$$K_n = \exp\left(\frac{-\Delta H_n + T\Delta S_n + zFV}{RT}\right) \tag{40}$$

where $\Delta H_n = \Delta H_0 + \Delta\Delta H$ and $\Delta S_n = \Delta S_0 + \Delta\Delta S$.

Functionally most important is the temperature range where $L_O \gg 1$ and $L_C \ll 1$. In this temperature range the temperature-sensitivity is the highest. Gating can be approximated using a two-state model in which the channel shuttles between states C_0 and O_n and open probability is given by:

$$P_{open} \approx \frac{1}{1 + \frac{1}{K^*}} \tag{41}$$

with

$$K^* = \exp\left(\frac{-\Delta H^* + T\Delta S^* + zFV}{RT}\right) \tag{42}$$

where $\Delta H^* = \Delta H_0 + n\Delta H_C + \Delta\Delta H$ and $\Delta S^* = \Delta S_0 + n\Delta S_C + \Delta\Delta S$.

Analogous to Equation (10), ΔH^* is related to the maximal value of $Q_{10,gating}$ at low open probabilities: $Q_{10,gating} \approx 10^{4.34\times\frac{(\Delta H^* - zFV)}{RT^2}}$

4.2.2 The Dual-Allosteric Coupling Model

An even more modular view of thermoTRP channel gating is represented by the dual-allosteric model (Brauchi et al. 2004), which is an adaptation of a model originally derived for large-conductance Ca^{2+}-activated K^+ channels (Horrigan and Aldrich 2002). In this model, the channel gate and distinct voltage and temperature sensors are envisaged as separate, allosterically coupled channel modules (Fig. 7).

The equilibrium between the resting (R_T) and activate (A_T) state of the temperature sensors is analogous to Equation (27):

$$L_T = \frac{A_T}{R_T} = \exp\left(\frac{-\Delta H_T + T\Delta S_T}{RT}\right) \tag{43}$$

whereas the equilibrium between the resting (R_V) and activated (A_V) state of the voltage sensor can be written as

$$L_V = \frac{A_V}{R_V} = L_{V0}\exp\left(\frac{zFV}{RT}\right) \tag{44}$$

where L_{V0} is the equilibrium constant at 0 mV (Note that this equation is equivalent to Equation (7) with $\Delta H = 0$ and $\Delta S = R\ln L_{V0}$).

The voltage and temperature sensors are allosterically coupled to opening of the channel, which is quantified by the allosteric coupling constants D_V and D_T, respectively. The equilibrium of the channel gate is given by:

$$\frac{O}{C} = D_V^i \times D_T^j \times K_G \tag{45}$$

where i and j represent the number of active voltage and temperature sensors, respectively, and K_G the equilibrium constant for channel gating when all sensors are inactive. K_G has been assumed to be voltage- and temperature-independent and $\ll 1$, and represents a lower limit to the channel's open probability. Interaction between voltage and temperature sensors can be defined by an additional allosteric factor E, which equals 1 in case the temperature and voltage sensors do not interact.

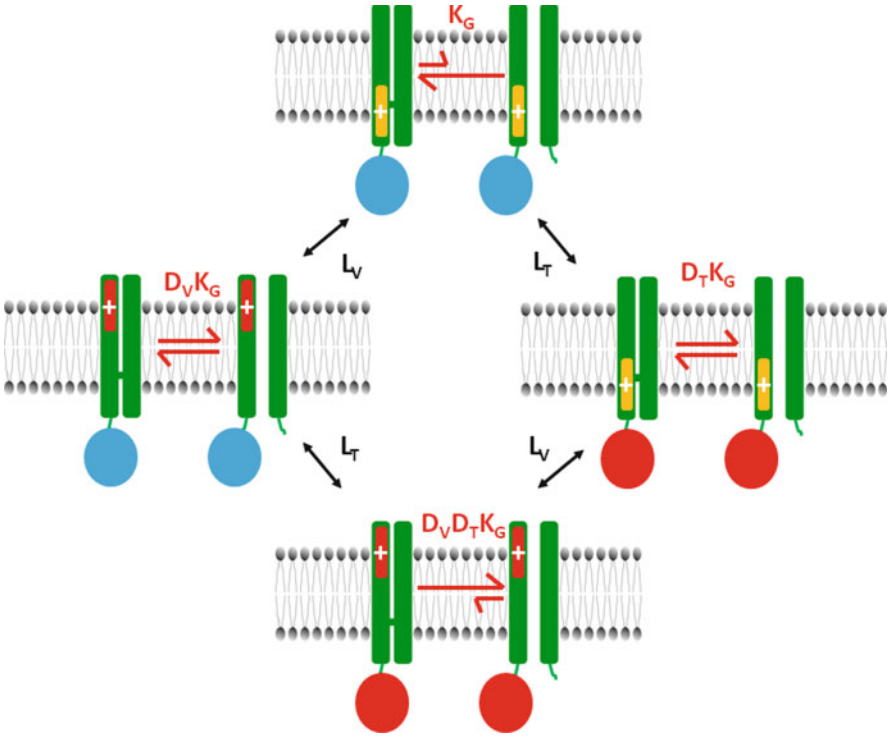

Fig. 7 Graphical representation of the dual allosteric model for a channel with one thermosensing and one voltage-sensing module. *Blue* and *red circles* represent thermosensing module in the resting and active state, respectively. The voltage sensor is represented by the rod with the *plus sign*, being intracellularly oriented and *orange* when in the resting state, and extracellularly oriented and *red* when in the active state

Assuming E = 1 and an equal number (n) of voltage and temperature sensors, the channel's open probability is given by

$$P_{open} = \frac{1}{1 + \frac{(1+L_V+L_T+L_VL_T)^n}{K_G(1+L_VD_V+L_TD_T+L_VL_TD_VD_T)^n}}. \tag{46}$$

When all voltage sensors are in the resting states (i.e. at very negative voltages, where $L_V \approx 0$ and $L_VD_V \approx 0$), Equation (46) simplifies to

$$P_{open} \approx \frac{1}{1 + \frac{(1+L_T)^n}{K_G(1+L_TD_T)^n}}. \tag{47}$$

The steepest temperature dependence of P_{open} occurs at temperatures where $L_T \ll 1$ and $L_TD_T \gg 1$, where

$$P_{open} \approx \frac{1}{1 + \frac{1}{K^{**}}} \tag{48}$$

with

$$K^{**} = \exp\left(\frac{-\Delta H^{**} + T\Delta S^{**}}{RT}\right) \tag{49}$$

where $\Delta H^{**} = n\Delta H_T$ and $\Delta S^{*} = n\Delta S_T + RlnK_G D_T{}^n$. This yield a maximal $Q_{10,gating}$ given by:

$$Q_{10,gating} \approx 10^{4.34 \times \frac{\Delta H^{**}}{RT^2}}. \tag{50}$$

5 What Is the Best Model?

Although, at first sight, the above-described models may seem quite different, it can be readily shown that the two-state and MWC-type model are actually special cases of the dual-allosteric model. The MWC-type model represents the case where allosteric coupling between channel gating and the voltage sensor(s) is very strong, i.e. that the channel is open when the voltage sensors are active, and closed when the voltage sensors are inactive. This is the case when $L_V \ll 1$ and $L_V D_V \gg 1$, where Equation (47) reverts to Equation (34), with $L_C = L_T$, $L_O = L_T D_T$ and $K_0 = K_G L_V D_V$. The two-state model represents the case where the allosteric coupling between channel gating and both the temperature sensor(s) and the voltage sensor (s) is very strong, i.e. when both $L_V \ll 1$ and $L_T \ll 1$, and $L_V D_V \gg 1$ and $L_T D_T \gg 1$. Now Equation (47) reverts to Equation (6), with $K = K_G \times (L_V D_V L_T D_T)^n$, or $\Delta H = n\Delta H_T$ and $\Delta S = n\Delta S_T + nRlnL_{V0} D_V D_T$.

When choosing the best model to describe the gating of thermoTRPs, one may be guided by Occam's razor, which recommends the use of the simplest model that adequately describes the available experimental data. In this respect it should be noted that the number of free parameters for the description of steady-state currents (or P_{open}), increases from 3 for the two-state model (ΔH, ΔS and z) to ≥ 8 for the MWC-type and dual allosteric model. For example, the steady-state data for TRPM8 and TRPV1 shown in Fig. 2 are adequately described by the two-state model. Fitting these whole-cell data with the more complex models can yield a comparable fit, but will inevitably lead to interdependence of parameters, resulting in non-uniqueness and unacceptable errors on some parameter estimates.

There are, however, experimental observations that may urge the use of the more complex models. For example, both the two-state and the MWC-type model predict that voltage-gated thermoTRPs can be fully opened and closed by voltage, independent of temperature (Fig. 8a). In contrast the dual-allosteric model predicts that the minimal ($P_{open,min}$) and maximal ($P_{open,max}$) open probability that can be achieved by voltage change with temperature (Fig. 8b), according to:

$$P_{open,\min}(T) = \frac{1}{1 + \frac{(1+L_T)^n}{K_G(1+L_T D_T)^n}} \geq 0 \tag{51}$$

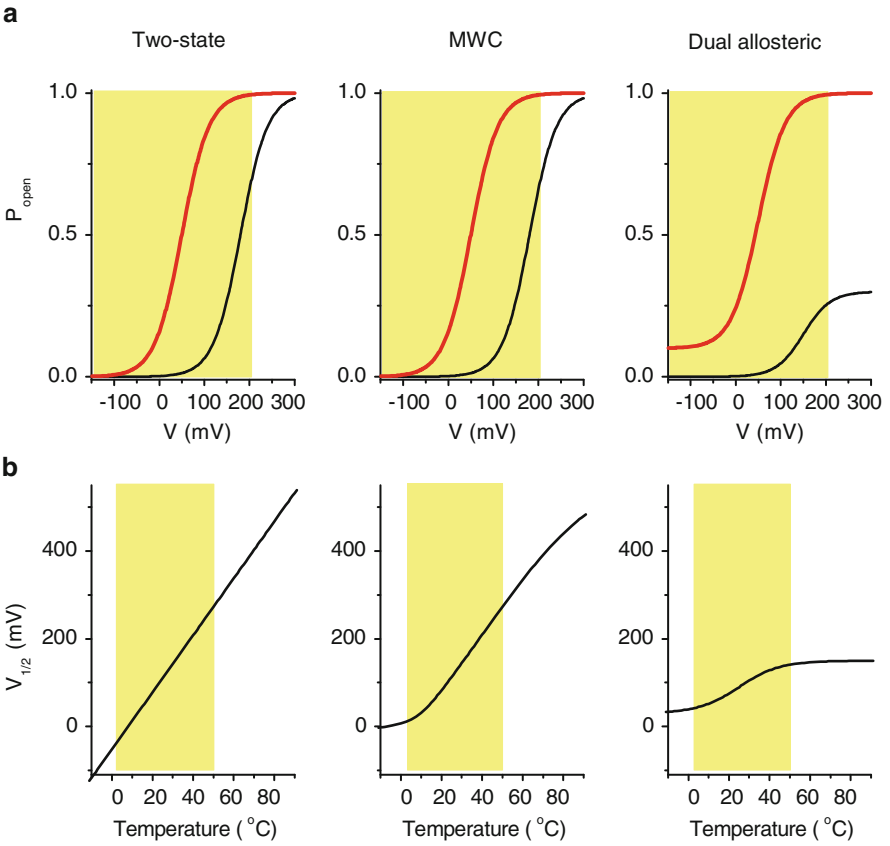

Fig. 8 Theoretical differences between the two-state, MWC and dual allosteric model, illustrated for a cold-activated channel. (**a**) Voltage-dependent activation curves at higher (*black*) and colder (*red*) temperatures. (**b**) $V_{1/2}$ in function of temperature. The *yellow backgrounds* indicate the voltage and temperature ranges that are practically amenable for steady-state whole-cell patch-clamp recordings

and

$$P_{open,\max}(T) = \frac{1}{1 + \frac{(1+L_T)^n}{K_G D_V^n (1+L_T D_T E)^n}} \leq 1. \tag{52}$$

Experiments suggesting that temperature alters $P_{open,max}$ have been taken as evidence for the dual allosteric model (Brauchi et al. 2004; Matta and Ahern 2007). It should be noted here that an accurate determination of $P_{open,max}$ of a thermoTRP is not at all trivial, and prone to errors for several reasons. First, $V_{1/2}$ values of voltage-dependent TRP channels are mostly in the positive voltage range, whereas z is generally low. For example, for TRPM8 we have determined a z of 0.92 and a $V_{1/2}$ value of approximately +200 mV at 37°C (Voets et al. 2007). Consequently,

depolarisations to extremely depolarised potentials (>+250 mV) are required to approach saturation, which is often not well tolerated in whole-cell patch-clamp recordings. Therefore, in most reports, $P_{open,max}$ is determined by extrapolation, inevitably inducing uncertainties. Second, deactivation of thermoTRPs is often very rapid ($\tau \ll 1$ ms), especially at higher temperatures (Voets et al. 2004). As a consequence, the use of tail currents to determine activation curves, as is generally done in the case of e.g. voltage-gated K^+ channels, can lead to an underestimation of P_{open}. Finally, overexpressing TRP channels in cell lines such as HEK or CHO can easily result in whole-cell current amplitudes of several tens of nanoAmperes at depolarised potentials, which, when not properly compensated, can easily provoke voltage-clamp errors of several tens of millivolts. Clearly, incorrect dealing with these issues inevitably leads to errors in estimating $P_{open,max}$. Functional measurements of thermoTRP channels in artificial systems (e.g. bilayers) may provide means to obtain more reliable estimates of $P_{open,max}$ at extreme voltages.

The temperature dependence of $V_{1/2}$ represents another potential discriminator between models. Indeed, whereas the two-state model predicts that $V_{1/2}$ changes linearly with temperature over the entire temperature range Equation (13), the MWC-type and dual-allosteric models predict saturation of $V_{1/2}$ at both low and high temperatures (Fig. 8b). At least for TRPM8, TRPV1 and TRPM5, studies have demonstrated a quasi-linear relation between $V_{1/2}$ and temperature in the physiologically relevant temperatures range (Voets et al. 2004; Talavera et al. 2005). However, again, the temperatures and voltages that can be reliably applied in whole-cell recordings are relatively restricted, and saturation at more extreme temperatures has not been reliably tested.

Finally, analysis of the kinetics of single-channel activity can yield a lower estimate of the total number of discernible closed and open states. Analysis of single-channel data for TRPV1 (Liu et al. 2003; Grandl et al. 2010) and TRPM8 (Fernandez et al. 2011) have indeed provided evidence for the existence of more than one open and closed state.

6 What Can We Learn from Structure-Function Studies (and What Not)?

A growing number of papers in recent years report structure-function analyses of thermoTRPs, aimed at understanding the molecular basis of their high temperature sensitivity (Vlachova et al. 2003; Brauchi et al. 2006, 2007; Voets et al. 2007; Grandl et al. 2008, 2010; Yang et al. 2010; Cordero-Morales et al. 2011; Yao et al. 2011). Generally, these studies apply site-directed or random mutagenesis to thermoTRPs and test the effects of these mutations on the thermosensitivity of channel gating following heterologous expression. These studies report identification of regions that specifically modulate thermosensitivity, which are sometimes put forward as thermosensor modules (Latorre et al. 2007; Yang et al. 2010; Cordero-Morales et al. 2011; Yao et al. 2011), analogous to the voltage sensor

module in the fourth transmembrane domain of voltage-gated K^+, Na^+ or Ca^{2+} channels (Tombola et al. 2006). In the case of TRPV1, studies have identified residues and regions that influence thermosensitivity in distal (Vlachova et al. 2003) and proximal (Brauchi et al. 2007) parts of the C-terminal tail, in the pore region (Grandl et al. 2010) and pore turret (Yang et al. 2010), and in the N-terminal region between ankyrin repeat domains and first transmembrane loop (Yao et al. 2011). Summarizing and interpreting the combined data of these different studies is not at all straightforward due to the diversity of methodology and analytical approaches and the (apparently) conflicting conclusions (Table 1; Fig. 9). A rough meta-analysis of these studies may lead to the conclusion that multiple regions, spread over the entire channel, determine the channel's response to changes in temperature, rather than a single, localized thermosensor module. Strikingly, there is not only disparity in the identified residues and regions but also quite substantial variation in quantitative parameters such as $T_{threshold}$, Q_{10}, and ΔH (both within and between studies), which, as discussed above, probably reflects the lack of robustness of some of these parameters as well as differences in methodology.

Does this mean that such structure-function studies are necessarily a wasted effort, as has been recently suggested (Clapham and Miller 2011)? To the contrary, determining the structures and structural rearrangements that underlie the high temperature sensitivity of thermoTRPs can be considered of comparable scientific interest as the search for the molecular nature and detailed mechanisms of the

Table 1 Overview of the literature on the structural basis of heat sensitivity in TRPV1

Reference	Quantification	Quotes
Vlachova et al. (2003)	Q_{10} and T_{thres}	". . ., our results provide evidence that the structural basis of the thermal sensitivity of the TRPV1 channel resides in the distal half of the C terminal."
Brauchi et al. (2007)	Q_{10}	"Our results show that the region located outside the TRP domain comprising the TRPV1 C-terminal amino acids Q727 and W752 is the minimal portion able to turn TRPM8 into a heat receptor."
Yang et al. (2010)	ΔH, ΔS	"These observations suggest that the turret is part of the temperature-sensing apparatus in thermoTRP channels, and its conformational change may give rise to the large entropy that defines high temperature sensitivity."
Yao et al. (2010)	Only qualitative	"Pore turret of thermal TRP channels is not essential for temperature sensing."
Grandl et al. (2010)	Loss of a long open state in single channel analysis.	"We used both random and targeted mutagenesis screens of rat TRPV1 and identified point mutations in the outer pore region that specifically impair temperature activation."
Yao et al. (2011)	ΔH, ΔS	". . .we demonstrate that temperature-gated channels possess localized structural components for detection of temperature changes. Our data converged to a fragment of approximately 80 residues on the N terminus of the channels that connects the ankyrin repeats to the first TM domain."

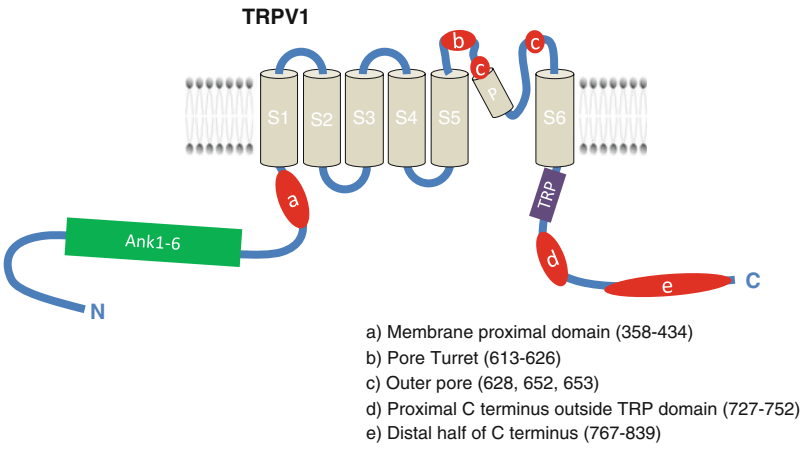

Fig. 9 Domains implicated in the thermosensitivity of TRPV1. *Red ovals* (*a–e*) delineate regions identified in different structure-function studies (see text and Table 1 for more details). Also indicated are the 6 Ankyrin repeats (Ank1-6), the 6 transmembrane domains (S1–S6), the pore helix (P) and the TRP domain

voltage sensor in classical voltage-gated cation channels. The mechanisms whereby these voltage-gated channels sense and respond to changes in the transmembrane voltage has dominated both the research of many top-level ion channel laboratories and the content of the top-level journals during the last decades (Catterall 2010). The combined and rigorous use of a variety of methods (e.g. site-directed mutagenesis, determination of total gating charge using gating current measurement and limiting slope methods, optical measurement of voltage sensor movements, electrophysiological analysis of the voltage sensor pathway, X-ray structure analysis of voltage gated channels and structure-based molecular modeling. . .) has provided important insights into the nature and motion of the voltage-sensor, which (gradually) progresses to a consensus on how voltage sensing works (Tombola et al. 2006; Catterall 2010). A similar rigorous approach will be required to further our understanding of the molecular basis of thermosensitivity in TRP channels.

7 Conclusions and Outlook

The steep temperature dependence of thermoTRPs lies at the basis of our bodies' ability to measure temperature, and understanding the detailed mechanisms underlying the striking thermal sensitivity of these channels is of fundamental biological/biophysical interest. Moreover, detailed knowledge of their *modus operandi* will assist exploiting thermoTRPs as targets for novel analgesic treatments. However, understanding the thermodynamic mechanisms of thermosensation and identifying the residues, regions and structural rearrangement responsible for the large enthalpy difference between a closed and open thermoTRP appears to be even more

demanding than the hunt for the voltage-sensor of voltage-gated channels and mapping of its voltage-dependent movements.

First, as illustrated above, there is no general consensus on the methods to determine ΔH for temperature-sensitive channels, which currently thwarts efforts to compare and combine results obtained in the different published papers on the molecular basis of thermosensitivity in thermoTRPs. Nevertheless, as outlined above, determination of the corrected $Q_{10,gating}$ at low open probabilities provides a model-independent estimate of the change in enthalpy upon opening of the channel, comparable to the limiting slope method for determination of the total gating charge movement required to open a voltage-gated channel. Moreover, it may become possible to use calorimetry to directly measure the amount of heat that is liberated/absorbed during gating of thermoTRPs. This would allow direct measurement of ΔH, comparable to the direct measurement of gating charge movement from gating currents in voltage-gated channels.

Second, whereas voltage sensing is limited to charged residues located within the transmembrane electrical field, temperature affects all atoms in the channel (and even in the interacting membrane lipids). Nevertheless, the developments in automated patch-clamp devices, combined with large-scale random mutagenesis may enable mapping the energetic contribution of most if not all residues in a thermoTRP.

Third, in contrast to voltage-gated Na^+ and K^+ channels, there is a general lack of crystal structures of integral TRP channels, despite, undoubtedly, intense efforts by many research groups. Nevertheless, there is no reason to believe that TRP channels are "uncrystallable", and it can be expected that in the coming decade we will see detailed images of the structure of various TRP channel. This may ultimately yield a precise view of the localized or global conformational changes that occur during gating of TRP channels, allow calculation of the contribution of domains, residues and even atoms to the thermodynamic properties of thermoTRPs.

Acknowledgements I wish to thank Bernd Nilius for his support, encouragements and comments on the manuscript, and all present and former members of the Laboratory of Ion Channel Research for enlightening discussions. Our work on thermoTRPs was supported by grants from the Belgian Federal Government (IUAP P6/28), the Research Foundation-Flanders (F.W.O.) (G.0565.07), and the Research Council of the KU Leuven (GOA 2009/07, EF/95/010 and PF-TRPLe).

References

Almers W (1978) Gating currents and charge movements in excitable membranes. Rev Physiol Biochem Pharmacol 82:96–190

Bandell M, Dubin AE, Petrus MJ, Orth A, Mathur J, Hwang SW, Patapoutian A (2006) High-throughput random mutagenesis screen reveals TRPM8 residues specifically required for activation by menthol. Nat Neurosci 9:493–500

Bandell M, Macpherson LJ, Patapoutian A (2007) From chills to chilis: mechanisms for thermosensation and chemesthesis via thermoTRPs. Curr Opin Neurobiol 17:490–497

Basbaum AI, Bautista DM, Scherrer G, Julius D (2009) Cellular and molecular mechanisms of pain. Cell 139:267–284

Bautista DM, Siemens J, Glazer JM, Tsuruda PR, Basbaum AI, Stucky CL, Jordt SE, Julius D (2007) The menthol receptor TRPM8 is the principal detector of environmental cold. Nature 448:204–208

Brauchi S, Orio P, Latorre R (2004) Clues to understanding cold sensation: thermodynamics and electrophysiological analysis of the cold receptor TRPM8. Proc Natl Acad Sci USA 101: 15494–15499

Brauchi S, Orta G, Salazar M, Rosenmann E, Latorre R (2006) A hot-sensing cold receptor: C-terminal domain determines thermosensation in transient receptor potential channels. J Neurosci 26:4835–4840

Brauchi S, Orta G, Mascayano C, Salazar M, Raddatz N, Urbina H, Rosenmann E, Gonzalez-Nilo F, Latorre R (2007) Dissection of the components for PIP2 activation and thermosensation in TRP channels. Proc Natl Acad Sci USA 104:10246–10251

Caterina MJ (2007) Transient receptor potential ion channels as participants in thermosensation and thermoregulation. Am J Physiol Regul Integr Comp Physiol 292:R64–R76

Caterina MJ, Schumacher MA, Tominaga M, Rosen TA, Levine JD, Julius D (1997) The capsaicin receptor: a heat-activated ion channel in the pain pathway. Nature 389:816–824

Caterina MJ, Rosen TA, Tominaga M, Brake AJ, Julius D (1999) A capsaicin-receptor homologue with a high threshold for noxious heat. Nature 398:436–441

Caterina MJ, Leffler A, Malmberg AB, Martin WJ, Trafton J, Petersen-Zeitz KR, Koltzenburg M, Basbaum AI, Julius D (2000) Impaired nociception and pain sensation in mice lacking the capsaicin receptor. Science 288:306–313

Catterall WA (2010) Ion channel voltage sensors: structure, function, and pathophysiology. Neuron 67:915–928

Chung MK, Lee H, Caterina MJ (2003) Warm temperatures activate TRPV4 in mouse 308 keratinocytes. J Biol Chem 278:32037–32046

Clapham DE, Miller C (2011) A thermodynamic framework for understanding temperature sensing by transient receptor potential (TRP) channels. Proc Natl Acad Sci USA 108:19492–19497

Colburn RW, Lubin ML, Stone DJ Jr, Wang Y, Lawrence D, D'Andrea MR, Brandt MR, Liu Y, Flores CM, Qin N (2007) Attenuated cold sensitivity in TRPM8 null mice. Neuron 54:379–386

Colquhoun D (1998) Binding, gating, affinity and efficacy: the interpretation of structure-activity relationships for agonists and of the effects of mutating receptors. Br J Pharmacol 125:924–947

Cordero-Morales JF, Gracheva EO, Julius D (2011) Cytoplasmic ankyrin repeats of transient receptor potential A1 (TRPA1) dictate sensitivity to thermal and chemical stimuli. Proc Natl Acad Sci USA 108:E1184–E1191

Davis JB, Gray J, Gunthorpe MJ, Hatcher JP, Davey PT, Overend P, Harries MH, Latcham J, Clapham C, Atkinson K, Hughes SA, Rance K, Grau E, Harper AJ, Pugh PL, Rogers DC, Bingham S, Randall A, Sheardown SA (2000) Vanilloid receptor-1 is essential for inflammatory thermal hyperalgesia. Nature 405:183–187

Dhaka A, Murray AN, Mathur J, Earley TJ, Petrus MJ, Patapoutian A (2007) TRPM8 is required for cold sensation in mice. Neuron 54:371–378

Fernandez JA, Skryma R, Bidaux G, Magleby KL, Scholfield CN, McGeown JG, Prevarskaya N, Zholos AV (2011) Voltage- and cold-dependent gating of single TRPM8 ion channels. J Gen Physiol 137:173–195

Grandl J, Hu H, Bandell M, Bursulaya B, Schmidt M, Petrus M, Patapoutian A (2008) Pore region of TRPV3 ion channel is specifically required for heat activation. Nat Neurosci 11:1007–1013

Grandl J, Kim SE, Uzzell V, Bursulaya B, Petrus M, Bandell M, Patapoutian A (2010) Temperature-induced opening of TRPV1 ion channel is stabilized by the pore domain. Nat Neurosci 13:708–714

Grivel F, Candas V (1991) Ambient temperatures preferred by young European males and females at rest. Ergonomics 34:365–378

Horrigan FT, Aldrich RW (2002) Coupling between voltage sensor activation, Ca2+ binding and channel opening in large conductance (BK) potassium channels. J Gen Physiol 120:267–305

Huang SM, Li X, Yu Y, Wang J, Caterina MJ (2011) TRPV3 and TRPV4 ion channels are not major contributors to mouse heat sensation. Mol Pain 7:37

Janssens A, Voets T (2011) Ligand stoichiometry of the cold- and menthol-activated channel TRPM8. J Physiol 589:4827–4835

Karashima Y, Talavera K, Everaerts W, Janssens A, Kwan KY, Vennekens R, Nilius B, Voets T (2009) TRPA1 acts as a cold sensor in vitro and in vivo. Proc Natl Acad Sci USA 106: 1273–1278

Latorre R, Brauchi S, Orta G, Zaelzer C, Vargas G (2007) ThermoTRP channels as modular proteins with allosteric gating. Cell Calcium 42:427–438

Lee H, Iida T, Mizuno A, Suzuki M, Caterina MJ (2005) Altered thermal selection behavior in mice lacking transient receptor potential vanilloid 4. J Neurosci 25:1304–1310

Liu B, Hui K, Qin F (2003) Thermodynamics of heat activation of single capsaicin ion channels VR1. Biophys J 85:2988–3006

Mahieu F, Janssens A, Gees M, Talavera K, Nilius B, Voets T (2010) Modulation of the cold-activated cation channel TRPM8 by surface charge screening. J Physiol 588:315–324

Matta JA, Ahern GP (2007) Voltage is a partial activator of rat thermosensitive TRP channels. J Physiol 585:469–482

McKemy DD, Neuhausser WM, Julius D (2002) Identification of a cold receptor reveals a general role for TRP channels in thermosensation. Nature 416:52–58

Monod J, Wyman J, Changeux JP (1965) On the nature of allosteric transitions: a plausible model. J Mol Biol 12:88–118

Moqrich A, Hwang SW, Earley TJ, Petrus MJ, Murray AN, Spencer KS, Andahazy M, Story GM, Patapoutian A (2005) Impaired thermosensation in mice lacking TRPV3, a heat and camphor sensor in the skin. Science 307:1468–1472

Morrison SF, Nakamura K (2011) Central neural pathways for thermoregulation. Front Biosci 16:74–104

Nilius B, Talavera K, Owsianik G, Prenen J, Droogmans G, Voets T (2005) Gating of TRP channels: a voltage connection? J Physiol 567:35–44

Park U, Vastani N, Guan Y, Raja SN, Koltzenburg M, Caterina MJ (2011) TRP vanilloid 2 knock-out mice are susceptible to perinatal lethality but display normal thermal and mechanical nociception. J Neurosci 31:11425–11436

Peier AM, Moqrich A, Hergarden AC, Reeve AJ, Andersson DA, Story GM, Earley TJ, Dragoni I, McIntyre P, Bevan S, Patapoutian A (2002a) A TRP channel that senses cold stimuli and menthol. Cell 108:705–715

Peier AM, Reeve AJ, Andersson DA, Moqrich A, Earley TJ, Hergarden AC, Story GM, Colley S, Hogenesch JB, McIntyre P, Bevan S, Patapoutian A (2002b) A heat-sensitive TRP channel expressed in keratinocytes. Science 296:2046–2049

Rohacs T, Lopes CM, Michailidis I, Logothetis DE (2005) PI(4,5)P2 regulates the activation and desensitization of TRPM8 channels through the TRP domain. Nat Neurosci 8:626–634

Romanovsky AA (2007) Thermoregulation: some concepts have changed. Functional architecture of the thermoregulatory system. Am J Physiol Regul Integr Comp Physiol 292:R37–R46

Smith GD, Gunthorpe MJ, Kelsell RE, Hayes PD, Reilly P, Facer P, Wright JE, Jerman JC, Walhin JP, Ooi L, Egerton J, Charles KJ, Smart D, Randall AD, Anand P, Davis JB (2002) TRPV3 is a temperature-sensitive vanilloid receptor-like protein. Nature 418:186–190

Story GM, Peier AM, Reeve AJ, Eid SR, Mosbacher J, Hricik TR, Earley TJ, Hergarden AC, Andersson DA, Hwang SW, McIntyre P, Jegla T, Bevan S, Patapoutian A (2003) ANKTM1, a TRP-like channel expressed in nociceptive neurons, is activated by cold temperatures. Cell 112:819–829

Talavera K, Yasumatsu K, Voets T, Droogmans G, Shigemura N, Ninomiya Y, Margolskee RF, Nilius B (2005) Heat activation of TRPM5 underlies thermal sensitivity of sweet taste. Nature 438:1022–1025

Talavera K, Nilius B, Voets T (2008) Neuronal TRP channels: thermometers, pathfinders and life-savers. Trends Neurosci 31:287–295

Togashi K, Hara Y, Tominaga T, Higashi T, Konishi Y, Mori Y, Tominaga M (2006) TRPM2 activation by cyclic ADP-ribose at body temperature is involved in insulin secretion. EMBO J 25:1804–1815

Tombola F, Pathak MM, Isacoff EY (2006) How does voltage open an ion channel? Annu Rev Cell Dev Biol 22:23–52

Tominaga M, Caterina MJ, Malmberg AB, Rosen TA, Gilbert H, Skinner K, Raumann BE, Basbaum AI, Julius D (1998) The cloned capsaicin receptor integrates multiple pain-producing stimuli. Neuron 21:531–543

Vlachova V, Teisinger J, Susankova K, Lyfenko A, Ettrich R, Vyklicky L (2003) Functional role of C-terminal cytoplasmic tail of rat vanilloid receptor 1. J Neurosci 23:1340–1350

Voets T, Droogmans G, Wissenbach U, Janssens A, Flockerzi V, Nilius B (2004) The principle of temperature-dependent gating in cold- and heat-sensitive TRP channels. Nature 430:748–754

Voets T, Talavera K, Owsianik G, Nilius B (2005) Sensing with TRP channels. Nat Chem Biol 1:85–92

Voets T, Owsianik G, Janssens A, Talavera K, Nilius B (2007) TRPM8 voltage sensor mutants reveal a mechanism for integrating thermal and chemical stimuli. Nat Chem Biol 3:174–182

Vriens J, Owsianik G, Hofmann T, Philipp SE, Stab J, Chen X, Benoit M, Xue F, Janssens A, Kerselaers S, Oberwinkler J, Vennekens R, Gudermann T, Nilius B, Voets T (2011) TRPM3 is a nociceptor channel involved in the detection of noxious heat. Neuron 70:482–494

Watanabe H, Vriens J, Suh SH, Benham CD, Droogmans G, Nilius B (2002) Heat-evoked activation of TRPV4 channels in a HEK293 cell expression system and in native mouse aorta endothelial cells. J Biol Chem 277:47044–47051

Xu H, Ramsey IS, Kotecha SA, Moran MM, Chong JA, Lawson D, Ge P, Lilly J, Silos-Santiago I, Xie Y, DiStefano PS, Curtis R, Clapham DE (2002) TRPV3 is a calcium-permeable temperature-sensitive cation channel. Nature 418:181–186

Yang F, Cui Y, Wang K, Zheng J (2010) Thermosensitive TRP channel pore turret is part of the temperature activation pathway. Proc Natl Acad Sci USA 107:7083–7088

Yao J, Liu B, Qin F (2010) Pore turret of thermal TRP channels is not essential for temperature sensing. Proc Natl Acad Sci USA 107:E125, author reply E126–E127

Yao J, Liu B, Qin F (2011) Modular thermal sensors in temperature-gated transient receptor potential (TRP) channels. Proc Natl Acad Sci USA 108:11109–11114

Zakharian E, Cao C, Rohacs T (2010) Gating of transient receptor potential melastatin 8 (TRPM8) channels activated by cold and chemical agonists in planar lipid bilayers. J Neurosci 30: 12526–12534

Zimmermann K, Lennerz JK, Hein A, Link AS, Kaczmarek JS, Delling M, Uysal S, Pfeifer JD, Riccio A, Clapham DE (2011) Transient receptor potential cation channel, subfamily C, member 5 (TRPC5) is a cold-transducer in the peripheral nervous system. Proc Natl Acad Sci USA 108:18114–18119